CHARACTERIZATION OF POLYMERIC MEMBRANES: SULFONATED POLYSULFONES

by

Yoonok Kang

Dissertation submitted to the Faculty of the
Virginia Polytechnic Institute and State University
in partial fulfillment of the requirements
for the degree of
DOCTOR OF PHILOSOPHY
in
Chemistry

APPROVED:

J. P. Wightman, Chairman

J. G. Dillard

M. A. Dinno

J. G. Mason

J. E. McGrath

J. F. Wolfe

September, 1981

Blacksburg, Virginia

TO MY LOVED ONES

ACKNOWLEDGEMENT

The author is indebted to numerous people who have provided tremendous support, including both intellectual and technical assistance.

The author is especially grateful to her advisor who, for four years of the graduate work, has been more than an academic advisor. As an academic advisor, he was always available when needed to provide encouragement and intellectual stimulation. But, he is also a man with great personal warmth, patience, and an unlimited supply of moral support. He has the ability to bring out the best in a student, and the author is forever grateful to have had the opportunity to know him as a person and to have associated with such a great mind.

The author greatly appreciates her committee members, and for their interest in the project and their time in going over the dissertation.

Further appreciation is extended to the following persons: and his co-workers, especially for providing raw SPSF polymers; of the Division of Forestry and Wildlife Resources at VPI & SU for performing SEM/EDAX analysis; of the Department of Physics at VPI & SU for his thoughtfulness

in allowing the author to use his experimental apparatus and for his genuine interest and many stimulating discussions; of the Department of Materials Engineering Science at VPI & SU for a thorough IR analysis;

of the Glass Shop of the Department of Chemistry at VPI & SU for the design of the IR cell holder for the membranes; the members of the Machine Shop in the Department at VPI & SU for the construction of the lucite cell for the electrical property studies; and

for her technical assistance.

The author is also grateful to OWRT for supporting this work under Contract #
and granting a Graduate Research Assistantship from Spring, 1979 to Spring, 1981.

TABLE OF CONTENTS

LIST OF TABLES

LIST OF FIGURES

I. INTRODUCTION

Water is one of the most vital natural resources utilized by man. The Water Resources Center (WRC) has projected that water consumption in the United States will be about 300 billion gallons per day in the year 2000.[1] Although the national water supply appears sufficient, regional and temporal shortages remain as serious problems. Water shortage is also a well-recognized problem world-wide, especially in the Middle East.

One way to meet the world's demand for water involves reliance on sea water which comprises 97% of the total surface water on the earth's crust.[2] Direct consumption of saline water is not possible, however, due to the physiological problem of dehydration. Therefore, the conversion of sea water to fresh water has been of interest for some time, and, in fact, the concept of desalination dates back to the ancient Greeks in the fourth century B.C. In the works of Aristotle's Problemata, it is stated:

> "Why is it that salt water when it is cold is not drinkable, but becomes more drinkable when it is heated, and when it is heated and then cooled? . . . when salt water is heated, the salt is boiled out, and, when it cools, is precipitated."[3]

Sailors of Aristotle's time and after obtained drinking water by collecting the evaporated water from the sea.

It is quite impressive that an optimistic prediction of the United States' capacity for desalination is about 30 billion gallons per day by the year 2000.[1] Modern desalination technology includes various techniques, such as distillation, ion exchange, and reverse osmosis. Of these techniques, the reverse osmosis membrane process has received much attention due to its relatively low energy requirement. Since the introduction of cellulose acetate reverse osmosis membranes by Loeb and Sourirajan,[4] in fact, the growth in the reverse osmosis technology has been phenomenal. As an example, a desalination plant is under construction in Yuma, Arizona which has a capacity of 95.7 million gallons per day processed only by reverse osmosis membranes. In Saudi Arabia, 50% of its present 141 million gallons per day capacity is provided by the reverse osmosis process.[5]

Significant efforts have been made to further improve the reverse osmosis desalination process and the search for better membrane materials is one such effort. Sulfonated polysulfone has been considered as a possible material for reverse osmosis membranes and the results of preliminary studies by various workers[6-8] seem very promising.

The objective of this study is the characterization of membranes prepared from sulfonated polysulfones of various degrees of sulfonation in order to determine

the feasibility of using these polymers for reverse osmosis membranes. The characterization process includes determination of the degree of sulfonation, water uptake capacity, contact angle measurements, ESCA analysis, scanning electron microscopy, and the measurement of the electrical properties.

II. LITERATURE REVIEW

A. Introduction

Reverse osmosis, or hyperfiltration, is a separation process which is achieved by passing a solution through an appropriate membrane under high pressure. A related but not identical process is ultrafiltration, where dispersed colloidal particles are separated by particle size on passage through a suitable filter. Ultrafiltration of salt from aqueous solution poses difficulties, however, due to the similarities in the sizes of the ions and the water molecules.

The first observation of salt filtration dates back to the mid 1930's. During the ultrafiltration studies, colloid chemists[9] observed rejection of KIO_3 in aqueous solution and attributed that rejection to the fact that the salt existed partially in the colloidal state. Later evidence against the colloidal state of salts was provided, however, and the previous results were reinterpreted as an ion-exchange rejection mechanism.[10]

Salt separation by membranes such as cellulose nitrate and cellophane has been reported by many workers, including Trautman and Ambard,[11] Hacker,[12] and Wintgren.[13] Unfortunately, these membranes showed very low (<10%) NaCl rejection for concentrations above 0.1 M.

B. Reverse Osmosis Desalination

The feasibility of desalination by reverse osmosis was introduced independently by Yuster et al. in 1958[14] and by Reid and Breton in 1957.[15,16] Among the various materials studied, both groups reported that cellulose acetate membranes exhibited the best salt rejection of greater than 98% for sea-water concentrations, although the flow rate of the process was very low. Reid and Spencer[17] applied greater pressure in their work, but the flow rate showed only about a 2-fold increase from 7 ml/hr/cm^2 at 135 atm to 17 ml/hr/cm^2 at 270 atm.

A significant achievement was made when Loeb and Sourirajan developed asymmetric membranes which enhanced the flux greatly.[4] According to Sourirajan, however, the recognition of the asymmetric nature of reverse osmosis membranes was accidental. In the course of a reverse osmosis study with commercially obtained Schleicher and Schuell type US-Ultrafine Superdense cellulose acetate membranes, the asymmetry of the membrane was noted.[18] It was observed that one side of the membrane was rough with smaller sized pores, whereas the other side was smoother and more porous, and desalination was observed only when the rough side was interfaced with the feed saline solution.

The first successful attempt to produce an asymmetric membrane in the laboratory was accomplished[4] through the

work of Dobry[19] and Biget[20]. Dobry reported that cellulose acetate dissolved in saturated solutions of Ca, Mg, Cu, and Zn perchlorate at room temperature and, further, the cellulose acetate saturated magnesium perchlorate solution could form into membranes. Later, Biget reported the coagulation of cellulose acetate in acetone with aqueous solutions of magnesium perchlorate and the formation of a cellulose acetate gel. Based on these studies, casting solutions of cellulose acetate containing water, acetone, and magnesium perchlorate were investigated. The composition and casting conditions of the first successful membranes are listed in Table I.

The fabrication of a successful membrane was followed by extensive work on improving the membranes further by studying the effect of variables involved in the film making process. The results of many such works are reported by Sourirajan.[21]

Table I.

Composition and Performance
of a Successful Asymmetric Cellulose Acetate Membrane
Developed by Loeb and Sourirajan[4]

Casting Solution Composition (wt. %)	
Cellulose acetate (acetyl content 39.8%):	22.2
Acetone	66.7
Water	10.0
Magnesium perchlorate	1.1
Casting Temperature	0 to -10°C
Temperature Treatment	75 to 82°C
Feed Concentration (wt. %)	3.5% NaCl
Operating Pressure	1500 psi
Product Concentration of NaCl	less than 500 ppm
Product Flux Rate	10 gal/day/ft^2 (4.6×10^{-4} g/cm^2-sec)

C. Sulfonated Polysulfone Membranes for Reverse Osmosis Desalination

The contribution of the classic Loeb-Sourirajan type asymmetric cellulose acetate membranes to the development of the reverse osmosis desalination process is significant. The shortcomings of such membranes were soon realized, however, including creep-induced compaction,[22] thermal[23] and biological degradation,[24] and hydrolysis.[25] Much attention has, therefore, been focused on improving the cellulose acetate membrane and on developing new membrane materials. The literature is abundant with accounts of the development of new membrane materials.[21, 26-28]

Sulfonated polysulfone is a sulfonated derivative of the sulfone containing poly (aryl ethers), poly (arylene ether sulfones), or polysulfones (PSF). The structure of a sulfonated polysulfone (SPSF) repeat unit is illustrated:[29]

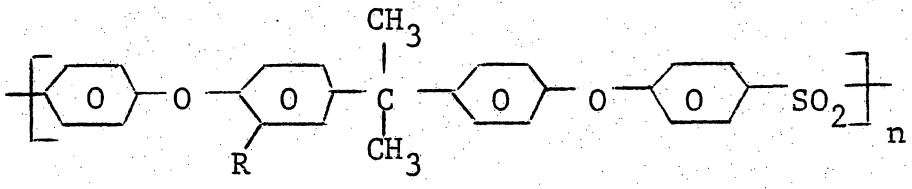

where R can be a free acid ($-SO_3H$), a salt ($-SO_3^-X^+$) or an ester ($-SO_3R$). The properties of PSF, in particular Bisphenol A-polysulfone (Bis A-PSF), which is the antecedent of the polymer illustrated above, have been studied.[30] Bis

A-PSF has been used as an asymmetric ultrafiltration/microfiltration membrane and as a porous, rigid support material in composite membranes.[31, 32] The reasons for the utility of this polymer as a membrane material are its superior strength, which gives resistance to creep-induced compaction and resistance to biological and chemical degradation, as well as wet-dry reversibility and, therefore, ease of handling.[32] Unfortunately, the poly (aryl ethers) are hydrophobic and thereby limited in their usefulness as reverse osmosis membranes for aqueous systems.

In the light of the discussion above, it is desirable to alter the chemical nature of PSF to induce a measure of hydrophilicity while maintaining the excellent physical character. Sulfonation has been known to dramatically alter a number of characteristics of polymeric materials (for example, dyeability,[33] tensile strength,[34] and, of particular interest to the present studies, hydrophilicity[35]). In fact, sulfonation has been used to improve the reverse osmosis performance of poly (phenylene oxide) membranes[36] as well as membranes of Bis A-PSF.[8,37-40]

The property changes resulting from sulfonation of Bis A-PSF have been investigated by Noshay and Robeson.[6] Some of their results are presented in Table II along with data relating to cellulose acetate (CA) for

Table II

Comparison of Mechanical Properties

	Tensile Modulus ($kPa \times 10^{-6}$)		Tensile Strength ($kPa \times 10^{-6}$)		Elongation (%)		Tg (^{o}C)
	Ambient	Wet	Ambient	Wet	Ambient	Wet	Ambient
SPSF-Na*							
D.S. = 0.0	2.48	----	7.03	----	50	---	180
D.S. = 0.1	2.05	1.83	6.90	5.65	7	14	180
D.S. = 0.5	1.60	1.08	6.27	3.81	25	98	240
D.S. = 1.0	1.21	0.24	3.86	0.83	17	30	300
CA	0.48(a)	0.32(a)	0.94(a)	0.49(a)	3.1(a)	18(a)	68.6(b)

*SPSF-Na represents Bisphenol A-polysulfone which has been sulfonated and neutralized to the sodium salt form. D.S. represents "degree of sulfonation" (i.e., the statistical fraction of repeat units which have been sulfonated). CA represents cellulose acetate.

Note: All data for SPSF-Na is taken from Reference 6. Film thickness = 0.254 mm.

Note: Data for cellulose acetate (film thickness = 0.088 mm) is taken from (a) Reference 61; and (b) Reference 26, p. 136.

comparison. The mechanical superiority of the polysulfone and its sulfonated derivative is obvious. Noshay and Robeson[6] included in their investigations limited flux and salt separation studies, using dense membranes of Bis A-PSF which were sulfonated and neutralized with a sodium counter ion (SPSF-Na). Even though their studies were restricted to dense membranes of the free acid and sodium salt sulfonated forms of the commercially available PSF (Union Carbide P-1700), their results were encouraging. Their results indicated that in order to optimize the strength/stability and flux/separation performance, the degree of sulfonation (DS) must be optimized at some moderate value. The term DS represents the statistical fraction of repeat units which are sulfonated.

The same base material, SPSF-Na, has been used by Rhone-Poulenc Industries to develop ion-exchange membranes for desalination.[8,37-40] Their research has concentrated on polymers of moderate DS and low molecular weight, a restriction imposed by their technique of sulfonation which may cause polymer degradation. While their method of membrane preparation is not entirely clear, it is evident that the Rhone-Poulenc membranes possess the desired structural asymmetry. In this form, the SPSF membranes have proven to be equal to and in some ways superior to CA membranes.

The Union Carbide P-1700 base material was also employed by Envirogenics Systems Company to investigate SPSF membranes for desalination.[7,41] Although their reports are comparable to those of Rhone-Poulenc and are encouraging, reproducibility of membrane performance appears to be a problem.

D. Membrane Characterization

It is important to characterize the reverse osmosis membrane in order to understand the processes involved. Only a limited number of attempts have been made to characterize these membranes, however, with particular emphasis on surface properties.

1. Electron Microscopy: Early work was done by Riley et al.[42,43] using a clever, but very tedious method involving transmission electron microscopy. Their work confirmed the asymmetric nature of the cellulose acetate membrane observed by Loeb and Sourirajan.

Development of scanning electron microscopy (SEM) introduced a powerful means of probing the membrane morphology.[44] Kesting investigated the effects of varying the swelling agent on the membrane morphology using SEM.[45] His continued extensive investigations of membrane morphology with SEM are reported in the literature.[26,46,47]

2. Contact Angle Measurements: Since the separation process involves the permeation of water through the membrane, the interaction of water with the membrane is very important. The extent of such interaction may be obtained from the measurement of contact angles. Zisman carried out extensive studies on the contact angles of a variety of liquids on various surfaces, including polymer

films. The determination of the critical surface tension of polymer films, using the Zisman series, has, in fact, become standard practice[48] and critical surface tensions for some typical polymers are given in Table III.[49]

The remarkable interest in this field is reflected in the three reviews on contact angles.[50-52] The earliest one[50] compiles basic works, such as the thermodynamic aspects of wetting, wettability by heats of immersion and the study of adhesion. The second review[51] includes a discussion of general concepts and experimental techniques with emphasis on low energy surfaces. The most recent review[52] includes the study of the dependence of contact angle on the drop size of the liquid and on the rate of the advancing and receding contact angles. Noshay and Robeson reported the water contact angles of polysulfone and totally sulfonated polysulfone as 70° and 52°, respectively.[6]

3. Electron Spectroscopy for Chemical Analysis (ESCA): Surface chemical composition is yet another important feature of a material in that the surface composition of any given polymer film can be markedly different from the bulk composition.[53] ESCA is a technique which can generally probe the top 50Å of a solid, and studies of polymer surfaces with ESCA are abundant in the

Table III.

Critical Surface Tensions for Some Polymers[49]

Polymer	γ_c, dyn/cm (20°C)
Polytetrafluoroethylene	18
Polyethylene	31
Polystyrene	33
Polyvinyl chloride	39
Polyhexamethylene adipamide (nylon 6,6)	46

literature.[54-56]

The rearrangement of a polymer surface, namely radiation grafted polymeric film upon dehydration, has been reported.[55] Thomas and O'Malley also predicted the topology of the polystyrene/poly (ethylene oxide) diblock copolymer surface using ESCA.[56] Further, depth profiling of the polymer can be achieved by variation of the photoelectron take-off angle. This angular-resolved ESCA technique results in enhanced surface analysis.[57-59]

Recently, Everhart and Reilley also reported the identification of functional groups on low density polyethylene formed during exposure to plasmas using derivitization methods containing an elemental tag.[60]

4. Electrical Properties: The electrical and electrokinetic properties of polymeric membranes[62-64] have received attention for some time, although studies on asymmetric cellulose acetate membranes have been reported only recently.[65-67] Demisch and Pusch[68] determined the electrical and electroosmotic coefficients as a function of the NaCl concentration. Kimjo and Sato,[69] however, studied the mobility of ions in asymmetric cellulose acetate and suggested the possible influence of bound water on ionic mobility within the membrane, thus effecting the salt separation.

Electrical properties of dense cellulose acetate membranes were also measured by Kimjo[70] based on the importance of the active dense layer. Kimjo reported a drastic reduction, of three orders of magnitude, in the mobility of the Na^+ and Cl^- ions in the dense membrane compared to the aqueous solution.

5. Water Sorption by Polymer: The extent and structure of sorbed water in a polymer sample has been studied by a number of workers. The results of such studies provide information on the compatibility of water and the polymeric material, and thus the nature and strength of the inter-and intra- molecular forces between water and the polymer.

Typically, water sorption study is approached through the analysis of sorption isotherms as a function of relative humidity. Polyethylene and polypropylene were found to follow Henry's law from 0 to 100% relative humidity.[71] Flory[72] and Huggins[73] modified the simple solution theory to be applicable to polymer solutions and their theory seems to fit rather well for non-polar polymer and solvent systems.

Another approach to the diffusion process is to consider the process in two steps: initial adsorption of water molecules on the membrane walls and subsequent

adsorption on the first layer. The multilayer physical adsorption theory (BET) was established by Brunauer, Emmett, and Teller,[74] and is widely used. Bull[75] and Pauling[76] employed the BET theory to interpret the results of water-sorption measurements and this was found to be very informative. Later study by White and Eyring[77] incorporated the effect of swelling in the analysis of isotherms. Another interesting study by Zimm and Landberg[78,79] reported a clustering theory where the solvent distribution in the polymer can be attained by the analysis of isotherms. Noshay and Robeson[6] determined the adsorption-desorption isotherm of water with SPSF-Na membranes and reported the apparent non-Fickian behaviour which was more extensive for greater degrees of sulfonation.

The structural analysis of sorbed water has also been of interest. Reid and Kuppers[80] concluded the presence of bound water within the cellulose acetate desalination membrane which is transported from site to site by hydrogen bonding. They also reported the presence of quasi-crystalline water.[80,81] A collective work on the interaction of water with polymers has also been published.[82] A recent report by Luck et al. indicated the presence of weakly bound water in desalination membranes, such as cellulose acetate and porous glass membranes.[83] In contrast, the presence of more restricted water in the vicinity of the membrane is reported

by proton NMR,[84,85] DSC,[86] and transport studies.[87] Belfort and Sinai[88] also reported an extensive study with pNMR to reconcile the discrepancy between pNMR and IR analysis of water structure.

E. Reverse Osmosis Technology

Since the introduction of the asymmetric membrane, the advancement in the science of reverse osmosis has been phenomenal. Broad applications of reverse osmosis can be found in many areas, including food technology, the paper industry, and waste water treatment, and reviews and progress in these fields are reported in the literature.[27,28,89]

Broader application and interest in reverse osmosis has brought about technological progress in membrane science. In 1964, Havens Industries introduced reverse osmosis desalination membranes "integrally lined within a porous fiberglass-reinforced tube," although the details of the manufacturing process were not disclosed.[90] This was followed by Loeb in 1966,[91] who pioneered the formation of tubular porous cellulose acetate membranes by gravity-drop techniques. Further achievements included the introduction of other types of membranes, such as grafted, composite, and hollow fiber membranes.[27,28] The greatest advantage of the hollow fiber membrane is the favorable ratio of membrane surface to pressure vessel volume.

F. Mechanisms

While the technological aspect has shown rapid growth, the mechanism(s) of the reverse osmosis process is still under debate. Discussions of the reverse osmosis separation mechanism across the Loeb-Sourirajan type porous cellulose acetate membranes, for example, are abundant in literature.[21,27,28,92] Reid and co-workers originally introduced the concept of the bound-water-hole-diffusion mechanism.[80] They reported that only the solvent and not the solute is adsorbed on the porous wall, thus filling the entire pore, and that the transport of water is by diffusion from site to site by hydrogen bonding. These authors also believed the sorbed water to be in a quasi-crystalline arrangement, thus excluding most ions.[81]

Lonsdale *et al.*[93], however, provided evidence against this feature by the measurement of diffusion coefficients. According to Lonsdale and co-workers, perfect membranes have a completely nonporous surface structure and the permeation through this membrane is through a homogeneous diffusion process.

Sourirajan, however, regards the separation process as proceeding via a preferential sorption capillary mechanism.[21,28] Here, water is preferentially sorbed at the membrane/solution interface, and passes through the membrane pores with a critical diameter.

III. EXPERIMENTAL

A. Materials

Polysulfone P-1700 was obtained from Union Carbide. Sulfonation of polysulfone to various degrees was performed by McGrath and co-workers. The detailed synthetic procedure is described elsewhere,[94] although a summary of the synthesis and some of the characterized properties are given in Appendix I.

The following degrees of sulfonation of the polysulfone were targeted: 0.2, 0.4, 0.5, 0.6, 0.8, and 1.0. The degree of sulfonation is defined as the number of sulfonated monomer units in every 10 total monomer units. For all degrees of sulfonation, except for 0.5, both the sodium and potassium salt of sulfonated polysulfone were synthesized. For the 0.5 degree of sulfonation, however, only the sodium salt was available.

For the sake of simplicity, sulfonated polymers are coded. For example, SPSF-Na (0.5) means the sodium salt of sulfonated polysulfone with a degree of sulfonation targeted for 0.5. The degree of sulfonation was determined with proton NMR analysis using a Varian EM390 NMR spectrometer by the integration of peak areas.[95] The NMR spectra were taken in CD_3Cl or DMSO for polysulfone or sulfonated polysulfone, respectively. The results of the NMR

analysis of the various polymers are given in Appendix I with the results of elemental analysis. Although the determined degree of sulfonation was lower than the targeted value, a good agreement between the two was seen in most cases.

Characterization processes were performed on the synthesized polymer powders, dense membranes, and asymmetric membranes. Since it is the dense part of the asymmetric membrane that is responsible for the salt separation, however, the focus of this study was on the characterization of the dense membranes. Water uptake study, contact angle measurement, IR sorbed water analysis, ESCA, and electrical property determination were, therefore, performed on dense membranes. Dense membranes are also referred to as polymer membranes, membranes, and polymer films. Of all the available polymer materials, the most extensive work was performed using SPSF-Na (0.5). Selection of this sodium salt polymer was based on the desire to limit ion exchange in desalination. The selection of the degree of sulfonation of 0.5 represents a compromise between the hydrophilic/hydrophobic balance and the structural stability as will be discussed later.

B. Preparation of Dense Membranes

Polymer solutions of 10 to 25 weight percent concentrations were prepared in the solvents DMF or DMSO, which were at least reagent grade. The polymer solutions were shaken overnight to promote mixing and dissolution of the polymer. The polymer solution was then cast on a glass plate using a doctor's knife (micron film applicator from Gardner). The height of the blade was adjusted to cast membranes between 8 mil (0.0203 cm) and 16 mil (0.0406 cm) in thickness.

The glass plates were annealed in air at 600°C for 15 hours prior to casting to ensure complete removal of residual polymers from the previous casting. Both the glass surface and the edge of the knife were rinsed with either acetone or solvent.

Cast membranes were dried in an oven with dry air circulation for 10 hours at ambient temperatures, and then for 15 hours at 80-120°C. The membranes were then cooled down to room temperature in the oven and peeled off the glass plate by moistening around the edges. By capillarity, a thin layer of water penetrated the area between the membrane and the glass plate, thus lifting the membrane. The peeled membranes were then wrapped loosely in aluminum foil and placed in a vacuum oven at 80-120°C for 15 hours. The membranes were then allowed to cool

to room temperature and were stored in a desiccator containing $CaCl_2$.

C. Degree of Sulfonation for Cast Membranes

It was necessary to monitor any changes in the degree of sulfonation which might occur during the drying process and/or to detect any interactions of polymers with solvents. The degree of sulfonation for the dried dense membranes was determined with a Perkin-Elmer 283 grating infrared spectrometer. The membranes were held by a Thomas film holder, and no other treatment was used in this study. The IR spectra were taken between 4000 cm^{-1} and 200 cm^{-1} using the normal mode operation with peak suppression. The typical scan time was 12 minutes and the response and slit program were set at 1 and N, respectively.

D. Water Uptake Study

A piece of each membrane, about 2 cm^2 was weighed and placed on an aluminum tray in a desiccator at various relative humidities. Relative humidity was controlled by varying the composition of aqueous H_2SO_4 solutions, as tabulated in Table IV. The measured relative humidities were lower than the values in the literature, possibly due to the reagent impurities and/or other experimental variables such as temperature.

30 ml of each solution was placed in a 50 ml beaker and put inside the desiccator. The relative humidity within each desiccator was measured with a YSI 91 HC dew point hygrometer. Water uptake was measured gravimetrically with respect to time using a Mettler 542 balance.

Initially, the membranes were stored over $CaCl_2$ until the weight was relatively constant. This weight was considered to be the base weight without any sorbed water. The membranes were then placed in the humidity-controlled desiccators. The membranes were weighed periodically and the difference between the base weight and the measured weight was taken to be the weight of the sorbed water.

TABLE IV.

Composition of H_2SO_4 (aq)
For Various Relative Humidities

wt% H_2SO_4	R. H.$_{literature}$	R. H.$_{measured}$
0	100	100
34	70.4	56
51	37.1	28

E. Contact Angle Measurements

Contact angles were measured on the dense membranes without further treatment. Two different methods were employed depending on the nature of the membranes. For sulfonated membranes, a 100 µl droplet of liquid was placed on the membrane's surface. The angle tangent to the liquid/air interface was measured by means of a goniometer within 10 seconds after the application of the droplet.

For the polysulfone membranes, the measurements were made using the apparatus shown schematically in Figure 1, which was patterned after the one described by Neumann and Good.[96] The apparatus consisted of a syringe pump with which the rate of the advancing and the receding processes were controlled. Steady state between the liquid droplet and the vapor was maintained by a cover with optical flats at both ends placed over the liquid drop. Introduction of a drop and measurement of the angle by a goniometer could therefore be performed without disturbing the system. Contact angles were measured on drops larger than 5 mm in diameter within 20 seconds after the introduction. Typical rates of injection or withdrawal were 1 ml/hour.

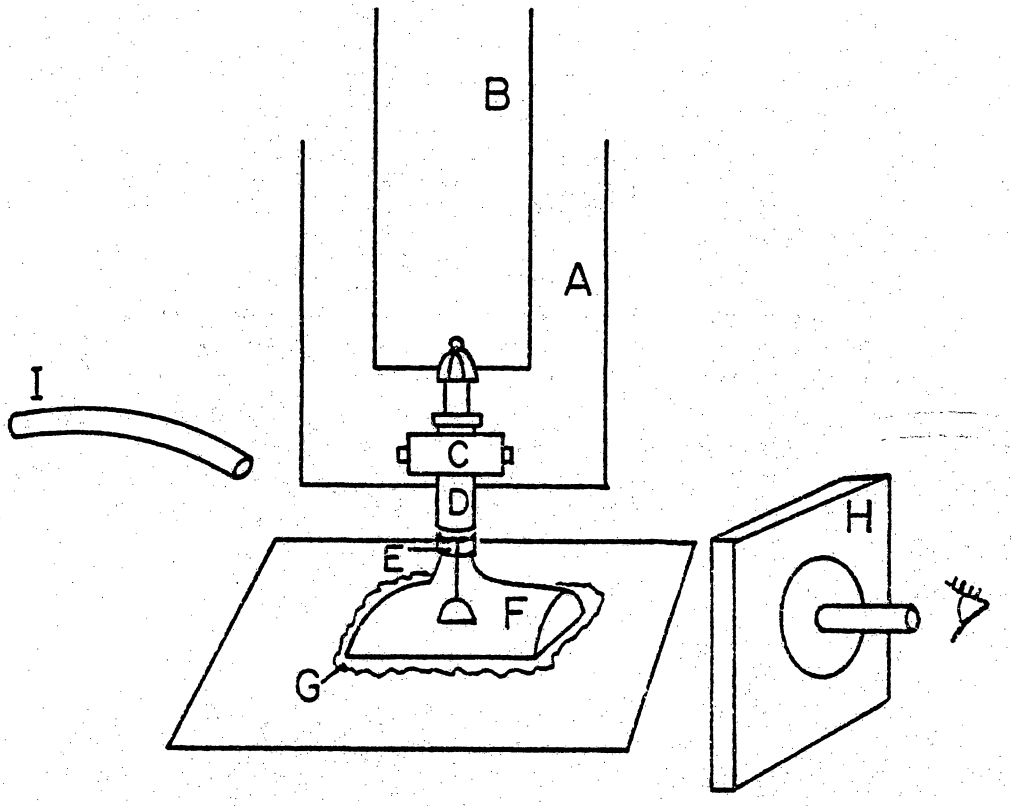

Figure 1. Apparatus for contact angle measurements.

A : Syringe pump (Model 352 Sage Instrument)

B : Gear box

C : Syringe holder

D : 5 ml syringe

E : Parafilm

F : Glass cover

G : Membrane

H : Goniometer

I : Fiber light

F. Ion Exchange Study

A known weight of SPSF-Na (0.5) or SPSF-K (0.6) dense membrane was placed in 10 ml of 0.1% KCl or NaCl solution, respectively, for 24 hours. The membrane was then removed from the solution, rinsed thoroughly with distilled/deionized water, and air dried. The salt solutions were analyzed with a Varian 175 atomic absorption spectrometer. Concentrations of sodium and potassium were determined using the 590.8 nm and 768.5 nm absorption band, respectively. The dried membranes before and after the ion exchange study were analyzed with ESCA and neutron activation analysis (NAA).

G. Electron Spectroscopy for Chemical Analysis (ESCA)

A duPont 650 ESCA electron spectrometer was employed with a magnesium anode (1254eV) as the x-ray source. The typical filament and anode currents were 2 amp and 20 mamps, respectively, when the x-ray voltage was set at 10 kV. The operating pressure was typically around $6X10^{-7}$ torr. Binding energies were calibrated by taking the background carbon 1s photopeak as 284.6 eV.

Membranes were punched and placed on a 1/4-inch diameter sample probe by means of double stick tape. The side of the membrane not touching the metal surface of the puncher was analyzed. The polymer powders were sprinkled directly on the double stick tape on the probe.

Quantitative analysis was performed by correcting the area under each photoelectron peak using tabulated photo cross-sections.[97] In some cases, the photoelectron peak was transferred to a computer by MADCAP and the peak was curve-fitted using GASCAP program.[98] The input parameters for GASCAP are: number of points in spectrum, number of peaks, peak position, peak width at half height, and peak height.

H. Scanning Electron Microscopy (SEM)

An AMR 900 scanning electron microscope was employed to study the membrane morphology. The microscope operates at 20KV and has an International 707 energy dispersive analysis of x-rays (EDAX) accessory.

Dried dense membranes were directly placed on copper tape on a 1/2" diameter aluminum sample stub. It was necessary, however, to pretreat the asymmetric membranes prior to the SEM study in order to prevent the collapse of pore structure due to dehydration.[45] The pretreatment process involved placing the membranes in a solution containing water, glycerol, and Triton X-100 of 69.5, 30, and 0.5 weight percent, respectively. The water used was distilled deionized; U.S.P. grade glycerol was obtained from Mallinckrodt; and Triton X-100 was provided by Rohm and Haas Company.

The order of mixing was found to be critical in order to produce a clear, homogeneous one-phase solution. 0.5 g of Triton was placed in a 150 ml beaker and 69.5 g of water was introduced drop-wise with rigorous mixing; glycerol was added last with constant stirring. The membranes were placed in the solution for 24 hours, removed, and air dried for 24 hours. The dried membranes were then freeze fractured under liquid nitrogen

and mounted on the copper tape. The freeze fracturing produced a freshly cleaved cross-section of the membrane. All the SEM samples were coated either with gold/palladium or carbon to ensure adequate conductivity and to avoid charging of the sample surface.

I. Water Structure Study with Infrared Spectroscopy (IR)

The structure of water sorbed by the membranes was investigated by near IR. A Cary 14 spectrophotometer was employed, and the water band at 19,000 Å was utilized for the analysis at the scan rate of 100 Å/minute. A special cell was constructed, as shown in Figure 2, for analysis of the membranes at 100% relative humidity. The cell had an outer jacket in which water was circulated to control the temperature of the system between 10 and 45°C. The desired humidity was obtained by placing a container with water at the end of a side arm connected to the neck of the cell.

Two CaF_2 windows were glued to the system in the optical path with epoxy. The membrane holder was constructed from pyrex glass. A magnet was attached at the top of the holder so it could be displaced in and out of the cell. A cross-shaped member ensured correct spacing of the holder within the cell. Membranes were placed in a slit produced by two glass rings joined at the bottom. To increase sensitivity, 7 sheets of membranes were placed in the system at one time.

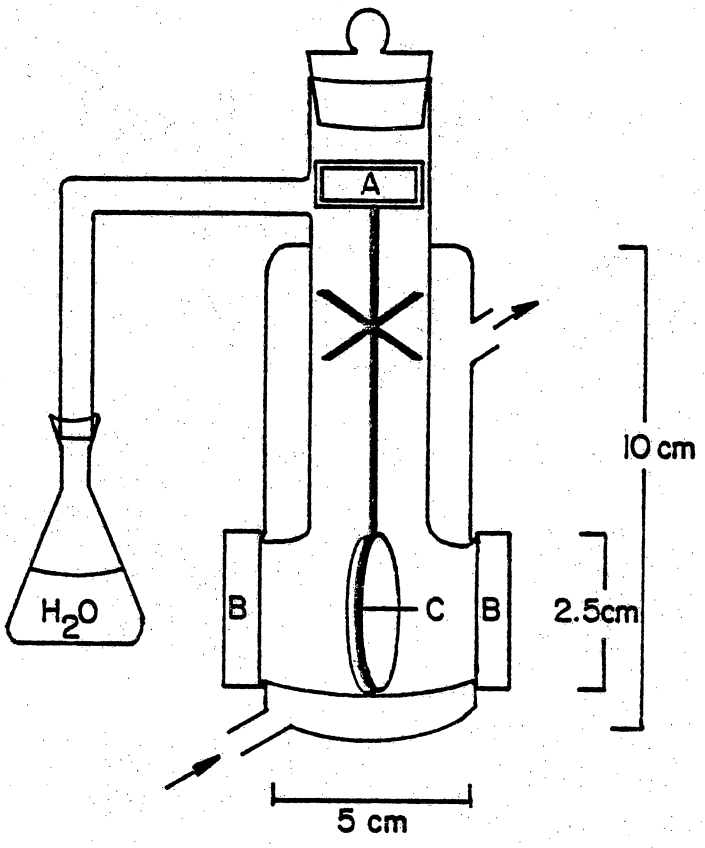

Figure 2. Schematic diagram of IR cell.

A : Magnet (inside a glass enclosure)

B : CaF_2 window

2.5 cm diameter

0.5 cm thick

C : Membrane (7 pieces)

J. Electrical Properties of Membranes

The transport of ions across the membranes was induced via a square pulse or transient current. Using the apparatus as shown in Figure 3, a picoamp current source was employed to send currents between 0.5 and 100 μA.

A membrane was placed in position A, dividing the lucite chambers into right and left, as detailed in the diagram of the cell in Figure 4. The solution in both chambers was circulated to and from the reservoir at the top via bubbling through a 95% O_2 and 5% CO_2 gas mixture. A water jacket around the reservoir allowed for the controlled temperature of the system. Current was sent via 3-layer agar electrodes connected to each end of the chamber. Preparation of the 3-layer agar electrode is described below.

The potential across the membrane was measured using calomel electrodes placed in the reservoirs, and the potential difference was plotted out on the chart recorder.

1. Preparation of Agar Solutions: The agar electrode consists of three separate layers described as follows:

*KCl agar: 2 gm of agar (Fisher, laboratory grade) and 34.7 gm KCl (Fisher, certified) were placed in 100 ml of glass distilled water. The solution was stirred

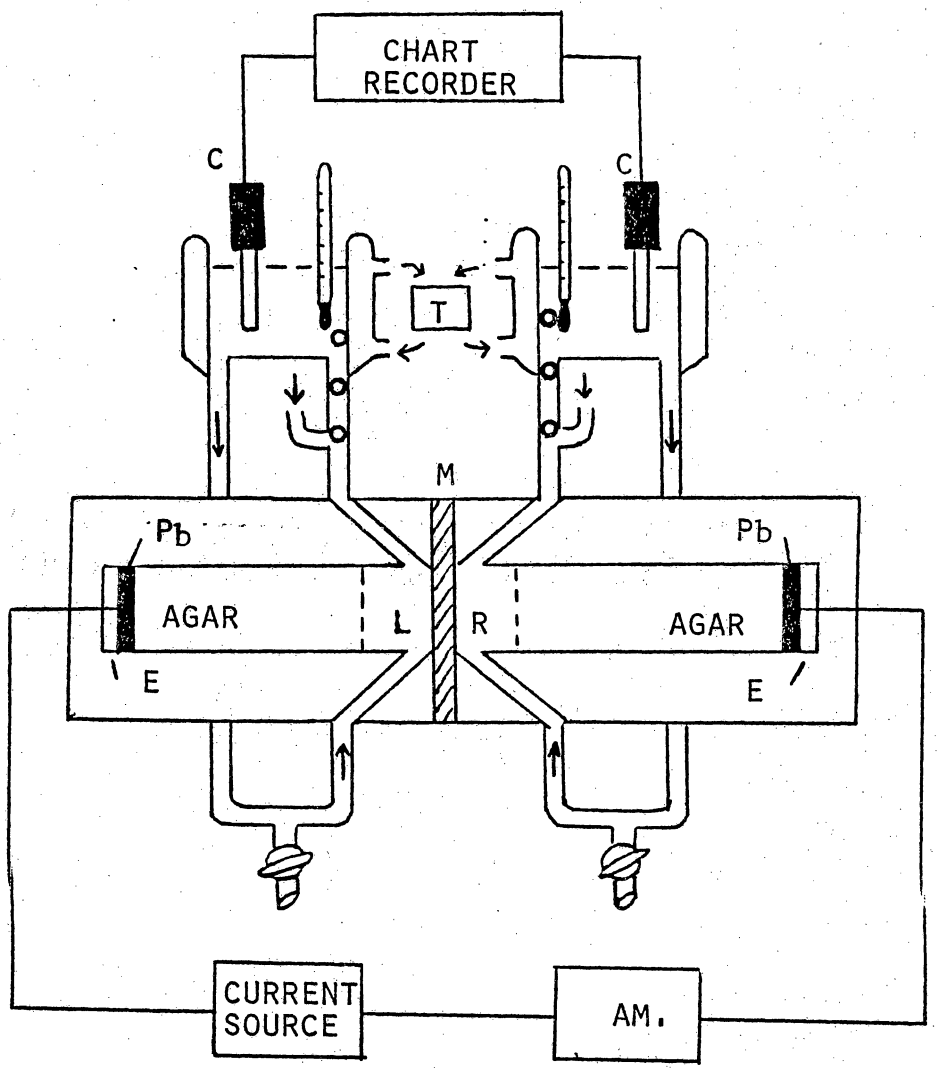

Figure 3. Diagram of apparatus for electrical property study.

AM = MICROAMMETER
C = CALOMEL ELECTRODES
E = CURRENT SENDING ELECTRODES
M = MEMBRANE
T = TEMPERATURE CONTROL SYSTEM

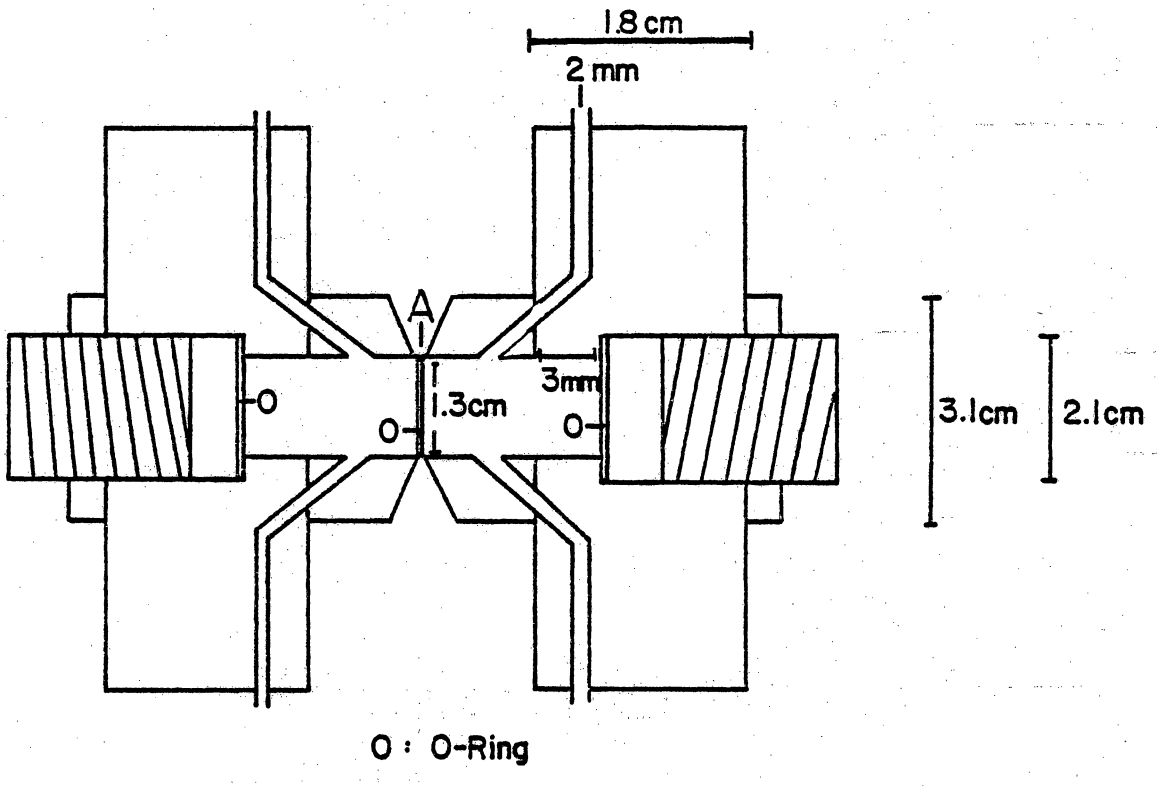

Figure 4. Diagram of cell for the electrical property study.

A : Membrane

well in a boiling water bath until it became clear.

*Pb acetate agar: 2 gm agar and 44.3 gm Pb acetate (Fisher, certified) were mixed with 100 ml of water in a boiling water bath. The final solution was light brown and opaque.

*Secretory Ringer agar: 2 gm agar was dissolved in 100 ml of Secretory Ringer solution. Secretory solution was prepared by mixing 102 ml of 1 M NaCl with 4 ml of 1 M KCl solution and diluting to 1 litre with distilled water.

2. Preparation of Agar Electrodes: The schematic diagram of an agar electrode is given in Figure 5. The electrical connection was made by a Pb coating at the end of the electrode. The agar solutions were introduced with a hot syringe, rinsed well with hot distilled water to avoid solidification in the syringe.

With the electrode in a vertical position, hot Pb acetate agar solution was introduced into the electrode through inlet A. The Pb acetate agar solution was allowed to set and a screw was placed in inlet A. Then, hot KCl agar solution was introduced via inlet B and allowed to harden, and a screw was placed in inlet B. Finally, Secretory Ringer agar solution was introduced through a hole at the tip of the electrode. The agar was allowed to flow over the tip to ensure the absence of any bubbles. The

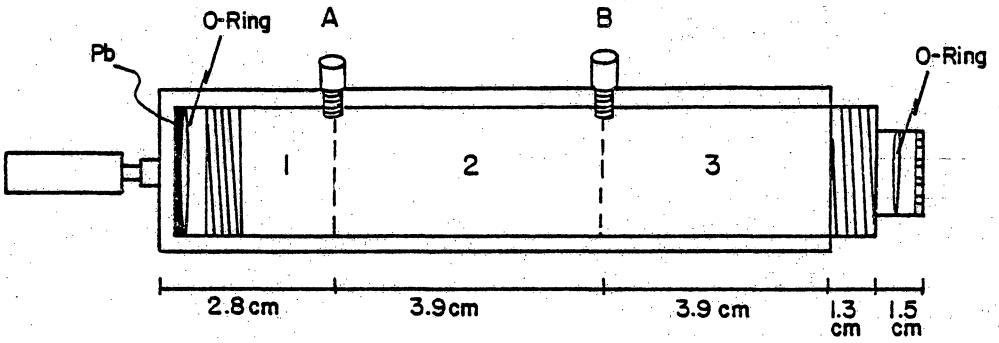

Figure 5. Schematic diagram of an agar electrode.

1 : Pb acetate agar

2 : KCl agar

3 : Secretory Ringer agar

A, B : Screw

excess agar at the tip was removed, however, before the electrode assembly was placed in the system.

3. Preparation of Electrolyte Solutions: Typically 0.599 M (3.5% NaCl solution) electrolyte solutions were prepared. The salts studied included NaCl (Sigma grade), KCl (Fisher ACS certified), $MgCl_2$ (Fisher, ACS certified), and choline chloride (Sigma). Glass distilled water was used as the solvent.

IV. RESULTS AND DISCUSSION

A. Degree of Sulfonation of Dense Membranes by Infrared Spectroscopy

The infrared spectrum of a polysulfone membrane between 3000 and 600 cm^{-1} region is shown in Figure 6. The spectra includes absorption bands at 1368 and 1010 cm^{-1} due to the methyl group and aryl ether stretching, respectively. These two bands were used in the quantitative analysis representing the polymer chain back bone.

In Figure 7, the infrared spectrum of a sulfonated polysulfone membrane is presented. Figures 6 and 7 were essentially identical except for an additional peak at 1028 cm^{-1} found only in the sulfonated polysulfone membrane. This additional, well-resolved peak is due to the symmetric O=S=O stretching of the sulfonate group and its intensity increased in accordance with the greater degree of sulfonation, as shown in Figure 8. Thus, the peak at 1028 cm^{-1} was selected to represent the extent of sulfonation for the quantitative analysis. A detailed peak assignment for the infrared absorption bands of sulfonated polysulfone was performed by Tran[99] and is given in Table V.

The quantitative analysis was performed by means of the baseline technique[100] as shown in Figure 9. The absorbance, A, was calculated by the equation:

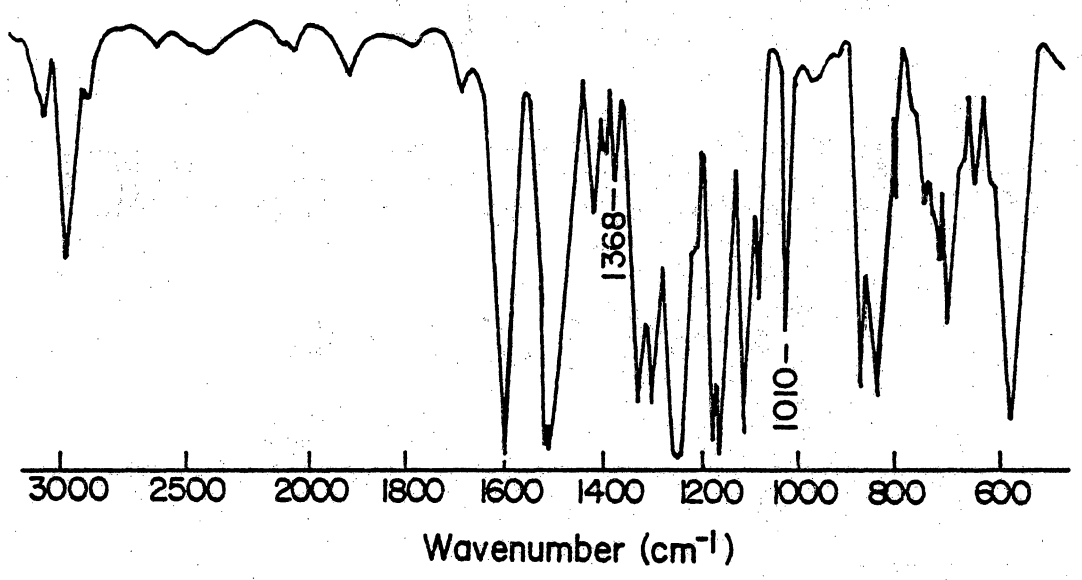

Figure 6. IR spectrum of polysulfone (PSF).

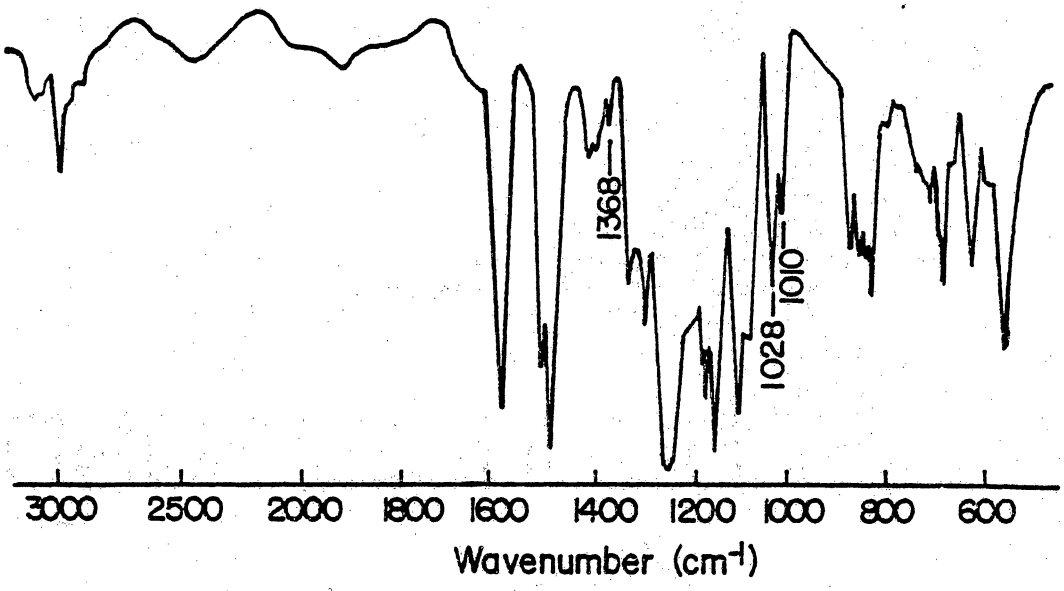

Figure 7. IR spectrum of sulfonated polysulfone (SPSF).

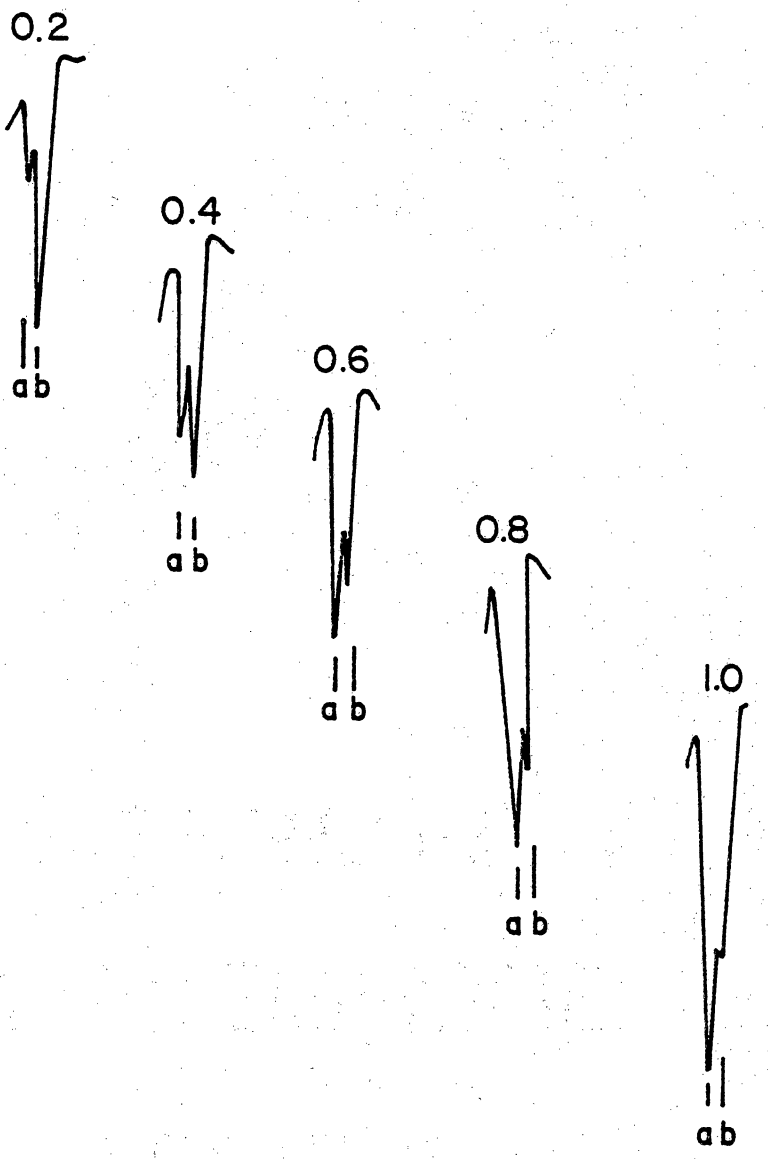

Figure 8. IR absorption bands of sulfonated polysulfone at (a) 1028 and (b) 1010 cm^{-1} : SPSF-Na.

Table V.

Infrared Peak Assignments
for Sulfonated Polysulfone [99]

Frequency (cm^{-1})	Assignments
3100 3078 3042	Aromatic C-H stretching vibrations.
2980 2880	Asymmetric and Symmetric C-H stretching vibrations involving entire methyl group.
1590 1508 1490	Aromatic C=C stretching.
1412	Asymmetric C-H bending deformation of methyl group.
1393 1368	Symmetric C-H bending deformation of methyl group.
1325 1298	Doublet resulting from asymmetric O=S=O stretching of sulfone group.
1245	Asymmetric C—O—C stretching of aryl ether group.
1172	Asymmetric O=S=O stretching of sulfonate group.
1152	Symmetric O=S=O stretching of sulfone group.
1108 1092	Aromatic ring vibrations.
1028	Symmetric O=S=O stretching of sulfonate group.
1010	Ring vibration of p-substituted aryl ether.
874 850	Out of plane C-H deformation of isolated hydrogen in 1, 2, 4 substituted phenyl ring.
832	Out of plane C-H deformation characteristic of p-substituted phenyl.
710 689 624	C-S stretching vibrations.

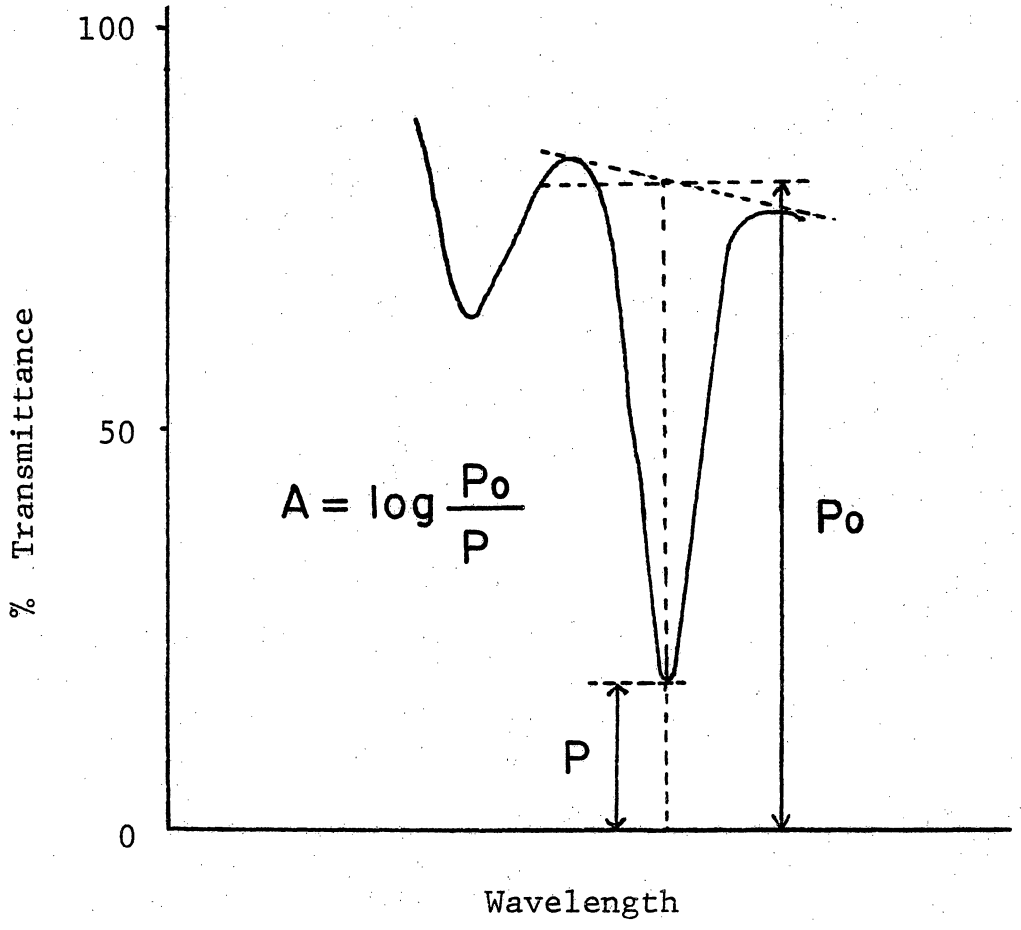

Figure 9. Base line method for determination of absorbance.

$$A = \log P_o/P \qquad (1)$$

where P_o and P, as defined in Figure 9, represent the intensities of the light before and after interaction with the sample. The degree of sulfonation was calculated based on Beer's Law:

$$A = \varepsilon C\ell \qquad (2)$$

where ε is the molar absorptivity coefficient, C is the molar concentration, and ℓ is the path length. The ratio of the two absorbances is proportional to the concentration ratio:

$$\frac{A_1}{A_2} = \frac{\varepsilon_1 C_1}{\varepsilon} \qquad (3)$$

and, thus, the amount of SO_3 group per monomer unit may be obtained from the value of the $A_{SO_3}/A_{Ph\text{-}O\text{-}Ph}$ or A_{SO_3}/A_{CH_3} ratio. The values of A_{SO_3}, $A_{Ph\text{-}O\text{-}Ph}$, and A_{CH_3} represent peak absorbances due to SO_3 ($1028cm^{-1}$), Ph-O-Ph ($1010cm^{-1}$), and CH_3 ($1368cm^{-1}$) groups, respectively. Table VI lists the values of peak absorbances and the ratios for SPSF-Na and SPSF-K. These values are averages of at least three measurements.

The values obtained by equation (3) are not absolute values because of the proportionality constant $\varepsilon_1/\varepsilon_2$. The proportionality constant, however, may be eliminated by

Table VI.

Infrared Peak Absorbances and Ratios for Sulfonated Polysulfones [99]

Polymer	A_{SO_3}	$A_{Ph\text{-}O\text{-}Ph}$	A_{CH_3}	$\frac{A_{SO_3}}{A_{Ph\text{-}O\text{-}Ph}}$	$\frac{A_{SO_3}}{A_{CH_3}}$	$\frac{A_{CH_3}}{A_{Ph\text{-}O\text{-}Ph}}$
SPSF-Na(0.2)	0.11	0.47	0.13	0.24	0.85	0.27
-Na(0.4)	0.22	0.29	0.07	0.75	3.14	0.24
-Na(0.6)	0.30	0.25	0.06	1.20	5.00	0.24
-Na(0.8)	0.36	0.23	0.05	1.56	6.56	0.22
-Na(1.0)	0.87	0.38	0.11	2.29	7.90	0.29
SPSF-K(0.2)	0.14	0.65	0.15	0.21	0.93	0.23
-K(0.4)	0.13	0.12	0.03	1.08	3.77	0.25
-K(0.6)	0.24	0.18	0.05	1.33	5.17	0.27
-K(0.8)	1.36	0.66	0.17	2.06	8.00	0.26
-K(1.0)	0.41	0.16	0.05	2.56	8.20	0.31

taking a double ratio with respect to a known value, as in:

$$\frac{A_1^x/A_2^x}{A_1^{known}/A_2^{known}} = \frac{C_1^x/C_2^x}{C_1^{known}/C_2^{known}} . \qquad (4)$$

The suffix "x" denotes ratios from a sample with unknown composition, and "known" denotes the ratios from a sample where the concentration ratio is known.

In this study, the degrees of sulfonation of the samples SPSF-Na(1.0) and SPSF-K(1.0) were assumed to be 1.0. The degrees of sulfonation for various samples were thus obtained by dividing the ratios in Table VI by the values for SPSF(1.0), and are tabulated in Table VII. The values of the two IR ratios were comparable. The results of NMR studies on the same powders are also listed in Table VII as a comparison. In the case of the SPSF-Na series, a good agreement was found between the IR and the NMR analyses. Such consistency indicates that there was no alteration in the degree of sulfonation during the fabrication process of dense membranes. With the SPSF-K series, however, the degrees of sulfonation calculated by the infrared analysis had to be multiplied by a factor of 0.87 since the NMR analysis for the highest degree of sulfonation was 0.87 and not 1.00. Such adjusted values are given in square brackets and those values compare well with the NMR results.

Table VII.

Degree of Sulfonation
for Dense Sulfonated Polysulfone Membranes
by Infrared in Comparison to NMR Results.[99]

Type	Target	NMR	IR-($A_{SO_3}/A_{Ph\text{-}O\text{-}Ph}$)		IR-(A_{SO_3}/A_{CH_3})	
SPSF-Na	0.2	.16	0.11		0.11	
	0.4	.34	0.33		0.40	
	0.6	.53	0.52		0.63	
	0.8	.68	0.68		0.83	
	1.0	1.00	1.00		1.00	
SPSF-K	0.2	.12	0.08	[0.07	0.11	[0.10
	0.4	.33	0.42	0.37]	0.46	0.40]
	0.6	.48	0.52	0.45]	0.63	0.55]
	0.8	.72	0.80	0.70]	0.98	0.85]
	1.0	.87	1.00	0.87]	1.00	0.87]

The relationship between the two methods, NMR and IR, is shown graphically in Figure 10. Here, the three peak absorbance ratios from Table VI are plotted against the degree of sulfonation as determined by NMR for the SPSF-Na. A good linear correlation is seen for the ratios of $A_{SO_3}/A_{Ph\text{-}O\text{-}Ph}$ and A_{SO_3}/A_{CH_3}. The ratio of $A_{CH_3}/A_{Ph\text{-}O\text{-}Ph}$ is independent of the degree of sulfonation, as expected, since both of these functional groups are in the polymer chain back bone, and, thus, are not affected by sulfonation.

A comparison between the SPSF-Na and SPSF-K membranes is shown in Figure 11, where the peak absorption ratio of $A_{SO_3}/A_{Ph\text{-}O\text{-}Ph}$ from Table VI is plotted against the degree of sulfonation, as determined by NMR. Although both SPSF-Na and SPSF-K series exhibited linear dependency, the slope of the two lines differed. This indicates that each salt requires a separate calibration curve for the determination of the degree of sulfonation for an unknown sample. A discussion of the difference in the slope for each salt is given by Tran[99] based on the size of the counter ions, which in turn influences the bond strength.

In summary, the degree of sulfonation of the initial polymer material was maintained during the membrane fabrication process. Further, the degree of sulfonation can be determined simply and effectively using infrared spectroscopy.

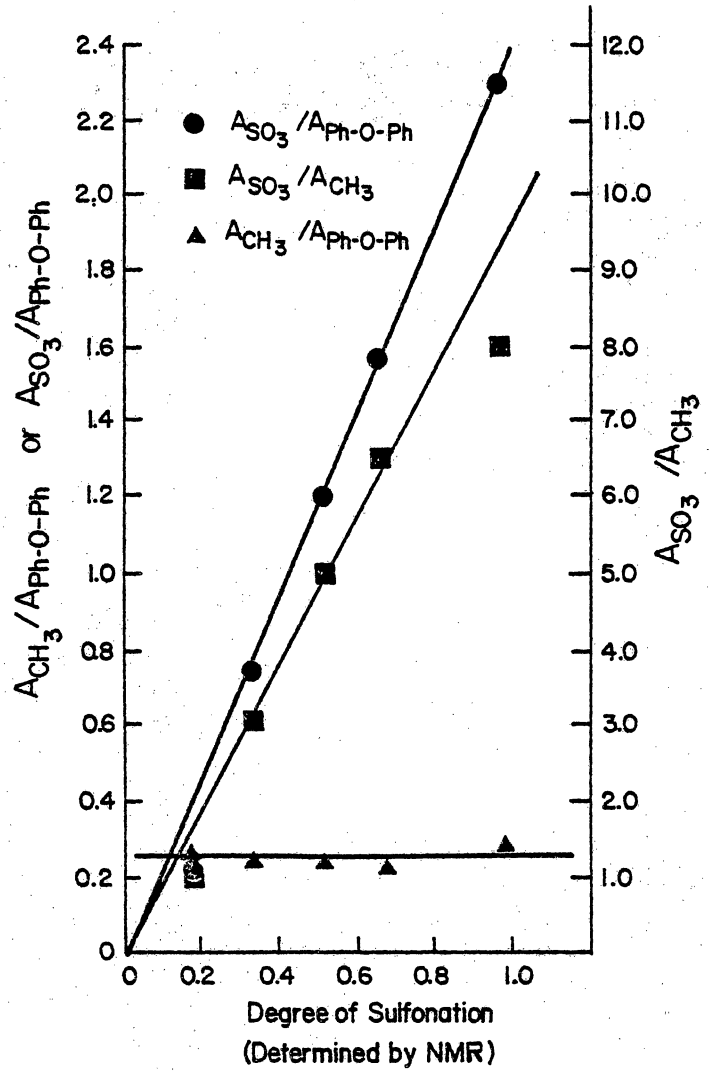

Figure 10. Calibration curves of IR and NMR methods for the determination of degree of sulfonation: SPSF-Na.[99]

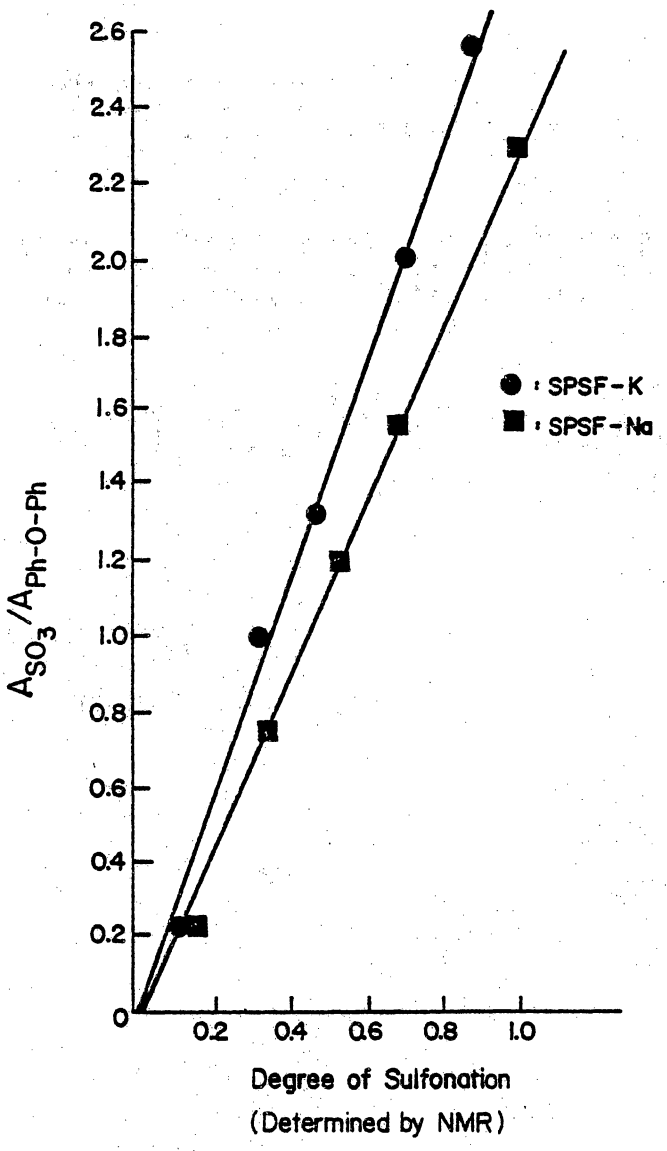

Figure 11. Effect of counter-ion on the IR-NMR calibration curve.[99]

B. Water Uptake by Dense Membranes

The weight of water sorbed in grams per gram of membrane versus time for the SPSF-Na and SPSF-K series at 100% relative humidity is plotted in Figures 12 and 13, respectively. The unsulfonated polysulfone (PSF) membrane showed negligible water uptake throughout the experimental time span, and, thus, the hydrophobic nature of polysulfone is clearly demonstrated. Water uptake did increase, however, with increasing degrees of sulfonation. This is self-consistent since the sulfonation introduces hydrophilicity into the polymer matrix. SPSF-Na(0.2) is omitted from the figure due to the presence of unwashed Na salt which remained in the system as determined by ESCA (see discussion in the ESCA section, p. 77). Although both series of membranes showed similar trends, it should be noted that the absolute amount of water sorbed by the SPSF-Na series is greater than that of the SPSF-K series for a given degree of sulfonation.

The total water sorbed per gram of membrane was obtained by extrapolation of the plateau, and the values are tabulated in Table VIII. The observed difference in the water uptake between the two series of membranes may, in part, be due to the formation of ionic clusters of different size. Macknight *et al.*[101] reported the dependence of the effective radius of a cluster on the radius of the counter ion, and that the hydration of the counter

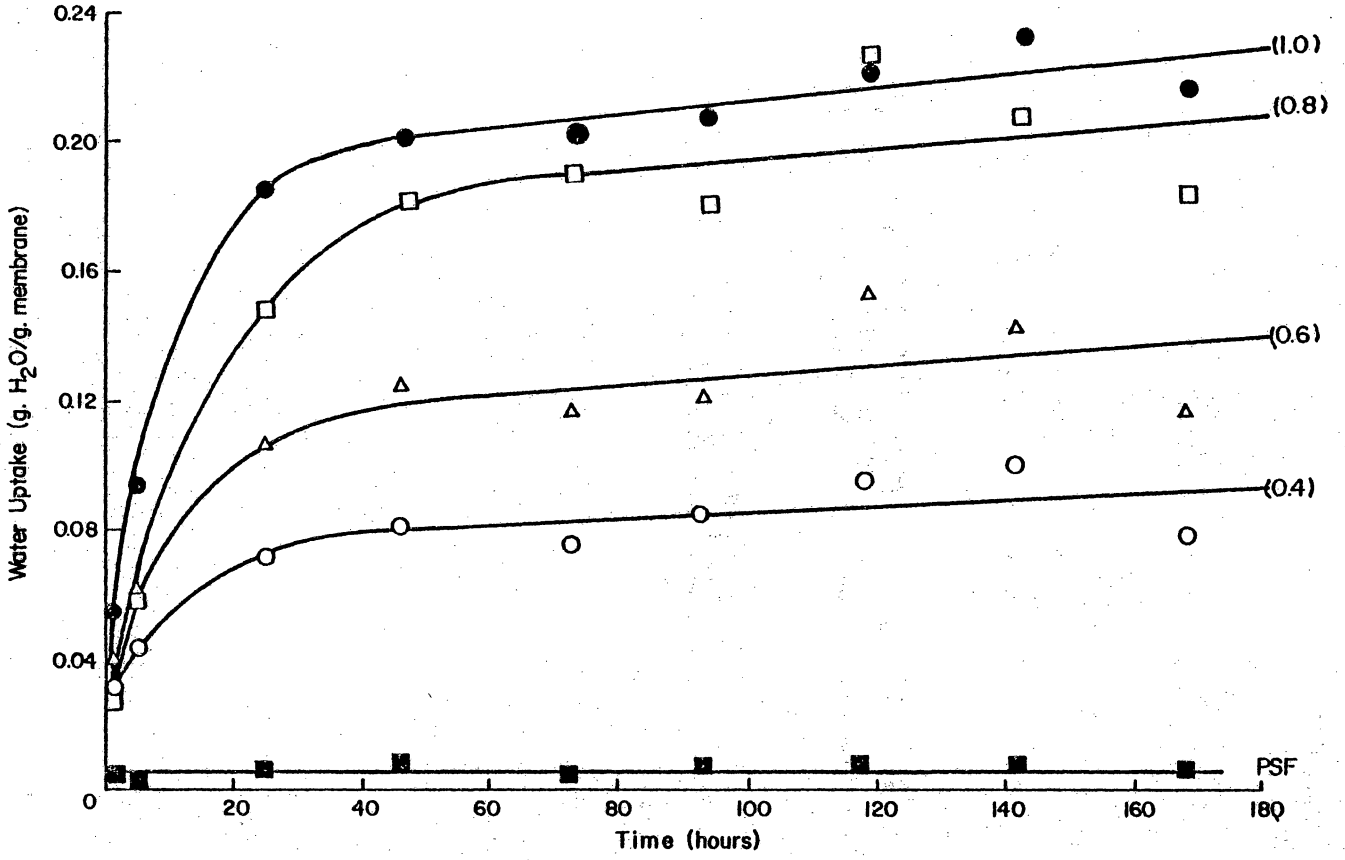

Figure 12. Water uptake by SPSF-Na dense membranes with respect to time at 100% relative humidity.

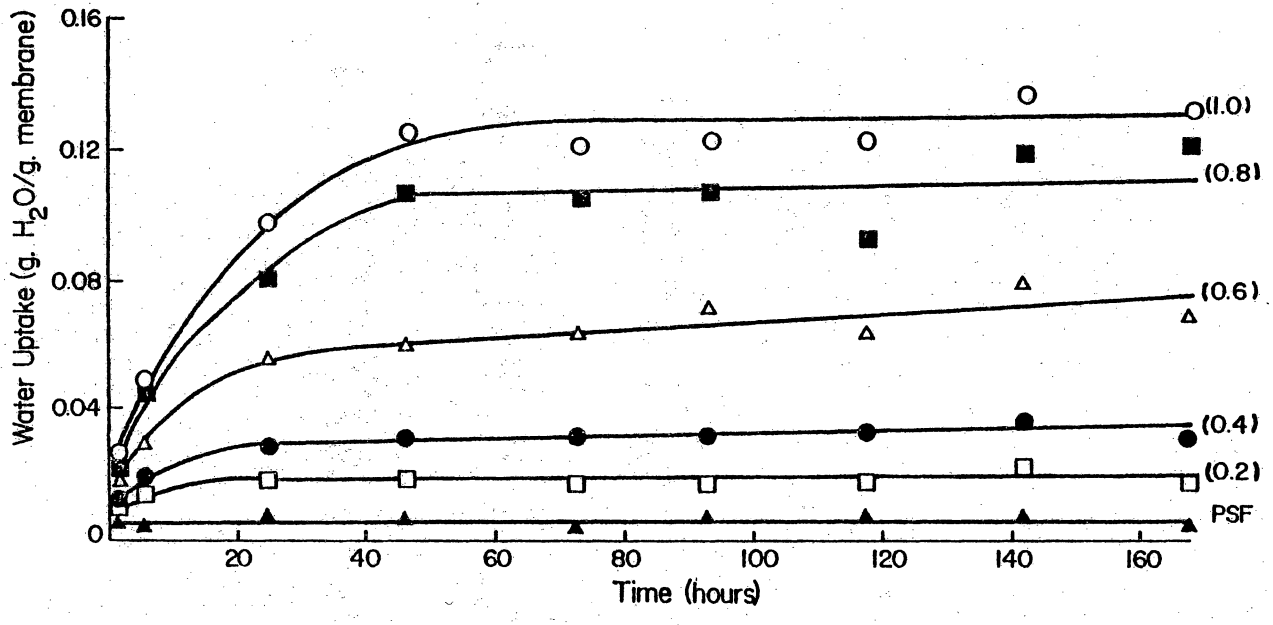

Figure 13. Water uptake by SPSF-K dense membranes with respect to time at 100% relative humidity.

Table VIII.

Total Water Sorbed by Dense Membranes

Membrane	H_2O (g)/Membrane (g)
PSF	0.006
SPSF-Na(0.2)	-----
(0.4)	0.075
(0.6)	0.140
(0.8)	0.190
(1.0)	0.192
SPSF-K(0.2)	0.017
(0.4)	0.029
(0.6)	0.053
(0.8)	0.106
(1.0)	0.122

ion was related to the addition of water.

Noshay and Robeson[6] reported water sorption of 5% to 61% for SPSF-Na(0.1) to SPSF-Na(1.0). These are greater values than the results of this study (1% to 19%), probably due to the difference in the experimental technique of sorption measurement. In their study, membranes were directly immersed in water and gently wiped dry before the weight measurement. Hence, a greater weight gain is reasonable for such a study as compared to the present one, although the trend observed was consistent with the present work.

Brousse et al.[8] also performed water sorption by immersion in water followed by a "superficial" drying process in which the membrane was pressed between two pieces of filter paper, and the values obtained ranged from 8% to 16%. These values are significantly lower than those of Noshay and Robeson, but closer to the present study. A comparison of these two studies implies probable error in the drying process to remove excess water involved in the immersion technique.

The kinetics of the water uptake by both SPSF-Na and SPSF-K membranes was rapid initially, but slowed down and eventually reached a steady state value. Alfrey et al.[102] and Jacques et al.[103] had suggested a method to interpret sorption kinetics where the uptake was assumed to follow

the relationship:

$$M_t = kt^n \qquad (5)$$

where M_t is sorption at time t, and k and n are constants. Geometric constants and the diffusion coefficient are included in k. The slope of a plot of log M_t versus log t is n, which provides information on the sorption mechanism. Diffusive behaviour is expected when n = 0.5, whereas relaxation behaviour is involved when n = 1. n is equal to zero when the equilibrium is reached. Figures 14 and 15 represent such log-log plots for SPSF-Na and SPSF-K membranes, respectively, where the log % water uptake is plotted against log time (hr). Both series of membranes exhibited slopes less than 0.5 and such anomalous, non-Fickian behaviour was also observed[102] in the water uptake by epoxy resin. Noshay and Robeson[6] also observed non-Fickian behaviour of sulfonated polysulfone membranes from the absorption-desorption studies. These authors reported that such non-Fickian behaviour similar to a swelling process increased with greater degrees of sulfonation.

The sorption isotherms of the membranes are given in Figure 16 and 17 for SPSF-Na and SPSF-K series, respectively. The amount of water sorbed per gram of membrane is plotted against the partial pressure of water at

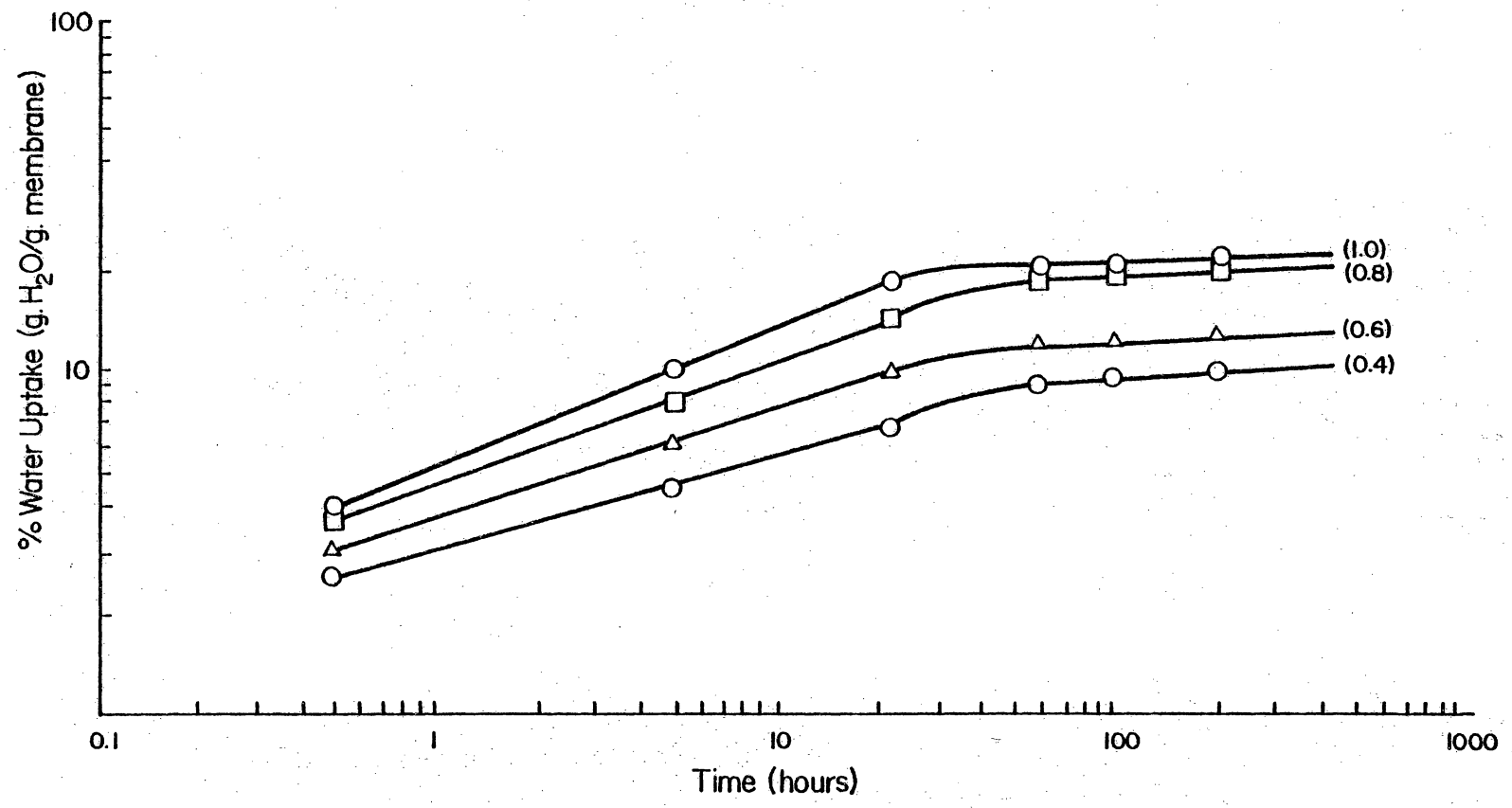

Figure 14. Log-log plot of % water uptake versus time (hour): SPSF-Na at 100% relative humidity.

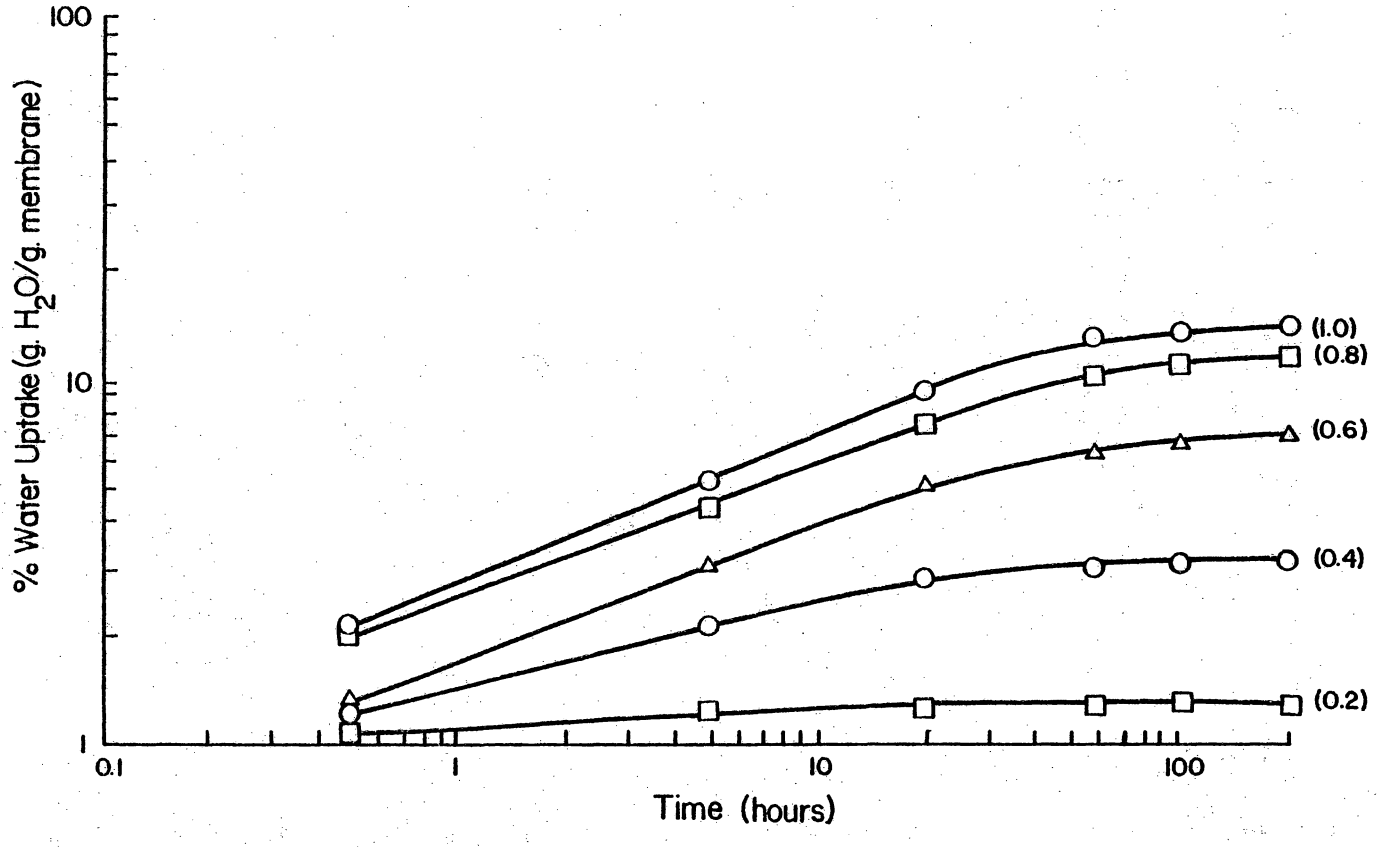

Figure 15. Log-log plot of % water uptake versus time (hour): SPSF-K at 100% relative humidity.

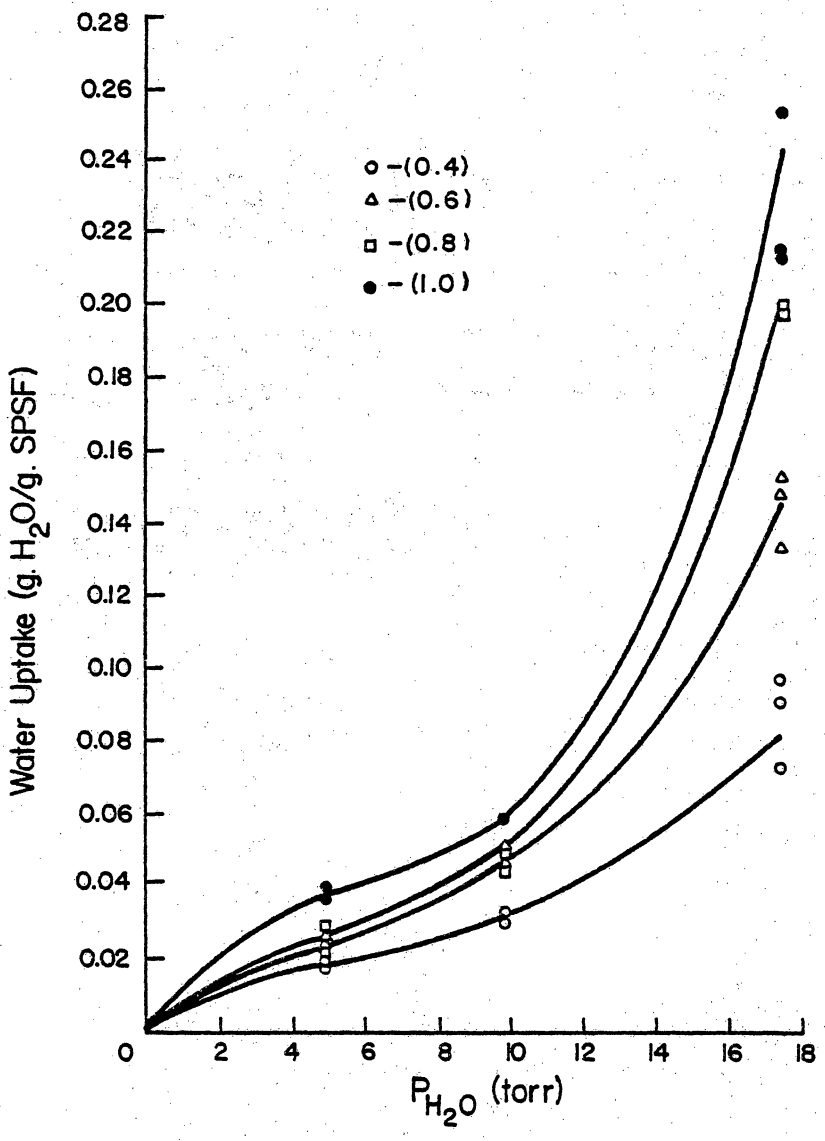

Figure 16. Sorption isotherm of SPSF-Na.

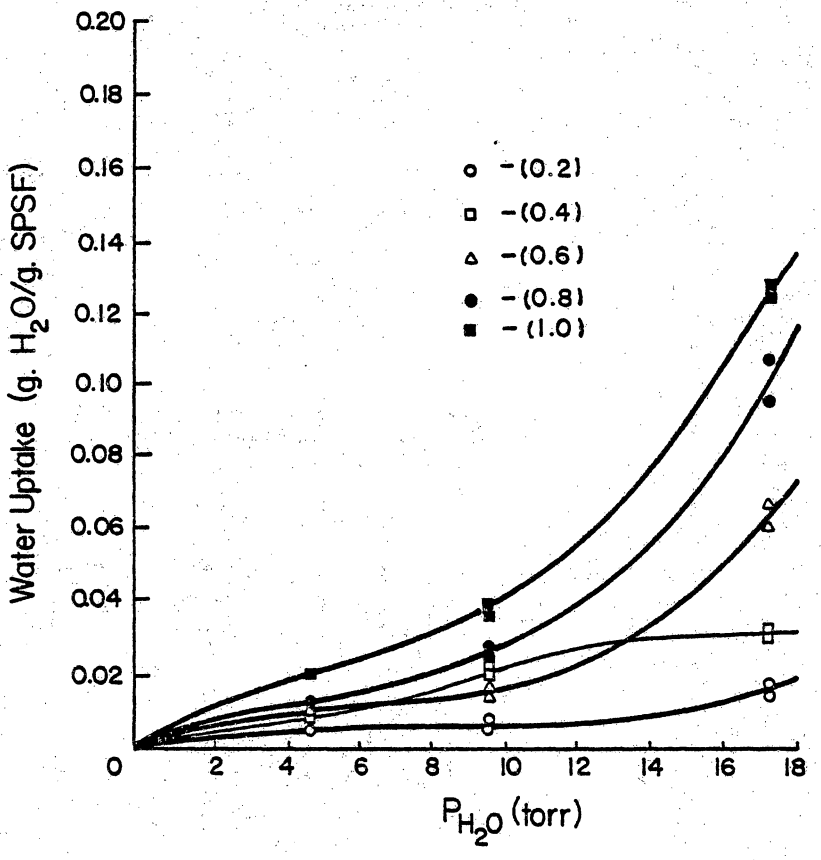

Figure 17. Sorption isotherm of SPSF-K.

different relative humidities. A comparison of the two isotherms indicates the consistently greater uptake of water by SPSF-Na membranes as compared to the SPSF-K membranes. The steep increase in the latter part of the isotherms indicates a possible cooperative sorption process due to the hydrogen bonding between water molecules. The increase may also be a result of swelling, as indicated by the non-Fickian behaviour, as the swelling process will open up more sites for the water to sorb.

In conclusion, sulfonation introduced hydrophilicity into an essentially hydrophobic material, polysulfone. The amount of water sorbed by the sulfonated polysulfone membranes was dependent on the nature of the counter ion. Finally, the mechanism for the water uptake was found to be non-Fickian for all the membranes tested and seems to involve swelling.

C. Contact Angle Analysis

The surface hydrophilicity was investigated by the measurement of the contact angle of water on SPSF membranes. The advancing and receding contact angles of water on polysulfone are listed in Table IX. A total of ten drops were measured for both right and left tangent angles, and the individual readings are listed to show the reproducibility. The average value of 20 readings are 80.1^{o} and 61.2^{o} for the advancing and receding angles, respectively. The drop size was about 0.7 cm in diameter, and the rate of introduction or withdrawal was 1 cc/hr.

Noshay and Robeson[6] reported a slightly lower value of 70^{o} for the advancing angle without any information on the drop size or the rate of application. Good and co-workers,[52,104] however, reported a significant dependency of the contact angles on the size of the droplet. For example, the advancing contact angle of water on Teflon FEP was 100^{o} and 116^{o} for droplets with diameters of 0.3 and 0.7 cm, respectively.

The difference between the advancing and receding angle is usually attributed to hysteresis, which may be caused by surface roughness and/or heterogeneity. A good discussion of hysteresis is given in two review articles.[51,52] Sulfonation introduced hydrophilicity into the polysulfone membranes, and, as a result, water droplets

Table IX.

Advancing and Receding Angles
of Water on Polysulfone (Top Side)

Advancing		Receding	
Left	Right	Left	Right
78.2	78.8	63.9	60.4
82.5	80.7	61.0	61.3
80.5	78.2	60.5	60.1
81.0	80.2	61.8	62.6
80.7	80.3	58.8	60.4
80.2	79.2	62.7	61.0
80.9	80.4	61.8	62.4
80.3	80.5	61.9	60.2
79.2	80.8	60.0	62.1
80.0	80.2	61.2	59.2
80.4 ± 1.1	79.9 ± 0.9	61.4 ± 1.4	61.0 ± 1.1
Ave.	80.1 ± 1.0		61.2 ± 1.3

interacted with the sulfonated polysulfone membranes. Shortly after the introduction of water drops onto the membrane, the membranes started to wrinkle, and this phenomenon was more rapid and extensive with higher degrees of sulfonation. For this reason, advancing and receding angles were not determined on the sulfonated polymer films, but instead, the contact angles of static drops were measured.

The reported values in Table X are the average of ten separate measurements. The "top" column indicates the side of the membrane interfaced with air and the "bottom" refers to the side interfaced with the glass plate during the drying process. Contact angles on the top side of the SPSF-Na series decreased with increasing degrees of sulfonation. This implies that the extent of surface hydrophilicity increases with higher degrees of sulfonation. This general trend was also detected with the SPSF-K series, although the extent of decrease was smaller compared to the SPSF-Na series. This was consistent with the results of the water uptake study in that for a given degree of sulfonation, SPSF-Na membranes had a greater hydrophilic nature than SPSF-K.

No apparent trend was observed for the bottom side of both series of membranes. This may be expected since the bottom side is sensitive to the conditions and

Table X.

Contact Angles of Water on Dense Membranes

	Top	Bottom
PSF	75.1°	73.5
SPSF-Na(0.2)	64.4	34.8
-Na(0.4)	66.4	46.0
-Na(0.6)	39.3	55.3
-Na(0.8)	32.2	41.1
-Na(1.0)	25.5	56.4
SPSF-K(0.2)	71.9	42.0
-K(0.4)	67.8	42.0
-K(0.6)	63.7	29.5
-K(0.8)	69.1	68.1
-K(1.0)	60.3	38.3

Precision: $\pm$ 4.5°

impurities present on the glass plate although the plates were annealed at 600° for 15 hours. Finally, it should be noted that the average value of the contact angle of a static drop of water on polysulfone (listed in Table X) falls between the advancing and receding angles listed in Table IX.

The energetics of the polysulfone membrane surface were characterized by measurement of the critical surface tension (γ_c). The determination of critical surface tension was done in accordance with Zisman's technique by plotting the cosine of the contact angle versus the surface tension of the liquid, as shown in Figure 18. Here, the value of γ_c for polysulfone obtained by extrapolation to zero contact angle ($\cos \theta = 1$) was 43.0 dyne/cm. The initial attempt to obtain γ_c for the sulfonated polysulfone membranes was not completed due to experimental difficulties. The major problem was due to the hydroscopic nature of both the sample and the liquids used, which resulted in film distortion. The γ_c value for cellulose acetate membrane was determined, however, for comparison and was found to be 37.0 dynes/cm. Thus, PSF is more wettable than CA by more liquids.

In summary, the top side of SPSF membranes exhibited greater hydrophilicity with increasing degrees of sulfonation. In addition, the surface of SPSF-Na membranes was more hydrophilic than the surface of SPSF-K membranes for

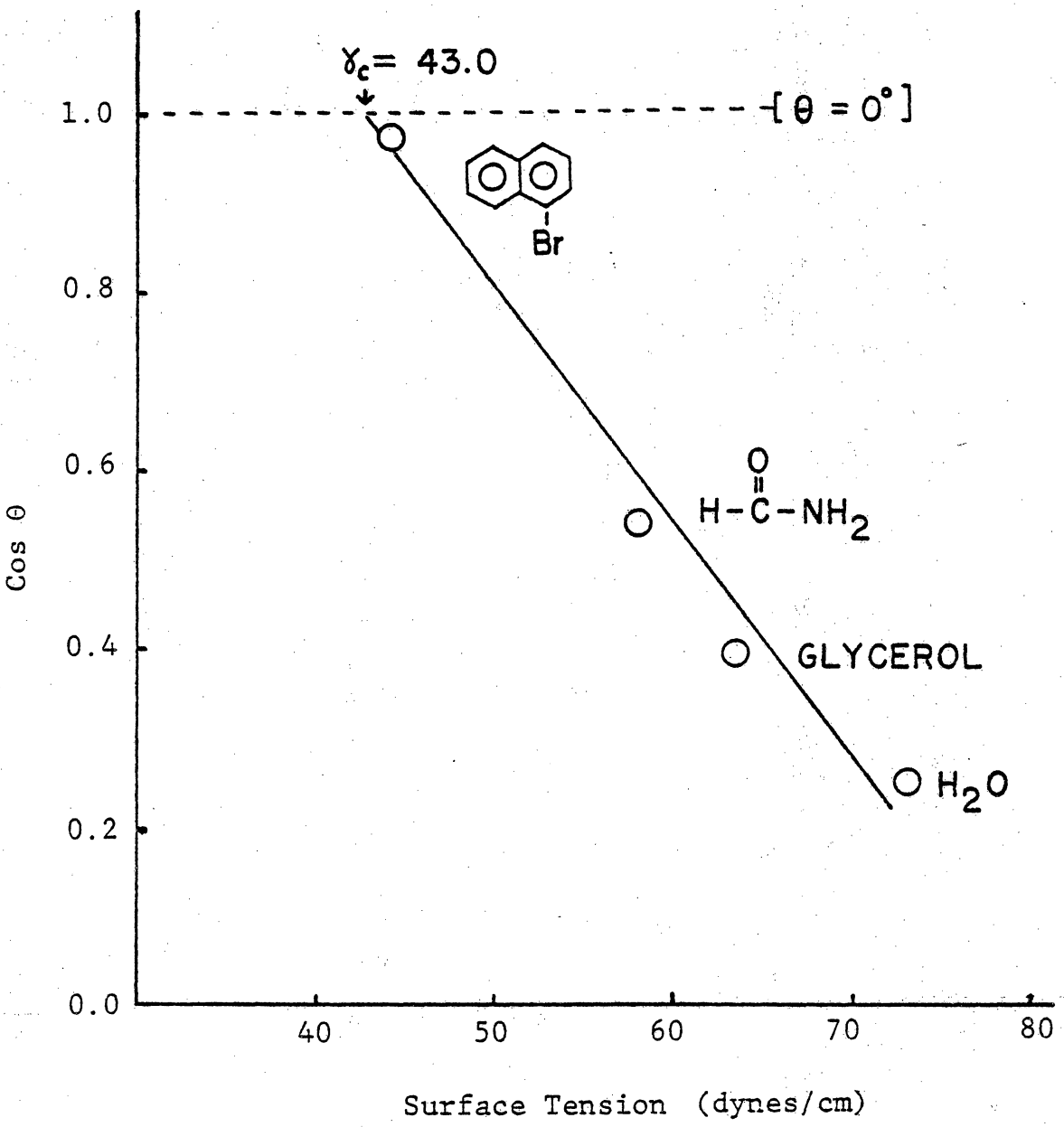

Figure 18. Critical surface tension (γ_c) of PSF membrane.

a given degree of sulfonation. These two observations were consistent with the bulk polymer membrane characteristics as determined from water uptake measurements. Thus, it can be concluded that in terms of hydrophilicity, the surface of SPSF membranes mimics the bulk membrane characteristics.

D. Structural Analysis of Sorbed Water

The structure of water sorbed by SPSF-Na (1.0) membranes was analyzed by near infrared spectroscopy (IR). The application of near IR to study water structure in the combination and overtone region has been reported by Luck.[105] Figure 19 gives the near IR absorption bands obtained with SPSF-Na (1.0) at 100% relative humidity over a period of 24 hours. The constant increase in the peak height, indicating an increase in the amount of sorbed water with respect to time, is in accordance with the result of the water uptake study. Table XI lists the values of the characteristic wavelength (λ_{max}) of the water combination band for bending ν_2 and stretching ν_3 at various temperatures. Within experimental error, λ_{max} did not show any temperature dependence. However, the comaprison of this λ_{max} with that of pure water, also listed in Table XI, indicates an interesting result. The λ_{max} of water in membranes is shifted to a shorter wavelength indicating that the water in SPSF-Na (1.0) has a weaker H-bond system compared to bulk water. A similar observation was made by Luck with cellulose acetate membranes.[83]

Although the present study is only preliminary in regard to the analysis of water structure in a SPSF membrane, it is still encouraging and exciting to obtain results in agreement with other types of membrane studies.

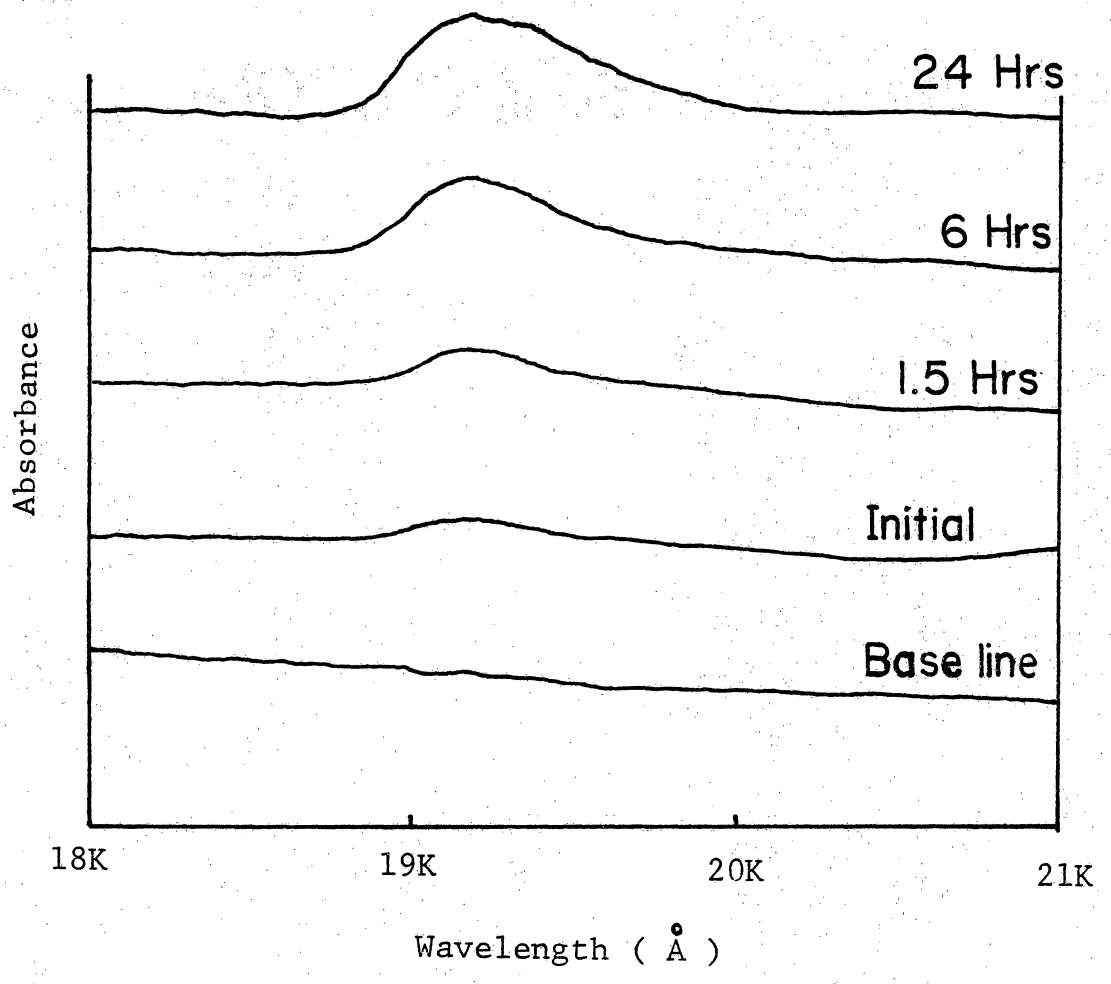

Figure 19. IR absorption band of SPSF-Na (1.0) at 100% relative humidity.

Table XI.

IR Absorption due to Water in SPSF-Na(1.0)

at 100% Relative Humidity

Temperature	λ_{max} (kÅ)
22.0°C	19.19
	19.19
20.0°C	19.19
	19.19
18.0°C	19.19
	19.18
16.0°C	19.18
	19.18
14.0°C	19.19
	19.20
12.0°C	19.19
	19.21
10.0°C	19.20
	19.21
22.0°C	19.19
	19.20
Ave.	19.19 ± 0.01
Pure water	19.31 ± 0.02

E. Electron Spectroscopy for Chemical Analysis

1. ESCA Analysis of SPSF Polymer Powders: ESCA analysis was performed on all SPSF polymers obtained to investigate the presence of any surface contamination and/or to verify the degree of sulfonation (D.S.) of the polymer. Sodium and potassium were detected in the corresponding Na and K salt SPSF polymers. Tables XII and XIII list the composite binding energies (BE) of the S 2s, Na 1s, or K 2p3, and O 1s photoelectron peaks for SPSF-Na and SPSF-K polymers.

In general, a good consistency was observed in the binding energies for the various polymers. A doublet in the Na photoelectron peak was noted for SPSF-Na(0.2) polymers, indicative of two types of Na. The higher binding energy photoelectron peak is probably due to residual sodium introduced into the polymer during the neutralization process. The presence of this residual compound in the polymer may explain the unusually high water uptake observed with the SPSF-Na(0.2) membrane.

Also listed in Tables XII and XIII are the values of the relative atomic ratios of the sulfur photopeak to the sodium or potassium photopeak. As can be noted, the tabulated values did not show any trend with respect to the degree of sulfonation. Furthermore, the values of the

Table XII.

ESCA Analysis of SPSF-Na Polymer Powder

D.S.	B.E. (eV) S 2s	B.E. (eV) Na 1s	B.E. (eV) O 1s	S/Na Exptl.	S/Na Calcd.
0.2	231.8	1073.8 1071.9	533.4	0.96	6
0.4	231.8	1071.6	532.1	1.42	3.5
0.5	231.9	1071.5	532.1	1.90	3.0
0.6	232.0	1071.8	532.2	1.22	2.67
0.8	231.1	1071.6	532.1	1.07	2.25
1.0	231.7	1071.9	531.7	1.49	2.0

Precision: $\pm$ 0.3 eV

Table XIII.

ESCA Analysis of SPSF-K Polymer Powder

D.S.	B.E. (eV) S 2s	B.E. (eV) K 2p3	B.E. (eV) O 1s	S/K Exptl.	S/K Calcd.
0.2	231.9	292.7	532.1	0.72	6
0.4	231.6	292.7	532.0	1.22	3.5
0.6	231.6	292.7	532.4	1.69	2.67
0.8	231.9	292.9	531.7	1.08	2.25
1.0	231.8	293.0	532.2	1.65	2.00

Precision: $\pm$ 0.3 eV

experimental S/Na and S/K ratios are consistently less than the calculated ratios based on the targeted degree of sulfonation listed in the final column. This may be due to the surface heterogeneity of the polymer powders such that the surface composition is different from the bulk composition.

Another reason for the above discrepancies may be the increasing amounts of sorbed water resulting from the increased hydrophilicity for the higher degrees of sulfonation. The nature of sorbed water may be such that it induces the migration of sodium ions to the surface as a result of interaction with SPSF. The nature of sorbed water is discussed in a later section. To verify this possibility, the temperature of the sample probe was raised. For this study, a SPSF-Na(0.5) membrane was employed and since its T_g was determined to be 218°C, the probe temperature was varied from 30° to 150°C.

Table XIV lists values of various atomic fraction ratios as determined by ESCA. The dependence of the atomic ratios on the probe temperature was determined to be minimal, and, thus, the disparate atomic ratios are not likely to be due to sorbed water. The final note in the analysis of polymer powder with ESCA is that the powder surface does not have the same stoichiometry as the bulk, although the explanation of such an observation

Table XIV.

Temperature Dependence of SPSF-Na(0.5) Polymer Powder on ESCA Analysis

Probe Temperature (^{o}C)	S/Na	C/Na	C/S	C/O	O/S
30	1.90	24.6	16.4	4.0	4.2
100	1.50	27.6	18.1	4.3	4.3
150	1.70	31.5	21.5	4.5	4.8

Precision: 15%

cannot be conclusive at this time.

2. ESCA of Dense Membranes: The surface chemical composition of dense membranes was determined using ESCA analysis and the results are tabulated in Tables XV and XVI for the SPSF-Na and SPSF-K membranes, respectively. Atomic fractions of C,S,O, and Na or K for both the top and bottom sides of the membrane are listed in addition to the values of the Na/S and the K/S atomic fraction ratios. Neither the top side nor the bottom side of the membrane showed any dependence of chemical composition on the degree of sulfonation. Therefore, ESCA analysis indicates that the actual degree of sulfonation at the membrane surface does not reflect the bulk degree of sulfonation but is some different value as a result of complex processes, a result similar to that with the polymer powders. These processes may include random orientation of polymer chains during the drying process, and interaction of polymer molecules of varying degrees of sulfonation with the solvent.

3. Comparison of Polymer Powders and Two Sides of Membrane:

The results of the last two sections indicate that the surface composition of polymer powders and membranes is different

Table XV.

ESCA Analysis of the Surface Chemical Composition of SPSF-Na Membranes

Membranes	Sides	Atomic Fractions C	Na	S	O	S/Na
SPSF-Na(0.2)	Top(T)	0.773	0.027	0.027	0.174	1.0
	Bottom(B)	0.754	0.033	0.030	0.183	0.91
(0.4)	T	0.783	0.013	0.026	0.179	2.00
	B	0.759	0.037	0.026	0.178	0.70
(0.5)	T	0.804	0.010	0.026	0.160	2.6
	B	0.719	0.012	0.043	0.228	3.58
(0.6)	T	0.763	0.018	0.033	0.186	1.83
	B	0.699	0.037	0.035	0.230	0.95
(0.8)	T	0.695	0.053	0.051	0.200	0.96
	B	0.648	0.067	0.056	0.229	0.84
(1.0)	T	0.820	0.007	0.030	0.150	4.29
	B	0.719	0.028	0.041	0.212	1.46

Table XVI.

ESCA Analysis of the Surface Chemical Composition of SPSF-K Membranes

Membranes	Sides	Atomic Fractions C	K	S	O	S/K
SPSF-K(0.2)	Top(T)	0.795	0.013	0.022	0.179	1.69
	Bottom(B)	0.723	0.029	0.035	0.214	1.21
(0.4)	T	0.768	0.031	0.028	0.174	0.90
	B	0.730	0.042	0.031	0.197	0.74
(0.6)	T	0.676	0.015	0.022	0.287	1.47
	B	0.878	0.018	0.009	0.094	0.5
(0.8)	T	0.765	0.019	0.028	0.189	1.47
	B	0.689	0.042	0.046	0.224	1.10
(1.0)	T	0.808	0.013	0.039	0.400	3.00
	B	0.847	0.019	0.023	0.111	1.21

from the bulk chemical composition. Through the courtesy of Dr. J. S. Jen of Corning Fiberglas, wide scan ESCA analysis was performed on SPSF-Na(0.5) powders and both sides of the SPSF-Na(0.5) dense membrane. The atomic fractions of the observed elements are tabulated in Table XVII. The Si photoelectron peak noted on the top side of the membrane was significantly reduced by the argon etching process (∿20 Å off), indicative of surface contamination. The Si peak observed on the bottom side of the membrane may be from the glass plate. ESCA was, thus, capable of detecting surface contamination (less than 20 Å thick) on the cast membranes. In general, both polymer powders and membranes had minimal contamination.

4. Angle-Resolved ESCA Analysis: Angle-resolved ESCA analysis enables one to obtain an enhanced surface analysis as shown schematically in Figure 20. Here, θ is the take-off angle, d is the sampling depth, and x is the distance normal from the surface. Since the sampling depth, d, is constant for a given sample, as the take-off angle, θ, decreases, the distance, x, which is equal to $d \cdot \sin \theta$, decreases. Thus, the effective sampling distance from the sample surface decreases resulting in enhanced surface analysis.

Table XVII.

Atomic Fractions of Elements Found in SPSF-Na(0.5) Polymer Powders and Membranes

Sample	Atomic Fractions				
	Na	O	C	S	Si
Polymer Powder	0.0295	0.1636	0.7341	0.0728	0
Membrane - Top	0.0166	0.1807	0.6935	0.0589	0.0503
Top (after 1 min Ar^+ sputtering)	0.0152	0.0326	0.8719	0.0688	0.0113
Membrane - Bottom	0.0235	0.2149	0.6448	0.0720	0.0448

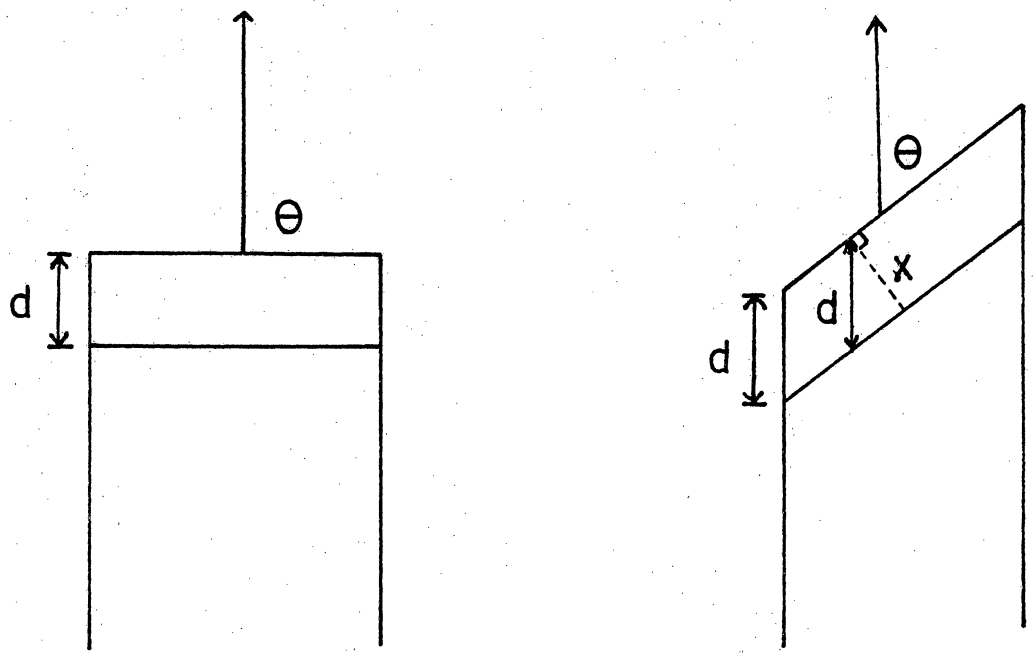

$$x = d \cdot \sin \Theta$$

Figure 20. Angle resolved ESCA.

d : Sampling depth

Θ : Take-off angle

Initially, the effective degree of sulfonation of the membrane surface and its distribution were investigated from the corrected photopeak area ratio of the two types of sulfur photopeak, namely sulfur from SO_2 and sulfur from SO_3^-. Thus, model compounds to obtain the value of the binding energies for the two sulfur peaks from diphenyl-dichlorosulfone and p-toluene sulfonic acid were chosen for $-SO_2-$ and $-SO_3^-$- groups, respectively. The determined binding energies and atomic fractions for the two compounds are tabulated in Table XVIII. Sulfonates ($-SO_3^-$-) have a higher binding energy compared to sulfones ($-SO_2-$) even though the oxidation state of the two sulfurs are both formally +6. This is due to the fact that sulfonates have three electronegative groups (oxygen) compared to two for sulfones. Thus, the sulfur in sulfonate is slightly more positive in nature and, therefore, has a higher binding energy.

The difference between the two sulfur peaks was determined to be 0.3 to 0.4eV. Using this value and a separation of 0.1 to 0.3eV for SO_3 and SO_2 oxygen peaks, the composite sulfur and oxygen peaks for the SPSF-Na(0.5) membrane were curve-fitted. The computer program employed for the curve fitting was GASCAP developed by G. Dulany.[98] Figures 21 and 22 show typical curve-fitted and curve-resolved peaks, respectively. Table XIX lists the curve-resolved

Table XVIII.

ESCA Analysis of Dichloro-diphenyl Sulfone (DDS)

and p-toluene Sulfonic Acid (p-TSA)

	DDS	p-TSA
B.E. (eV)		
S	231.7 ± 0.2	232.0 ± 0.1
Cl	200.1 ± 0.1	
O	531.2 ± 0.1	531.3 ± 0.1
Na		1070.6 ± 0.2
A.F.		
O/Cl	0.9 ± 0.1	
S/Cl	0.33 ± 0.02	
S/O	0.35 ± 0.02	0.33 ± 0.02
S/X		0.61 ± 0.03

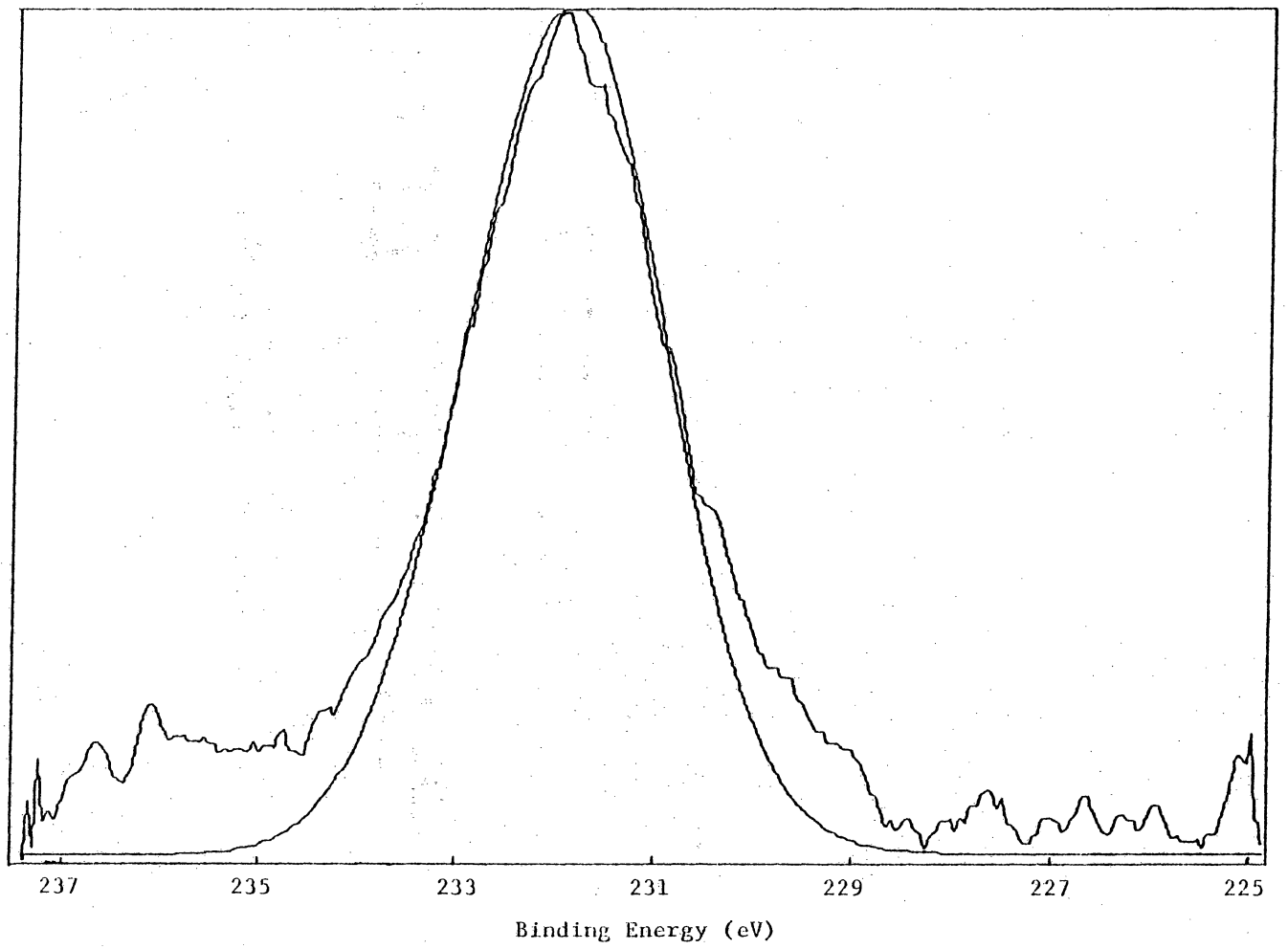

Figure 21. Curve fitted S 2s peak for SPSF-Na (0.5).

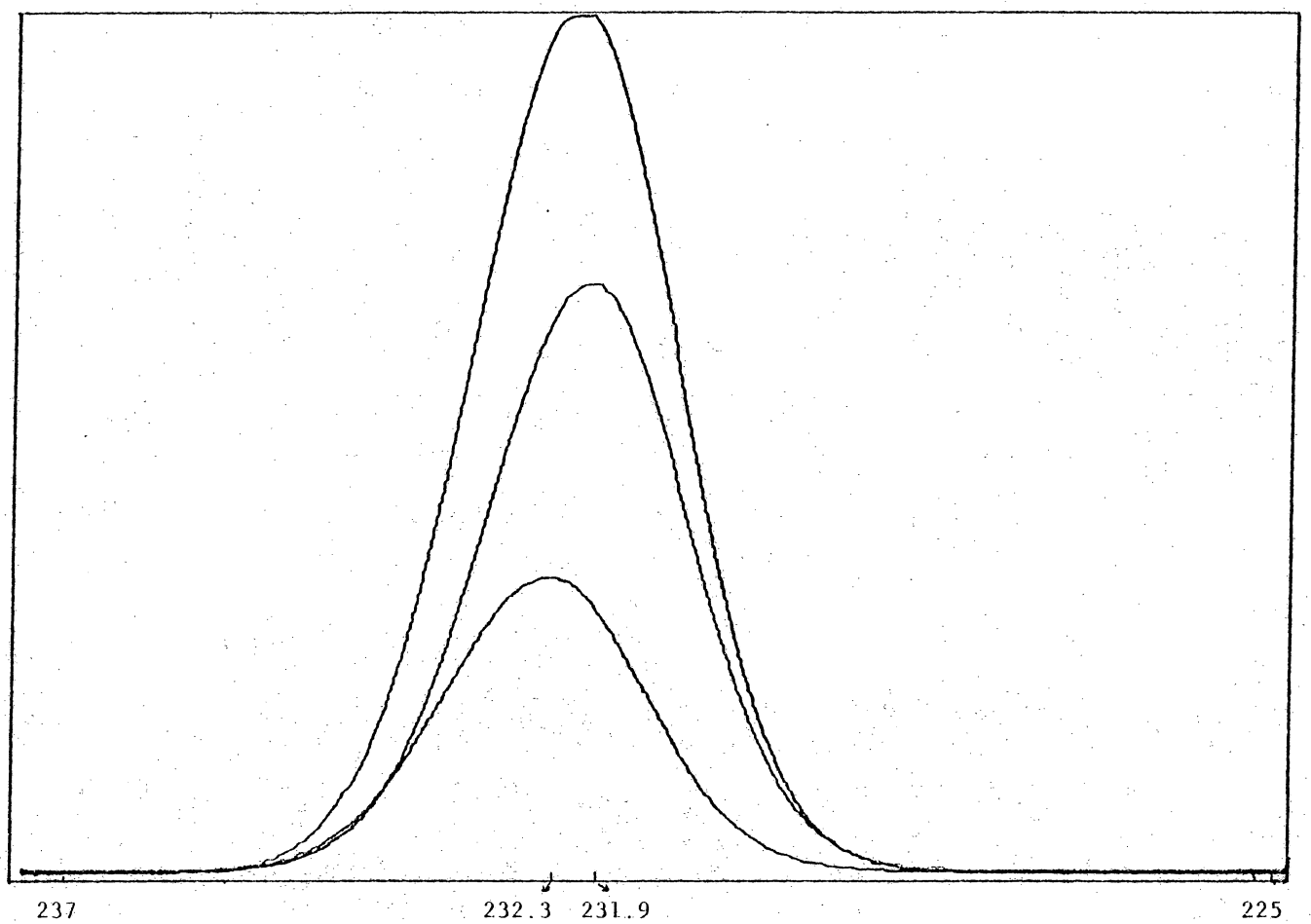

Figure 22. Curve resolved S 2s peak for SPSF-Na (0.5).

Table XIX.

Curve-Resolved ESCA Analysis of SPSF-Na(0.5)

Element		B.E.* (eV)
O 1s	C-O-C	533.7
	$-SO_3X$	532.1
	$-SO_2-$	531.9
S 2s	$-SO_3X$	232.4
	$-SO_2-$	232.0
Na 1s		1072.0

*Background C 1s: 284.6

Precision: $\pm$ 0.3 eV

binding energies for SPSF-Na(0.5). The observed values are consistent with the reported literature values.[106]

The 0.3eV separation between the two peaks, however, was found to be too small to allow a quantitative resolution of the two peaks by the present technique. Figure 23 shows the composite peak of two peaks separated by 0.3eV whose relative ratios were varied between 1:4 and 1:1. It is clear that the fittings are quite close for the two cases and that to retrieve quantitative information from the study may be erroneous.

The information regarding the surface composition compared to the bulk was thus accomplished by considering the angle-resolved total peak areas under the sulfur and the sodium photoelectron peaks.

The experimental and calculated values of the atomic ratios for SPSF-Na(0.5) polymer are compared in Table XX. A good correlation was noted in most cases except where sodium was involved. Calculated values for sodium were about a factor of 1.8 greater in the experimental values. A similar discrepancy of 1.6 was also noted in the case of the sodium salt of p-toluene sulfonic acid used as a model compound (see Table XVIII). The basis for the normalizing factor is not determined at this time, although other inorganic salts also showed such discrepancies, as noted in Table XXI. The present

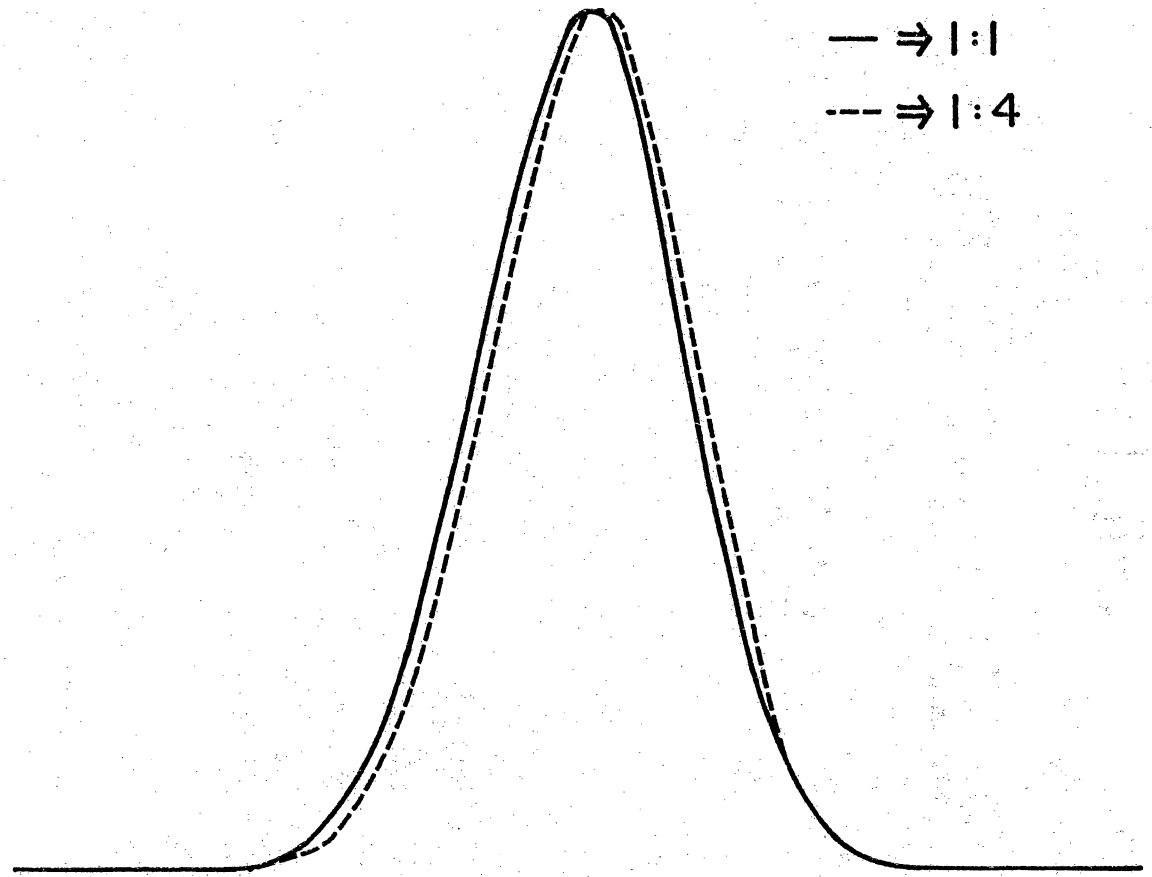

Figure 23. Theoretical composite ESCA peaks of 2 peaks separated by 0.3 eV with varying relative ratios.

Table XX.

Analysis of SPSF-Na(0.5) Polymer with ESCA

Atomic Ratio	Exptl.	Calcd.
S/Na	1.9	3.3
C/O	4.5	3.8
C/S	18.4	19
C/Na	34.0	64
O/S	4.2	4.9

Table XXI.

Atomic Ratios of Various Salts By ESCA

Salt	Uncorrected	Corrected
$NaCl$	Na : Cl 1 : 1	
$K_2Cr_2O_7$	K : Cr : O 2 : 1 : 3.4	1.3 : 1 : 3.5
K_2SO_4	K : S : O 3 : 1 : 4.2	2 : 1 : 4.2
$NaC_2H_3O_2$	Na : O 1.2 : 1	0.8 : 1
Na_2SO_4	Na : S : O 3.4 : 1 : 3.8	2.2 : 1 : 3.8
$Li_2SO_4 \cdot H_2O$	Li : S : O 3.3 : 1 : 3.9	2.2 : 1 : 3.9

discussion will be based on the trend in the values of the atomic ratios.

The result of the 90^{o} normal mode analysis is compared with the surface enhanced 30^{o} electron take-off angle in Table XXII. A change in the atomic ratios was noted only in the decreased values for S/Na and C/Na. This indicates the presence of more sodium on the surface of the polymer powder compared to the bulk. The spatial distribution of elements on the polymer powder is compared with the film in Table XXIII. In contrast to the powder sample, the value of the atomic ratios for the film showed a minimal dependency on the electron take-off angle. This indicates greater chemical homogeneity across the cross-section of the membrane compared to the polymer powders.

Table XXIV compares the cross-sectional chemical distribution between SPSF-Na and SPSF-K membranes. Unlike SPSF-Na membranes, the relative concentration of counter ions on the surface decreased in SPSF-K, as evidenced by the increased values in S/X and C/X ratios. Such enhanced concentration of sodium ions on the SPSF-Na membrane surface, when compared to the SPSF-K membrane surface, may explain the greater surface hydrophilicity of SPSF-Na membranes determined by the water uptake and by the water contact angle measurements.

Based on the angle-resolved ESCA analysis, the

Table XXII.

Depth Profile of SPSF-Na(0.5) Polymer with ESCA

Atomic Ratio	90^{o}	30^{o}	
S/Na	1.9 ± 0.2	0.7 ± 0.1	(3.3)*
C/O	4.5 ± 0.9	4.7 ± 0.5	(3.8)
C/S	18.4 ± 0.9	18.9 ± 1.9	(19)
C/Na	34.0 ± 3.8	13.7 ± 2.4	(64)
O/S	4.2 ± 0.8	4.0 ± 0.5	(4.9)

*Calculated values

Precision: 15%

Table XXIII.

Comparison of Polymer Powder and Film Surface Composition with ESCA: SPSF-Na(0.5)

	Powder		Film	
	90°	30°	90°	30°
S/Na	1.9	0.7	2.3	1.7
C/O	4.5	4.7	3.7	4.5
C/S	18.4	18.9	20.4	21.2
C/Na	34.0	13.7	45.5	35.6
O/S	4.2	4.0	5.5	4.8

Precision: $\pm$ 15 %

Table XXIV.

Comparison of Angle-Resolved ESCA of SPSF-Na and SPSF-K Membranes

	SPSF-Na(0.5)		SPSF-Na(1.0)		SPSF-K(0.6)		SPSF-K(1.0)	
	90°	30°	90°	30°	90°	30°	90°	30°
S/X	2.3	1.7	4.7	.65	1.4	2.8	3.0	6.6
C/O	3.7	4.5	4.0	3.9	3.8	4.9	5.8	5.5
C/S	20.4	21.2	11.3	15.7	27.6	35.0	20.7	24.6
C/X	45.9	35.6	52.6	10.1	37.8	96.6	62.1	162.6
O/S	5.5	4.8	2.8	4.0	7.3	7.19	3.6	4.5

X : Na or K

Precision: ± 15 %

following conclusions can be made. Firstly, the polymer powder surface composition is more heterogeneous compared to the surface of cast membranes. Secondly, the counter ion concentration on the surface is greater for SPSF-Na membranes compared to SPSF-K membranes in accordance with the lower contact angles of water and higher water uptake capacity for SPSF-Na membranes.

F. ESCA Analysis of Asymmetric Reverse Osmosis Membranes

Reverse osmosis membranes, before and after use in the desalination test cell, were analyzed by ESCA. Also, membranes having different fluxes and separation efficiencies were analyzed to examine any apparent differences. The test membranes were dried in air prior to ESCA analysis. Table XXV lists the binding energy (BE) and the atomic fraction (AF) for the membranes studied. In all cases, a very good consistency was found in the BE values. Membrane (1) gave practically no flux, whereas membrane (2) showed good flux in one case and not in the other, although they were cut from the same sheet of membrane.

In general, no significant differences in the ESCA parameters were noted between any of the membranes investigated. The relatively high sulfur AF for unused membrane (2) and the high oxygen AF for membrane (2), which gave a good flux, is noteworthy, however. Wide scan ESCA spectra were obtained on membranes that gave a good and a bad flux in the desalination cell. The results are tabulated in Table XXVI. In addition to carbon, oxygen, sodium, and sulfur, which were expected, small peaks attributed to nitrogen and silicon may be due to contamination, although the overall level of contamination was minimal. A peak at 51.4 eV could not be identified.

Table XXV.

ESCA Results of Asymmetric SPSF-Na(0.5) Membranes

Before and After Use in the Desalination Test Cell

Membrane	Sample		B.E. Na 1s	B.E. S 2s	B.E. O 1s	A.F. Na	A.F. S	A.F. O	A.F. C	Flux g/hr(25°C)	Sep'n %
1	Unused	-T	1071.5	231.9	532.2	0.002	0.010	0.184	0.803		
		-B	1071.6	231.8	532.4	0.002	0.008	0.181	0.809		
	used	-T	1071.5	231.7	532.2	0.001	0.004	0.138	0.857	0.1108	~50
		-B	1071.5	232.0	532.2	0.003	0.012	0.182	0.804		
2	Unused	-T	1071.5	231.8	532.0	0.002	0.028	0.162	0.809		
		-B	1071.6	231.7	532.2	0.002	0.026	0.156	0.816		
	Used (Good flux)	-T	1071.9	232.1	532.2	0.004	0.014	0.300	0.682	1365	0
		-B	1071.5	232.0	532.1	0.005	0.012	0.196	0.787		
	Used (Bad flux)	-T	1071.6	232.0	532.2	0.003	0.017	0.189	0.790	<.5	
		-B	1071.3	231.7	531.8	0.002	0.015	0.169	0.814		

Table XXVI.

Wide Scan ESCA Results on Reverse Osmosis Membranes

Sample	C 1s	O 1s		N 1s		Na 2s		S 2s		Si 2p1,3		
	A.F.	B.E.	A.F.	B.E.	A.F.	B.E.	A.F.	B.E.	A.F.	B.E.	A.F.	B.E.
Bad Flux												
Top	0.721	532.1	0.196	399.7	0.040	63.4	0.018	231.8	0.015	102.3	0.010	51.4
Bottom	0.787	532.2	0.105	399.7	0.020	63.4	0.016	231.9	0.012	102.7	0.013	51.2
Good Flux												
Top	0.798	532.2	0.129	399.7	0.023	264.0*	0.008	231.7	1.005	102.2	0.036	51.2
Bottom	0.751	532.2	0.181	399.7	0.019	63.3	0.019	232.0	0.017	102.5	0.014	51.4

*Na Auger line (KLL)

In conclusion, the performance of the reverse osmosis membrane cannot be explained by the ESCA analysis based on the present study. Similarities in the surface chemical composition of the membranes discussed indicate that some other factors are more influential in determining the membrane performance - at least at this stage. Probable factors may be physical homogeneity and reproducibility of the prepared membranes.

G. Ion Exchange Capacity

The ion exchange capacity (IEC) of asymmetric SPSF-Na and SPSF-K membranes was investigated. It is of great importance to understand the IEC of the membranes since the actual desalination process involves solutions of various electrolytes with sodium chloride as the major component. In addition, the information of the IEC may be useful in both the synthesis and the membrane fabrication process. For example, if one type of salt form is easier to produce or handle, then the material so available may easily be ion exchanged to a salt with a different counter ion in the final step to yield the desired salt form.

Initially, 0.1% KCl and NaCl solutions showed an absence of Na and K, respectively. However, after being equilibrated with SPSF-Na and SPSF-K, respectively, a significant level of Na and K were detected in the solution by atomic absorption spectroscopy. The extent of ion exchange was calculated based on the weight % of salt per gram of each polymer membrane, and was found to be about 78% for SPSF-Na(0.5) and about 76% for SPSF-K

In terms of an equivalence number, the IEC is 0.822 meq/g and 0.929 meq/g for the SPSF-Na(0.5) and SPSF-K(0.6), respectively. These values are in good agreement with the results obtained by Brousse *et al*[8]. They employed the

IEC as a means of identifying various sulfonated polysulfones, and it ranged from 0.635 to 1.020meq/g obtained by titration. It is reasonable to assume that since 0.5 and 0.6 degrees of sulfonation are the mid-degrees of sulfonation, the ion exchange capacity would also be in the mid-range of about 0.800 meq/g. Noshay and Robeson[6], employing the titration method of Fisher and Kunin,[107] reported a value of 1.15meq/g for SPSF-Na(0.5) which is slightly higher than the present results.

Dried membranes, after the ion exchange study, were analyzed by NAA and the result was 92% exchange for SPSF-Na and 63% for SPSF-K. The overall exchange of about 80% was greater than expected. The ESCA analysis provides additional support for extensive ion exchange. Figure 24 shows the ESCA spectra of the Na 1s and K 1s photoelectron peaks for SPSF-Na(0.5) before (A, B) and after (C, D) the ion exchange study. A very strong Na 1s peak (A) is seen initially at an attenuation of 1K. Since the polymer is the Na salt, there was no K photoelectron peak (B) present initially. The small peak observed was the $\pi^* \leftarrow \pi$ transition of the carbon shake-up peak. After the ion exchange, the Na photoelectron peak (C) decreased significantly. Note not only the decrease in intensity, but the fact that the attenuation is only 500. In addition, a strong K photoelectron peak is observed (D). The two peaks are

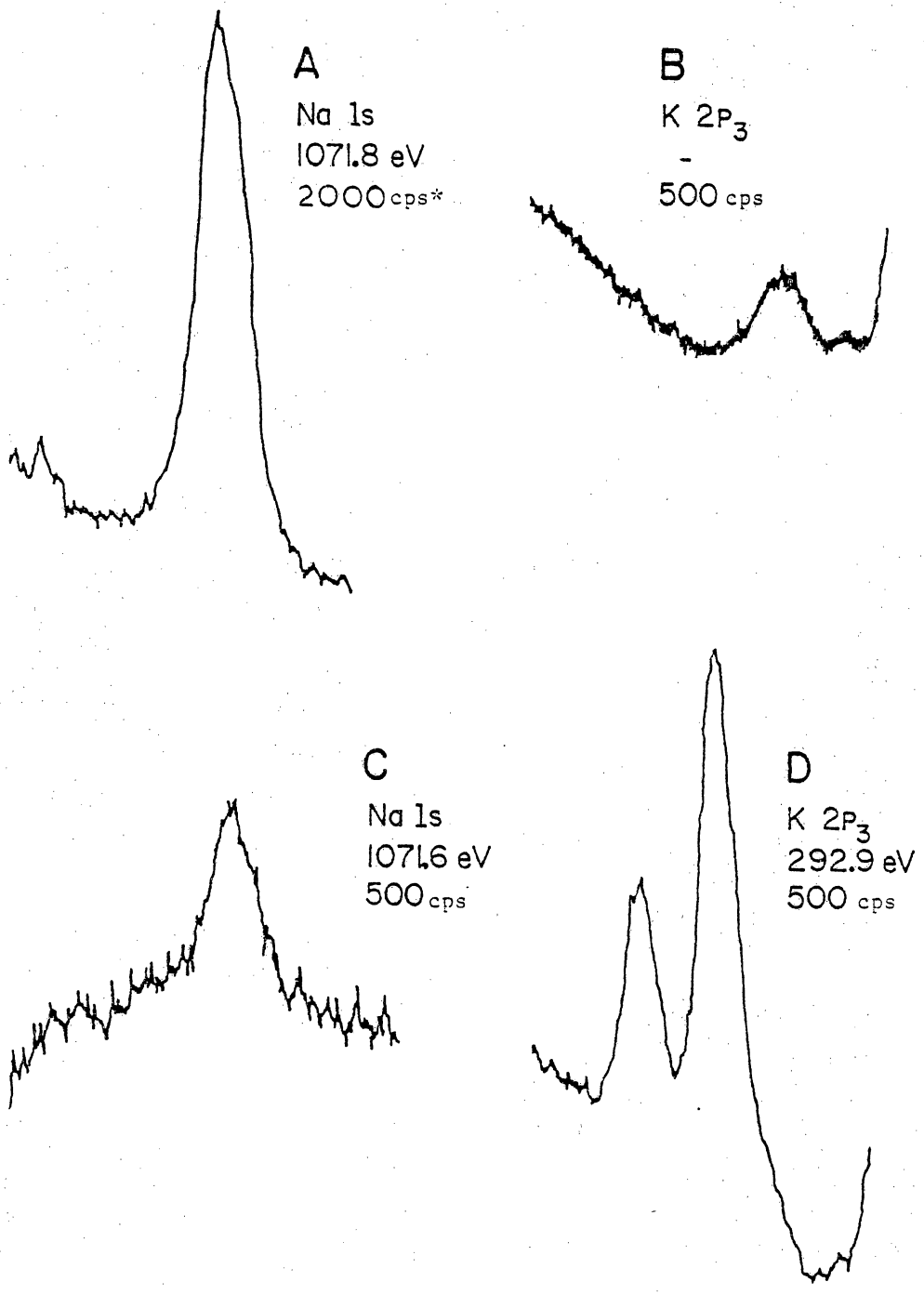

Figure 24. Photoelectron peaks of Na and K in SPSF-Na (0.5) before (A,B) and after (C,D) the ion exchange study.

*cps : counts per second

for the 2p1 and 2p3 photoelectron peaks. Combining the results of ESCA, NAA, and AA, the ion exchange process does not occur just at the membrane surface but throughout the bulk of the membrane.

H. Electrical Properties of Dense Membranes

1. Transient Current in NaCl (aq) System: The voltage response of dense SPSF-Na (0.5) membranes to constant direct current showed a "square pulse-like" increase in the overvoltage as shown in Figure 25. The term 'overvoltage implies the membrane potential difference (MPD) which is the potential difference across the membrane as a result of applied current. Thus the MPD used in this study is different from the intrinsic membrane potential. The intrinsic membrane potential of SPSF membranes was less than 2 mV. The observed shape of the curve was similar for both directions of the applied current. This supports the symmetric nature of the dense membrane across the current conducting channels.

Further, the shape of the curve was independent of the magnitude of current density and the temperature of the system. This is in contrast to the results of a similar study performed on a biological membrane,[108] the gastrointestinal epithelium, or the stomach of a frog. The difference may be due to the sensitivity of an active membrane to temperature. The SPSF-Na membranes have good thermal stability and thus are not likely to show any sensitivity to a temperature variation between 9^{o} and $30^{o}C$.

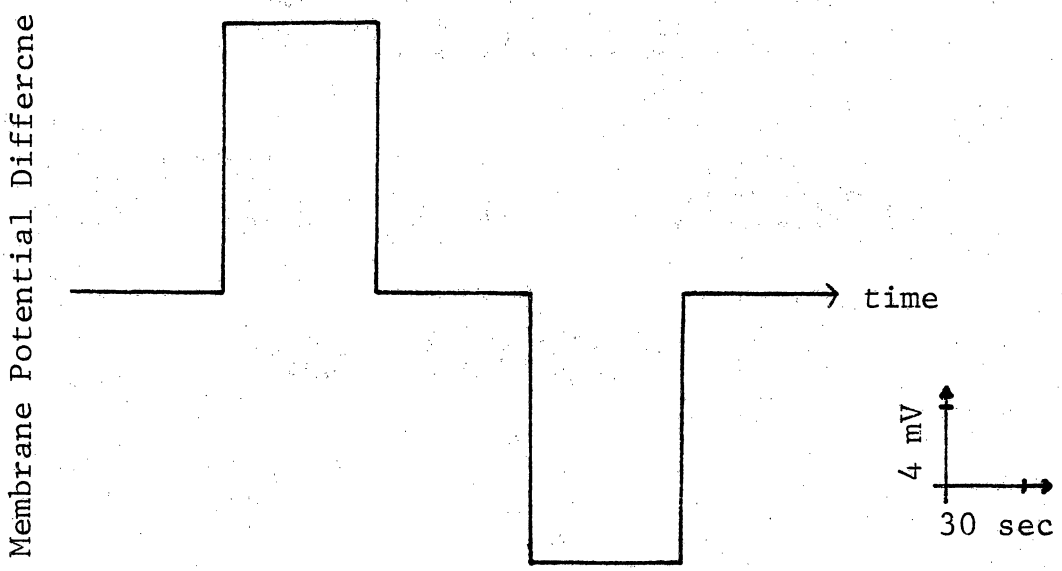

Figure 25. Overvoltage response to 0.5 μA current density in NaCl(aq)/SPSF-Na (0.5)/NaCl(aq) system.

The values for the MPD due to the various current densities applied for a period of 1 minute are plotted as a function of the magnitude of the applied current in Figure 26. Here, it is clear that the NaCl/membrane NaCl system followed ohmic behaviour to a reasonable extent, although a slight deviation was observed at current greater than 40 μA.

The effect of temperature of this ohmic behaviour was also investigated and the result is shown in Figure 27. Again, the MPD is plotted against the current, and, as it can be seen, for a given current density, the MPD increased as the temperature of the system decreased. Good linearity was observed for each temperature studied.

2. Transient Current in Other Electrolyte Systems: The electrolyte system was varied to investigate the nature of the current-carrying ions. Because the initial approach was to change the size of the cation, NaCl(aq) was first replaced by choline chloride(aq). In this system, a significantly greater resistance was observed as compared to the NaCl(aq) system, as shown in Figure 28. This figure includes results obtained from four different systems, namely choline chloride/membrane/choline chloride, NaCl/membrane/choline chloride, choline chloride/

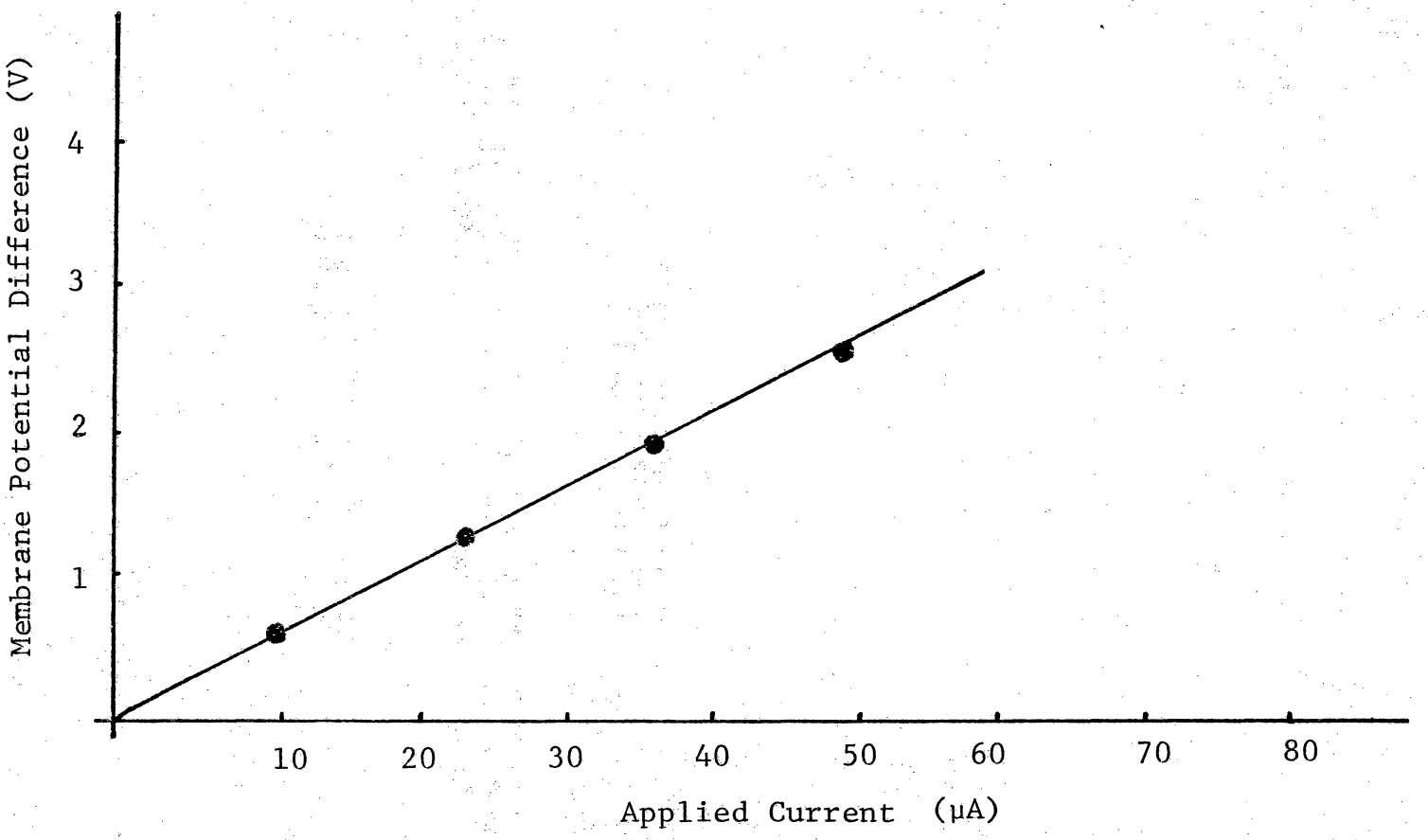

Figure 26. The study of ohmic behaviour of SPSF-Na (0.5) at 23°C for NaCl(aq) system.

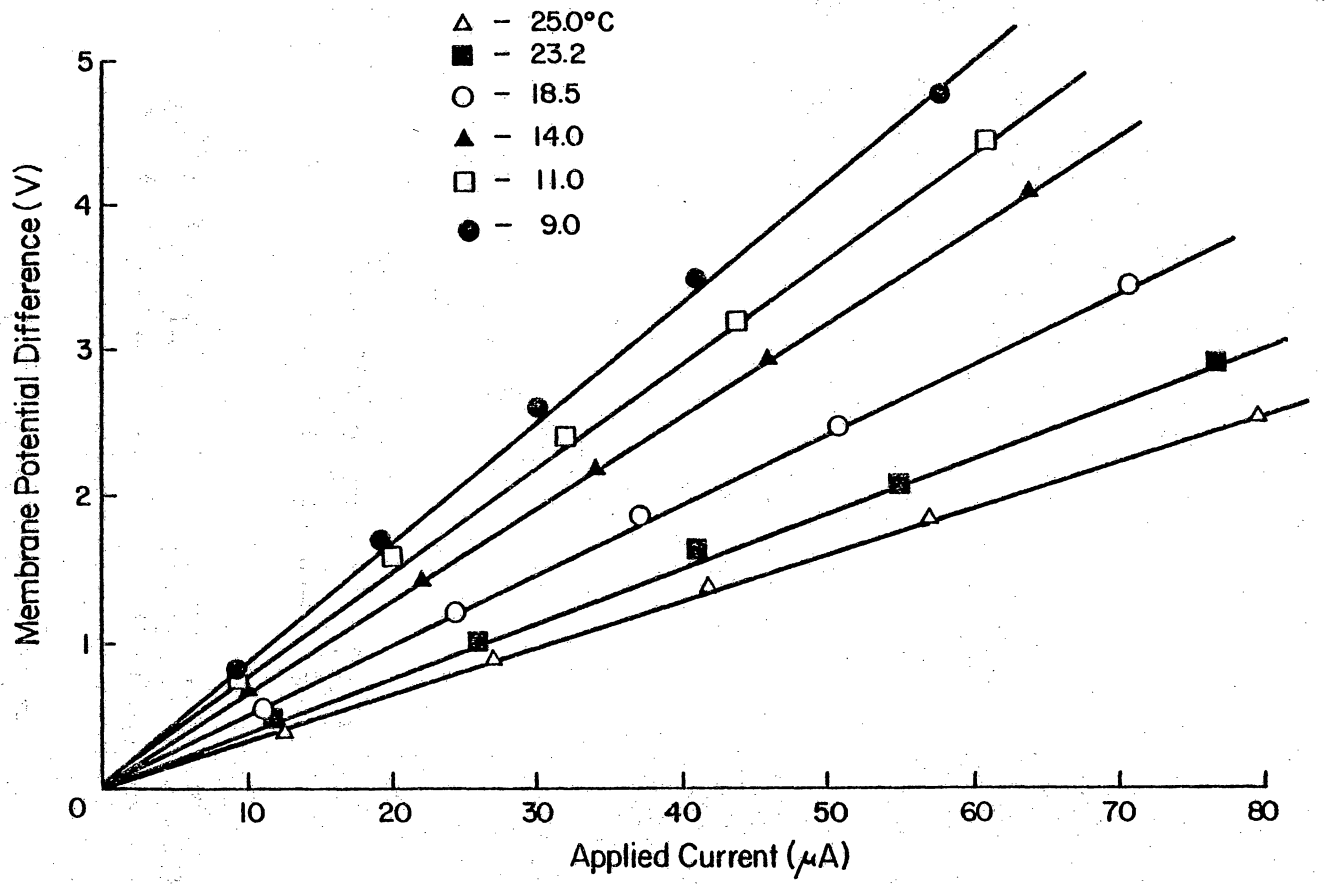

Figure 27. Temperature dependence of membrane potential difference: SPSF-Na (0.5).

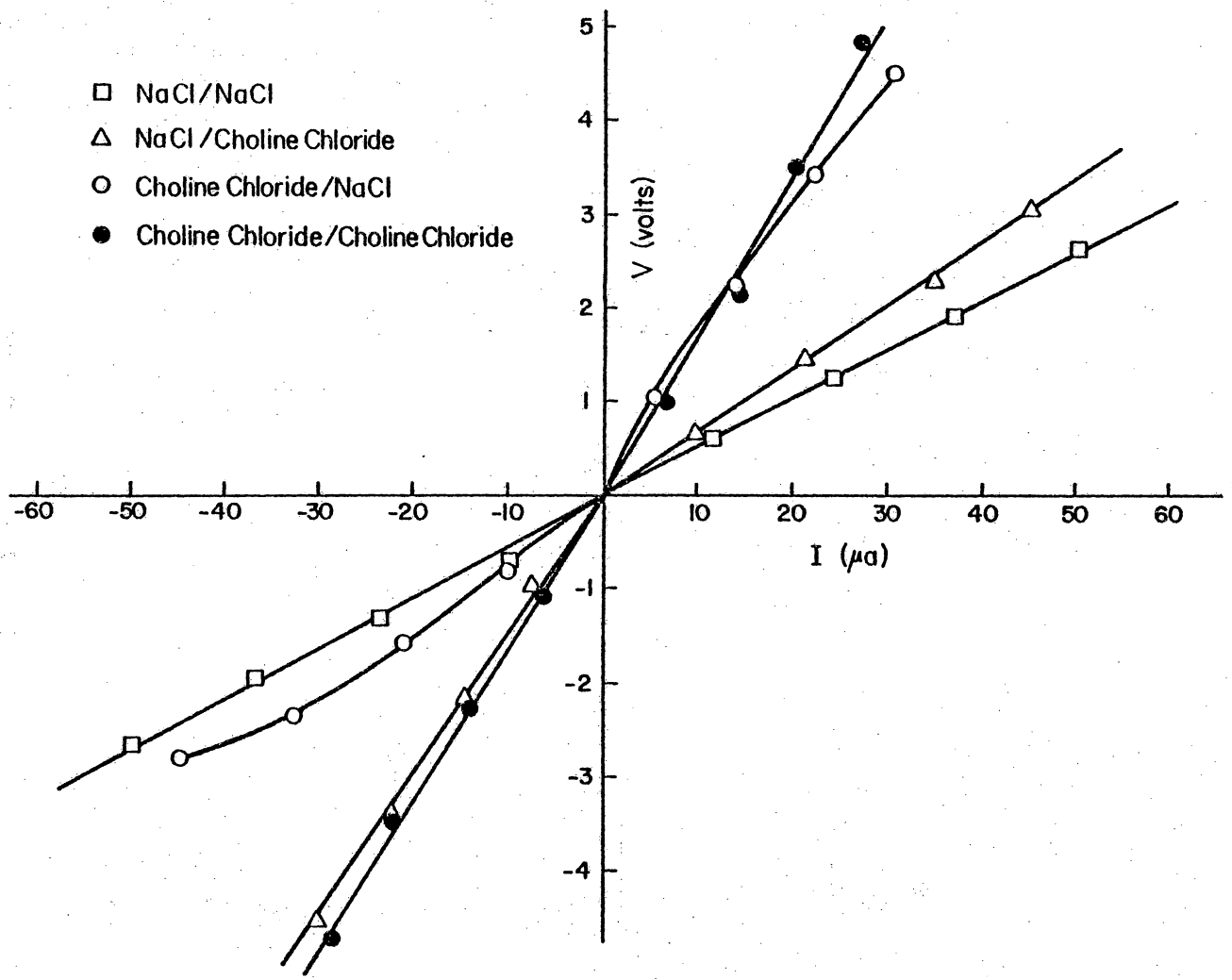

Figure 28. Membrane potential difference for NaCl and choline chloride systems: SPSF-Na (0.5)

membrane/NaCl, and finally, NaCl/membrane/NaCl as a comparison. It is also important to note at this point that the first quadrant represents the system when the current is passed from the left-hand chamber through the membrane to the right-hand chamber. The reverse current direction is plotted in the third quadrant.

A comparison of the NaCl/membrane/NaCl system and the choline chloride/membrane/choline chloride system in the first quadrant indicates a 3-fold increase in the MPD for the latter system. For the NaCl/membrane/choline chloride system, the positive direction of applied current induces the migration of Na^+ ions across the membrane from left to right and of Cl^- ions from the right to the left. Thus, in principle, the transport phenomenon in this system is similar to the NaCl/membrane/NaCl system. This was indeed the case and the MPD approximated the values obtained for the NaCl/membrane/NaCl system as shown in Figure 28. By the same token, the plot of the MPD for the choline chloride/membrane/NaCl system was about the same as for the choline chloride/membrane/choline chloride system. The same results were obtained with the reverse current as shown in the third quadrant. Thus both the NaCl/membrane/NaCl and choline chloride/membrane/choline were symmetrical across the origin whereas the NaCl/mem-

brane/choline chloride and choline chloride/membrane/NaCl systems showed a break at the origin showing a dependency of the current direction. It can be concluded that the resistance of the system was affected by the nature of the cations.

The effect of the anion was investigated by using $NaClO_3$(aq) and the results are given in Figure 29. Again, four types of systems were considered: $NaClO_3$/membrane/$NaClO_3$, NaCl/membrane/$NaClO_3$, $NaClO_3$/membrane/NaCl, and NaCl/membrane/NaCl. As is clearly shown in Figure 29, however, the electrical behaviour was indifferent to the change in the nature of the anion. In conclusion, therefore, the effect of the cations and the anions on the electrical resistance indicated that the cations play an important role in the ion transport process through the current-carrying channel, although the transport mechanism needs to be investigated further.

3. Activation Energies ($E_a^{\neq}$) for Ion Transport:

The activation energies for the ion transport process were calculated on the basis of Arrhenius' law, namely:

$$\underline{R} = A\, e^{E_a^{\neq}/RT} \quad [109,110] \qquad (6)$$

where $\underline{R}$ is the resistance, $E_a^{\neq}$ is the activation energy,

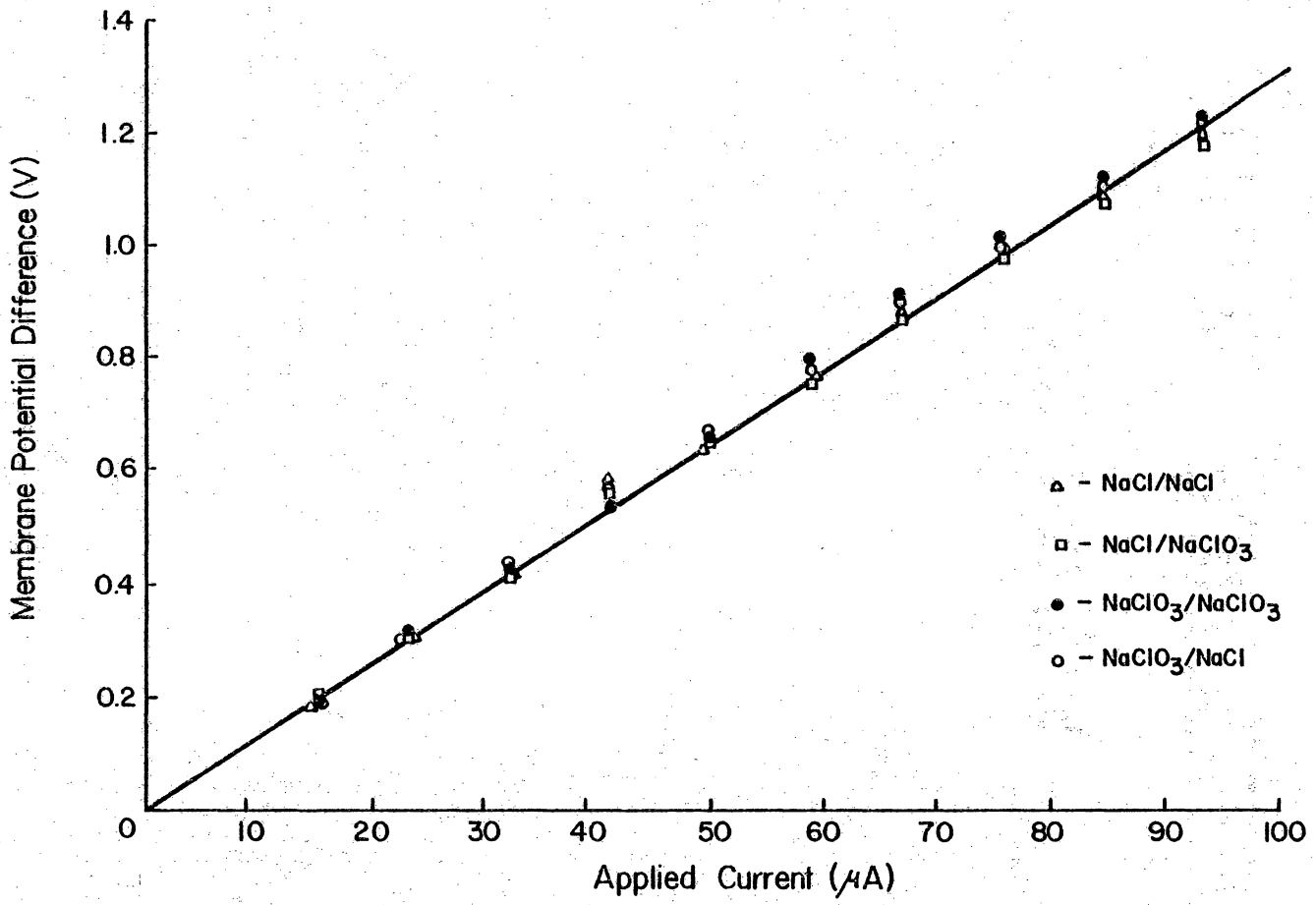

Figure 29. Membrane potential difference for NaCl and $NaClO_3$ systems: SPSF-Na (0.5).

R is the gas constant, T is the Kelvin temperature, and A is a constant. Therefore, in this study, the natural log of resistance was plotted against 1/T to obtain the value of $E_a^{\neq}$ which would be the slope of a plot such as that shown in Figure 30. The system plotted is for SPSF-Na(0.5) in NaCl solution, and a relatively linear Arrhenius plot was obtained for temperatures between 40 and 9°C with a possible break at ~18°C. This is quite different from the results obtained with the gastrointestinal epithelium[108], where a distinct break in the curve was observed in the vicinity of 16°C,

This break in the Arrhenius plot around 16°C, which indicates a change in the activation energy, has been observed in other systems, including the surface tension of water[111], and many biological systems.[112] By simple deduction, it can be concluded that the common factor between all of the above systems is water, and the extreme sensitivity of the active biological membrane to the structural changes of water may be reflected in the sharp break in the Arrhenius plot. It is understandable, then, that a thermally stable, inactive SPSF membrane would be relatively insensitive to the water structure and show a very small, if any, break in the Arrhenius plot.

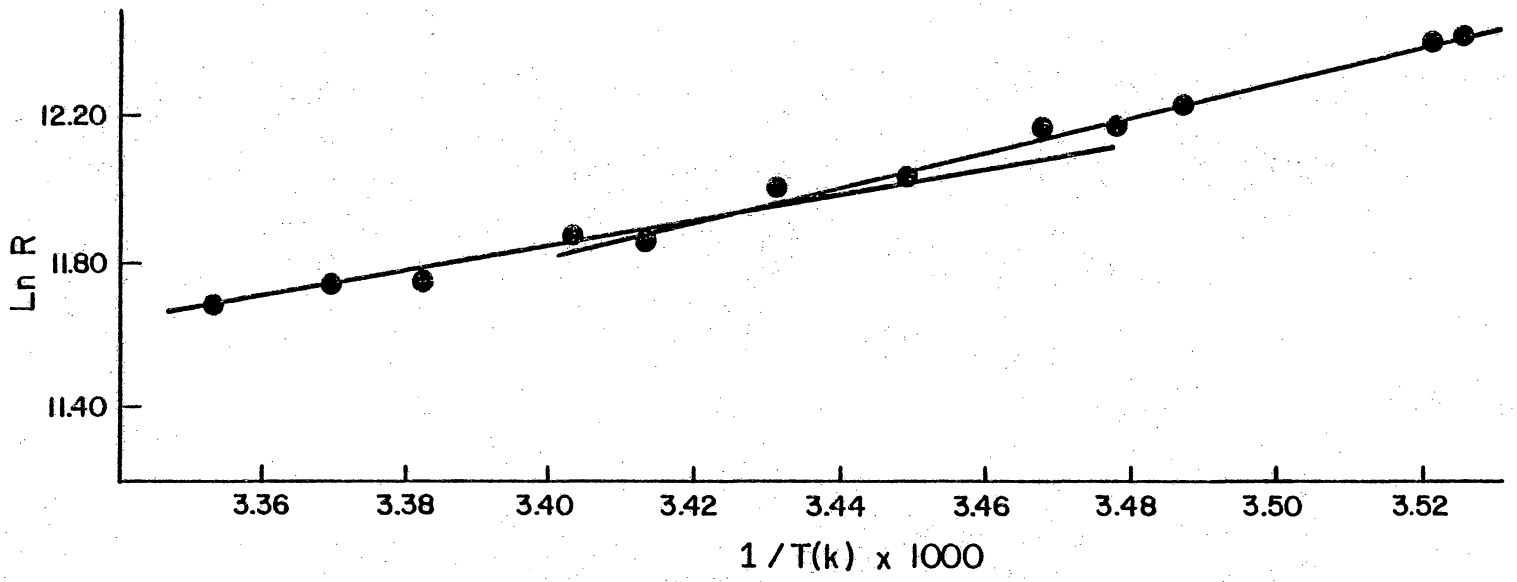

Figure 30. Arrhenius plot of SPSF-Na (0.5) in NaCl system.

The effects of membrane thickness and various electrolyte systems on the magnitude of the $E_a^{\neq}$ were also investigated. The three thicknesses of cast SPSF-Na(0.5) membranes used were 8, 12, and 16 mil. The thickness of the dried membranes were 0.57, 0.98, and 1.4 mil, respectively.

The activation energies for the three membranes are tabulated in Table XXVII. These values for the activation energies compare well with the activation energies of desalination of SPSF membranes (8 to 10 kcal/mole) reported by Vinnikova and Tanny.[113] It is interesting to note that the value of $E_a^{\neq}$ remained relatively constant for all three thicknesses. Such results indirectly indicate that the transport of ions across the membrane is not dependent on the membrane thickness, and that the energy barrier for the process is similar for the different thicknesses for the membrane investigated. It appears, then, that the main contribution to the energy barrier is the initial interaction of ions with the membrane at the membrane/solution interface. Obviously, this initial step is present in any membrane, and, thus, the secondary step of ion transport within the membrane either contributes much less to the process or has the same $E_a^{\neq}$ value regardless of the membrane thickness.

Table XXVII.

Activation Energies ($E_a^{\neq}$) of SPSF-Na(0.5) Membranes at i = 0.5 μA in NaCl(aq) Systems

Thickness		
Cast (mil)	Dry (mil)	$E_a^{\neq}$ (kcal/mole)
8	0.57	8.7 ± 0.8
12	0.98	9.2 ± 0.1
16	1.4	9.4 ± 0.1

Table XXVIII lists the effect of the nature of the electrolytes on the activation energy. Although the resistances were higher for $MgCl_2$(aq) and choline chloride (aq) systems as compared to NaCl(aq), the value of $E_a^{\neq}$ was about the same. This rather surprising result may be interpreted as follows: The average value of $E_a^{\neq}$ for ion transport across the SPSF-Na(0.5) membrane was found to be around 9 kcal independent of the membrane thickness and the nature of the electrolyte solution. Comparison of this $E_a^{\neq}$ value to the value of 13 kcal[114] for the disruption of bound water indicates that the ion transport process may involve the breakage of bound water. In addition, similarities in the energy barrier for the NaCl. and $MgCl_2$ systems can be interpreted as having similar transport mechanisms.

The notably lower activation energies for the choline chloride system can be understood as follows: Choline ions, being relatively large ions, may not pass through the membrane channel. Thus, the energy barrier for the choline transport process can be regarded as infinite. Then, the actual conduction process must be carried out by the chloride ion or breaking free water. This model is supported indirectly by making the comparison that the activation energy of free water disturbance by electrolyte is 3.3 kcal/mole[114].

Table XXVIII.

Effect of Electrolytes on $E_a^{\neq}$ of 8 mil SPSF-Na(0.5) Membrane

System	$E_a^{\neq}$ (kcal/mole)
NaCl / NaCl	9.2
$MgCl_2$ / $MgCl_2$	8.6
ChCl/ChCl*	2.4
3.5% NaCl solution resistance	3.3

*ChCl : Choline Chloride

Precision: 20%

4. Model of the Current-Carrying Channel: This investigation was performed by analyzing the shapes of the voltage response to a series of transient current pulses of 50 μA. The system studied was NaCl/membrane/choline chloride. Figure 31 shows the trace of the voltage response to 3 sequential current pulses from the left chamber to the right (positive current), followed by another 3 pulses in the reverse direction (negative current).

The initial pulse in the positive direction showed an instantaneous spike which decreased and then reached a plateau. The values listed by each spike are the overvoltage. By the second and third pulses, the magnitude of the spike decreased further and the height of the voltage response also decreased.

The negative current induced an 'exponential-like' shape, and the height of the response increased with the series. It should be noted here that the positive current induced migration of Na^+ ions from the left chamber to the right and that the converse holds true for the negative current.

Based on curve analysis, the following deductions were made: (1) For the positive current, the initially high MPD indicates high resistance, and the decrease in

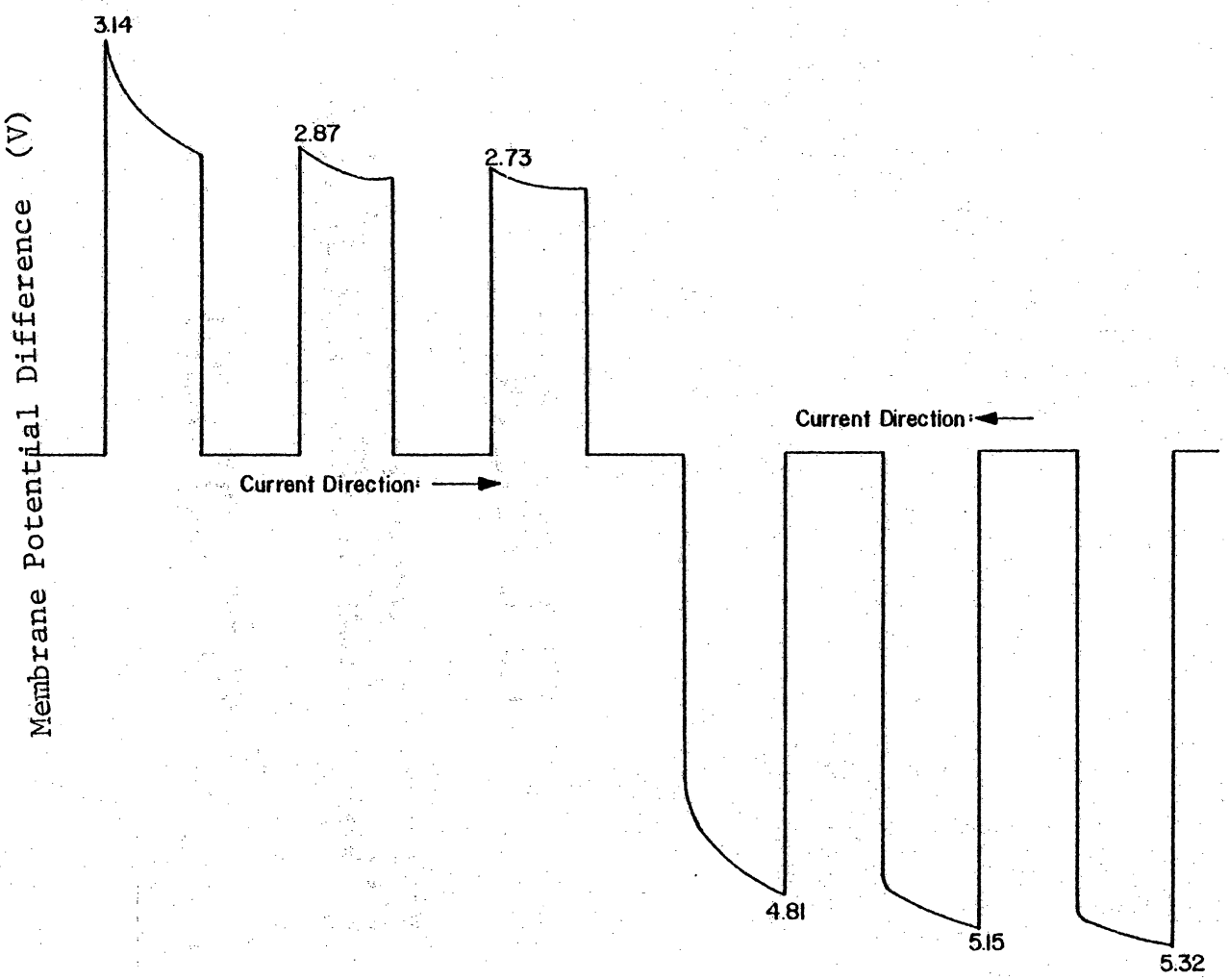

Figure 31. Overvoltage response to transient current by SPSF-Na (0.5).
System: NaCl/membrane/choline chloride Current: 50 μA

the response height reflects a reduction in the resistance. Thus, as the Na^+ and Cl^- ions pass through the membrane, the resistance decreased. (2) For the negative current, continuous migration of choline ions and Cl^- ions increased the resistance of the system. Combining these two deductions and the fact that Cl^- ions are present in both systems, one very simple interpretation would be that the transport of Na^+ ions opens up the current-carrying channel whereas the choline ions block the channel.

The results obtained for the $MgCl_2$(aq) system were similar to the other systems except for one interesting aspect. The MPD in response to the applied current was not reversible for the magnitude of the current density. The initial MPD up to 0.5 μA was about the same as for the NaCl(aq) system. At current densities greater than 10 μA, however, the values of MPD increased to values similar to those obtained in the choline chloride system and remained high even if 0.5 μA current was subsequently applied.

Table XXIX lists the conductivities of the various systems at three sequential currents of 0.5, 40, and 0.5 μA. The explanation for the conductivity results which provide the basis for the construction of the channel model is as follows: consider a channel with a certain radius as shown in Figure 32. The size of the hydrated

Table XXIX.

Conductivity of SPSF-Na(0.5)
in Various Electrolyte Systems

System	Applied current 0.5μA	50(20)μA	0.5μA
NaCl/NaCl	15.4*	18.0	16.7
$MgCl_2/MgCl_2$	11.0	(3.5)	(3.9)
$NaCl/MgCl_2$	(6.6)	(5.9/3.9)	(5.7)
NaCl/NaCl	13.7	15.8	
KCl/KCl	19.2	19.2	19.2
NaCl/KCl	19.2	19.2	19.2
NaCl/NaCl	15.4	17.1	15.4
ChCl/ChCl**	(3.5)	(3.3)	(3.5)
NaCl/ChCl	(5.6/4.6)	(5.6/3.4)	
NaCl/NaCl	11.0	14.5	12.8
LiCl/LiCl	12.8	15.0	13.3
NaCl/LiCl	13.2	15.8	13.3

*Units : μmho · cm^{-2}

**ChCl : Choline Chloride

Precision: 20%

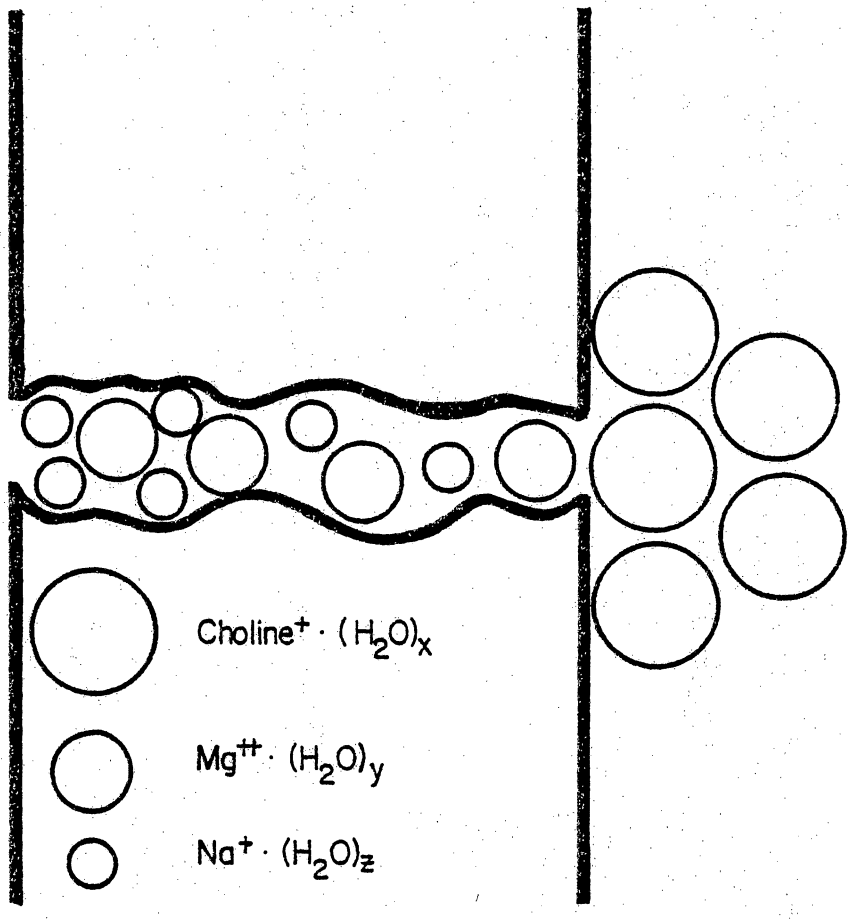

Figure 32. Model for current channel of SPSF-Na (0.5).

Na^+ ions and the choline$^+$ ions are smaller and larger, respectively, relative to the channel radius. Thus, a higher resistance may be expected for the choline system, although the actual channel pathways are not impaired at low and high current densities. Supposing that the hydrated Mg^{2+} ions are about the same size as the channel size, then a low current densities, Mg^{2+} ions might migrate through the membrane like the Na^+ ions. With an increase in the current density, however, a large quantity of Mg^{2+} ions would push into the membrane and clog up the current channel. This simple model is consistent with the experimental results. While the proposed model calls for further verification, techniques developed in keeping with this model could be very useful in determining the channel size of a variety of polymer membranes.

5. Electrical Properties of Membranes of Different Degrees of Sulfonation:

The effect of degree of sulfonation on the resistance of the system was also investigated. Table XXX lists the conductivity for the various systems studied. As can be seen, polysulfone showed the lowest conductivity and the conductivity increased with increasing degree of sulfonation. In fact, the conductivity of the SPSF-Na(1.0) membrane was identical to the solution conductivity. Hence

Table XXX.

Conductivity of Various Systems

Membrane	Conductivity (μmho . cm^{-2})
Polysulfone	1.65
SPSF-Na(0.5)	21.4
SPSF-Na(1.0)	(59600)
Solution	(59600)

Applied Current: 0.5 μA (50 μA)

System: NaCl / Membrane / NaCl

Precision: 20%

it can be concluded that the increase in the sulfonation swells the membrane, which results in larger channels. This in turn may explain the poor performance of polysulfone with a high degree of sulfonation as a desalination membrane, although a certain degree of sulfonation is essential to impart hydrophilicity and produce the necessary flux.

In conclusion, the uniqueness of the electrical property studies made it possible to obtain information concerning the channel size and the activation energy for electrolyte transport across the membrane. In addition, by simply measuring the membrane resistance with the present apparatus, membrane performance may be predicted as will be discussed in the next section.

I. Electrical Properties and Membrane Performance

Electrical properties were measured for various membranes after the reverse osmosis desalination process to study the possible correlation between electrical properties and membrane performance. Membranes were air-dried upon removal from the reverse osmosis cells and placed in the electrical property measurement apparatus described earlier. The results of this study are given in Table XXXI. The tabulated values for the resistance have been corrected for the solution (all 0.599N) resistance of 16.6, 22.8, and 11.4 ohm.cm^2 for NaCl, choline chloride, and $MgCl_2$, respectively.

In regard to membrane performance, a well-established trend was noted as the degree of sulfonation increased. The polysulfone membrane gave practically zero flux. However, the membrane flux improved significantly with increasing degree of sulfonation, and the increase in the flux paralleled the increase in the degree of sulfonation. At the same time, a decrease in the salt rejection was observed for the greater degree of sulfonation. The membrane conductivity was very small for the polysulfone membrane and there was minimal dependence of the conductivity on the particular electrolyte system. Thus, it could be concluded that the size of the ion transport channel in the polysulfone membrane is small, indeed.

Table XXXI.

Membrane Performance and Electrical Properties

Membrane	Flux(g/min)	Rejection(%)	R (ohm . cm^2) NaCl/NaCl	R (ohm . cm^2) ChCl/ChCl*	R (ohm . cm^2) $MgCl_2/MgCl_2$	G (μmho . cm^{-2}) NaCl/NaCl	G (μmho . cm^{-2}) ChCl/ChCl	G (μmho . cm^{-2}) $MgCl_2/MgCl_2$
PS	$6.7x10^{-6}$	- - - -	$1.89x10^{6}$	$1.12x10^{6}$	$1.43x10^{6}$	.528	.894	.701
SPSF-Na (0.4)	$7.38x10^{-3}$	95.9	$5.0x10^{1}$	$1.69x10^{3}$	$6.50x10^{2}$	$3.03x10^{4}$	$6.00x10^{2}$	$1.57x10^{3}$
(0.6)	$8.02x10^{-3}$	92.3	4.2	$2.32x10^{2}$	$6.56x10^{1}$	$2.38x10^{5}$	$4.31x10^{3}$	$1.52x10^{4}$
(0.8) A(thick)	$5.39x10^{-2}$	86.2	1.00	8.4	$1.56x10^{1}$	$1x10^{6}$	$1.19x10^{5}$	$6.4x10^{4}$
B(thin)	$1.34x10^{-1}$	82.8	0	2.7	0	- - -	$3.75x10^{5}$	- - -
(1.0)	$1.42x10^{-1}$	65.6	0	0	0	- - -	- - -	- - -

*ChCl : Choline Chloride

Precision: 20%

For the sulfonated membranes, however, the membrane conductivity was significantly greater and eventually showed no resistance for the highest degree of sulfonation. In addition to the higher membrane conductivity, the difference between the three electrolyte systems was minimal for the highest degree of sulfonation. For example, with SPSF-Na(0.4), the conductivity for the NaCl, choline chloride, and $MgCl_2$ electrolyte systems varied by an order of magnitude. However, with SPSF-Na(1.0), there was no significant difference in conductivity between the three electrolyte systems.

Thus, the following conclusions can be made from this study: (1) The membrane conductivity has to be > 1 $\mu mho \cdot cm^{-2}$ for the membrane to be suitable as a reverse osmosis membrane. (2) The ion transport channels should have a critical diameter that differentiates between electrolytes to give different values for the electrical conductivity. (3) These electrical property measurements provide a quick determination of the suitability of a membrane to be used in a reverse osmosis desalination process.

J. SEM Analysis of Asymmetric Membranes

Formation of an asymmetric membrane is a very delicate process and can be an art in itself. Success depends upon many variables and complex interactions between one or many components at each stage of the preparation process. Casting solution components, drying time, drying temperature, and the nature of the gelation bath are only a few of the many variables.

SEM photomicrographs of cross-sections of dense (A) and asymmetric (B) membranes are compared in Figure 33. As can be seen, dense membranes (A) do not have any porous structure within the cross-section. The bright lines shown in photo (A) are simply the edges of uneven planes introduced during the freeze-cracking process.

In contrast to the dense membranes, the cross-section of the asymmetric membrane (B) clearly shows its asymmetric nature. Fortunately, a portion of the membrane top layer was removed during the freeze-cracking process. The transition from the dense region of about 5μ to the porous region of about 250μ was well presented, as indicated by the chipped region. It should also be pointed out that the swollen asymmetric membrane is much thicker than the completely dried dense membrane. Kesting *et al.*[115] reported a similar value of 4μ for the thickness of the dense layer. It is this dense or active layer that is considered

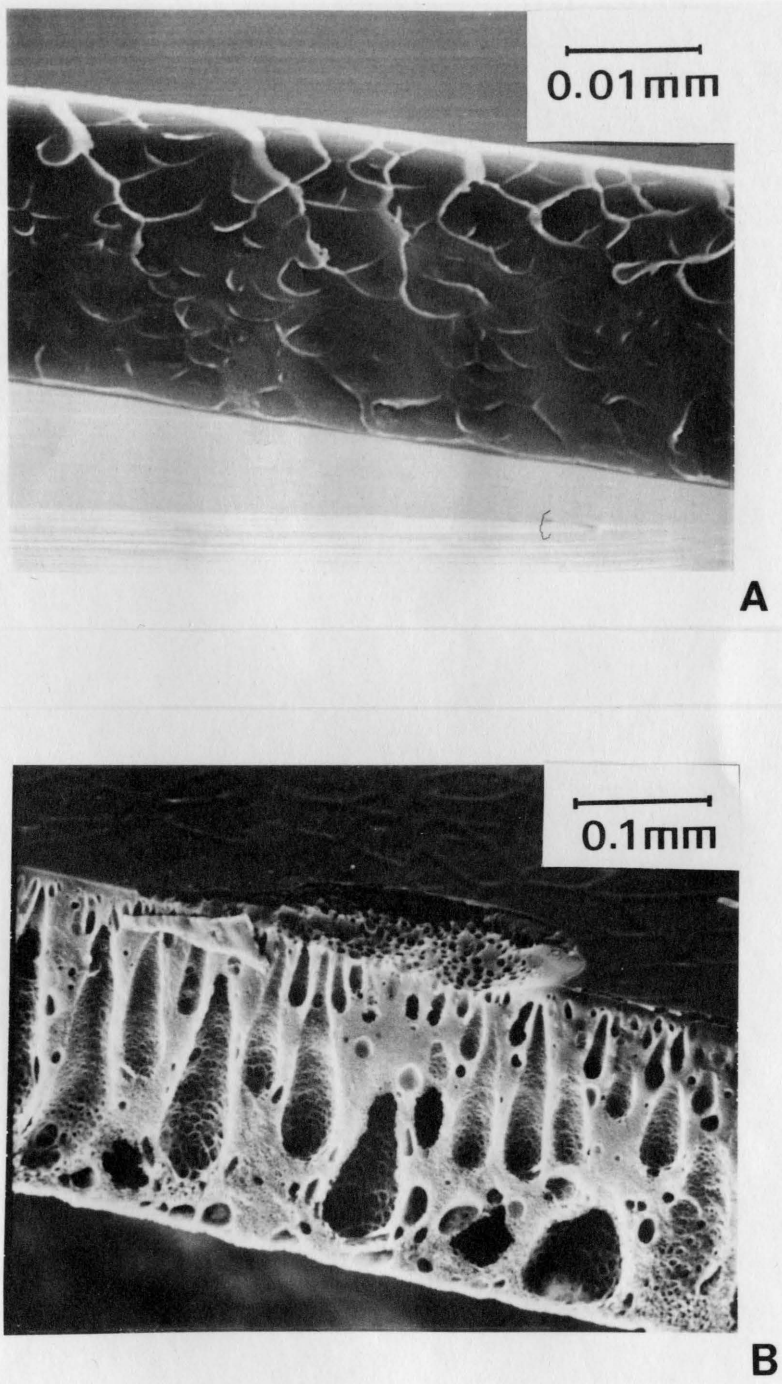

Figure 33. SEM photomicrographs of SPSF-Na(0.5) membrane cross-section.
A - dense (X200)
B - symmetric (X200)

to have effective resistance to solute transport.

Representative SEM photomicrographs of asymmetric SPSF-Na membranes are presented in Figures 34 - 38. The membranes were prepared by different methods as detailed in Appendix II. The effect of preparation on the membrane morphology is significant. Figure 34 is an SEM of a membrane prepared from a 70/30 mixture of γ-butylolactone and methanol solution and gelled in t-butanol. The membrane had almost a perfect asymmetry except for a rather thick dense layer.

An SEM photomicrograph of a membrane prepared from a $CaCl_2$ and DMF mixture is shown in Figure 35. The cross-section of the membrane (B) had huge macrovoids and the top side of the membrane (A) had pin holes. Photo (C) is the magnified cross section, and it is quite interesting to note the apparent similarity between this photo and the morphology of the asymmetric region found in Figure 34(B).

Figure 36 represents an SEM photomicrograph of an asymmetric membrane cast from a solution of acetone, H_2O, maleic acid, and dioxane. The cross-section indicates a gradual transition from a dense region into a region with small pores and then into a macropore region. The magnified asymmetric region indicates quite a different structural network of the membrane as compared to the previous two sets of photomicrographs (Figs. 34 and 35). Such differences

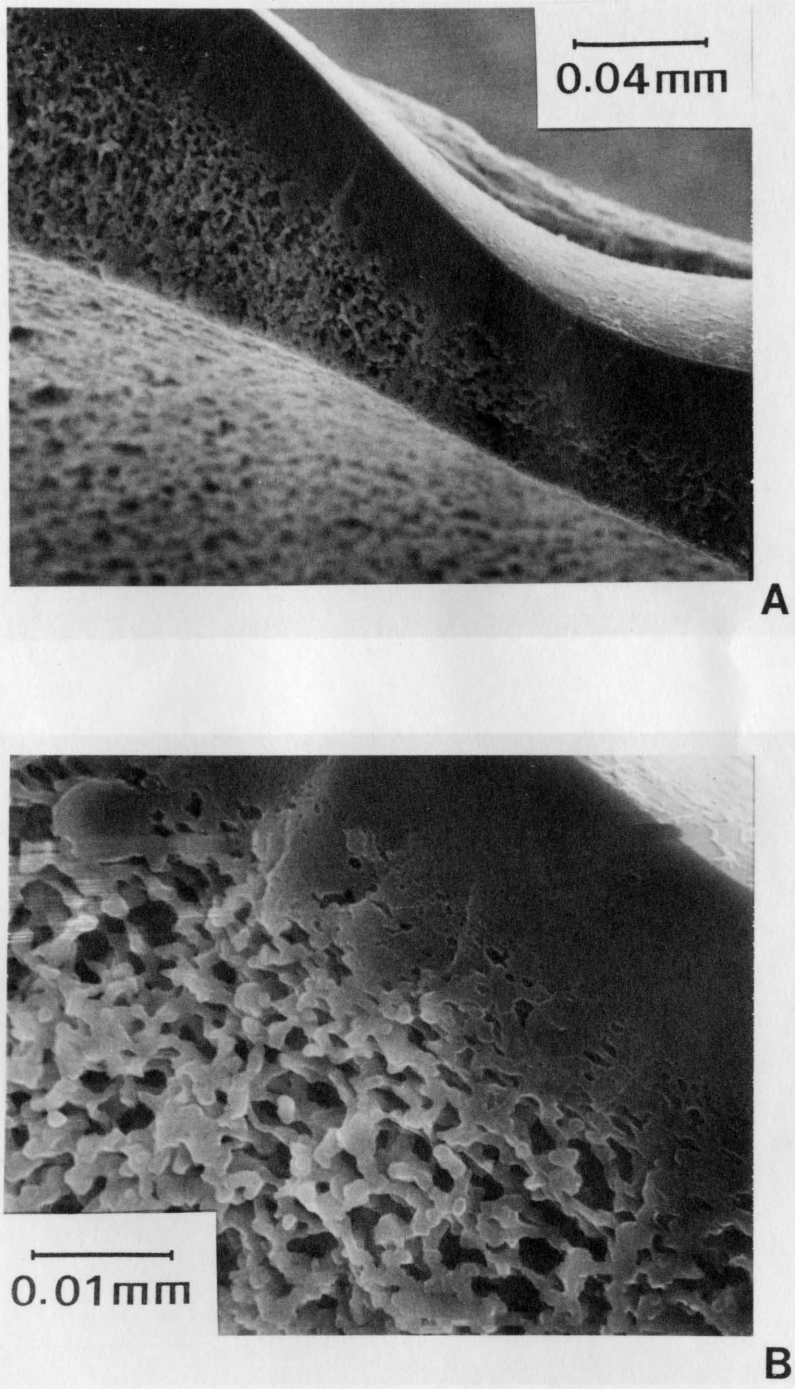

Figure 34. SEM photomicrographs of SPSF-Na (0.5) membrane cast from 70/30 mixture of γ-butyrolactone and methanol solution and gelled in t-butanol. A - X470 B - X1900

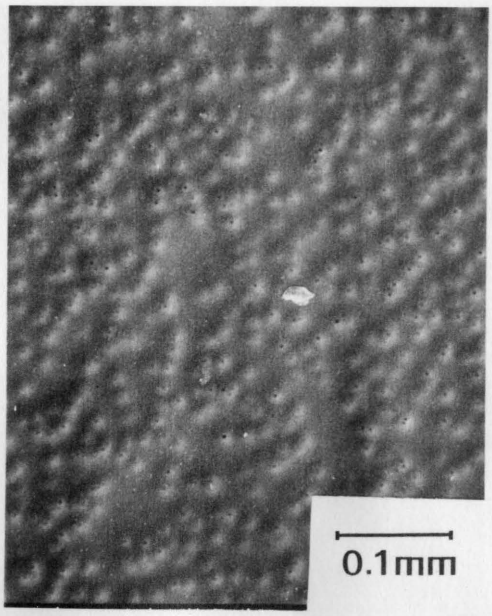

A

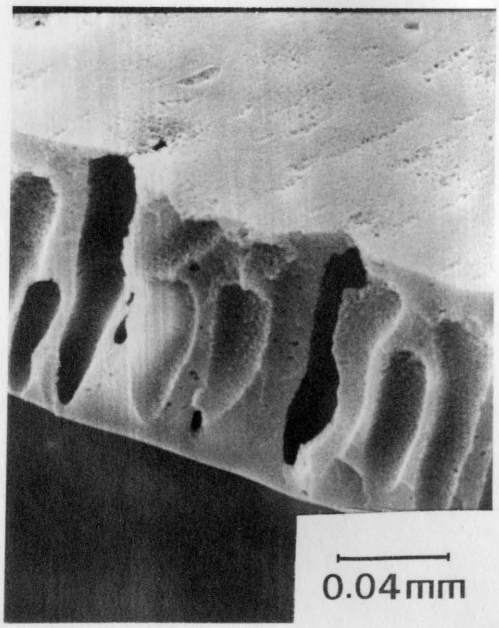

B

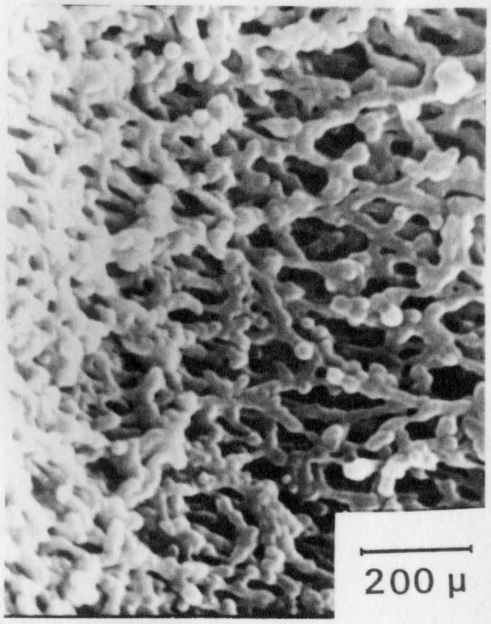

C

Figure 35. SEM photomicrographs of SPSF-Na (0.5) membrane prepared from $CaCl_2$/DMF solution gelled in H_2O.
A: Top (X200) B: Cross-section (X500)
C: Magnified detail structure of the cross-section (X10000)

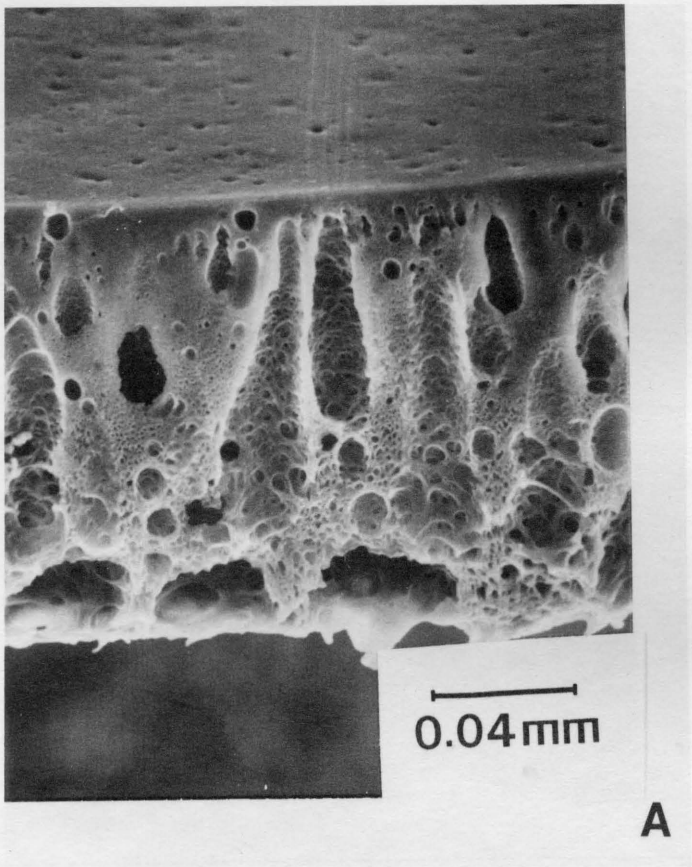

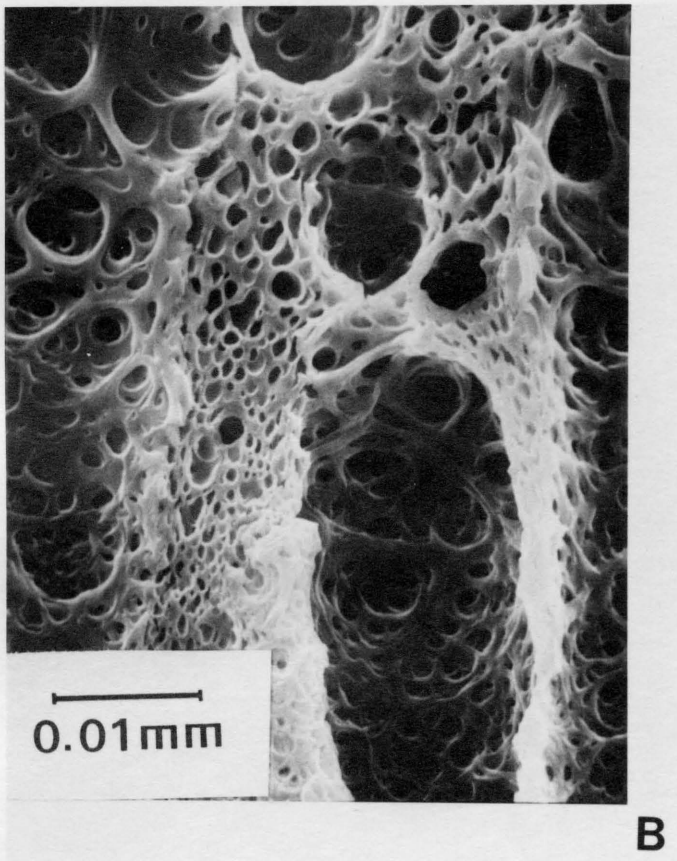

Figure 36. SEM photomicrographs of SPSF-Na (0.5) membrane cast from a mixture of acetone, maleic acid, H_2O, and dioxane gelled in H_2O. A - X500 B - X200

may be due to the difference in the interaction with the wet membrane and the gelation media.

Figure 37 is the membrane produced from the same casting solution as in Figure 36 , but cast cold. Comparison of Figures 36 and 37 indicates that the cold process shrank the membrane in general, as evidenced by the narrower cross-section and shrinkage in the fine structures of the membrane in Figure 37. The cold process membrane still contained a significant number of pin holes on the top surface of the membrane (not shown), however.

Preparation of an asymmetric membrane was attempted from DMF solution with maleic acid as a swelling agent. This procedure produced a membrane with small pores evenly distributed throughout the membrane cross-section, as shown in Figure 38 .

Figures 39 and 40 compare the same asymmetric membranes before (Fig. 39) and after (Fig. 40) the reverse osmosis desalination operation. Membranes were cast from a solution of acetone, maleic acid, H_2O, and dioxane similar to the one shown earlier (see Figs. 36 and 37), but at a higher polymer concentration. Photo (A) in Figure 39 shows the top side of the membrane and it shows the presence of some pin holes. This membrane had about 20-30% salt rejection, whereas the others showed no separation. The higher rejection could

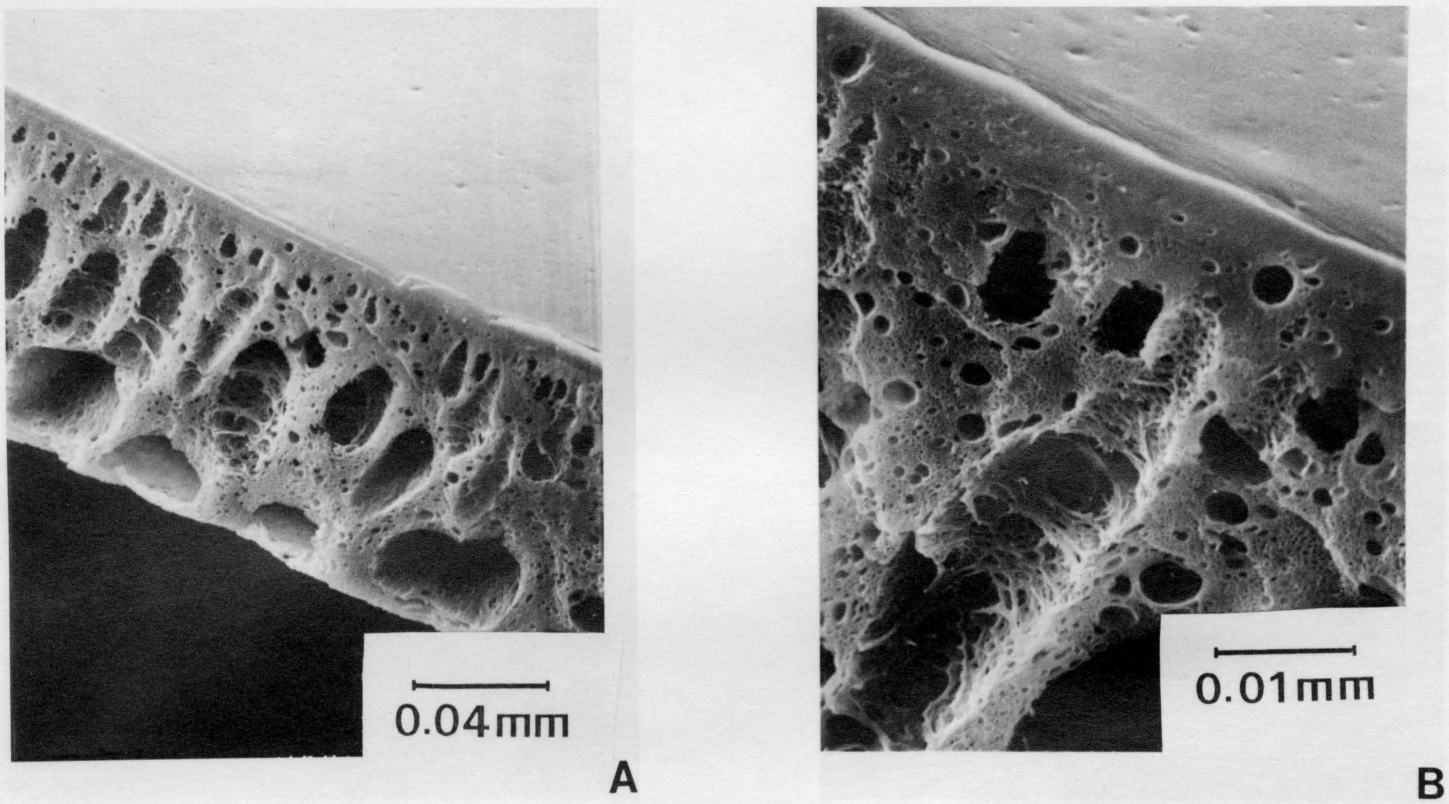

Figure 37. SEM photomicrographs of asymmetric SPSF-Na (0.5) membrane cold cast from a mixture of acetone, maleic acid, H_2O, and dioxane solution gelled in H_2O. A - X500 B - X200

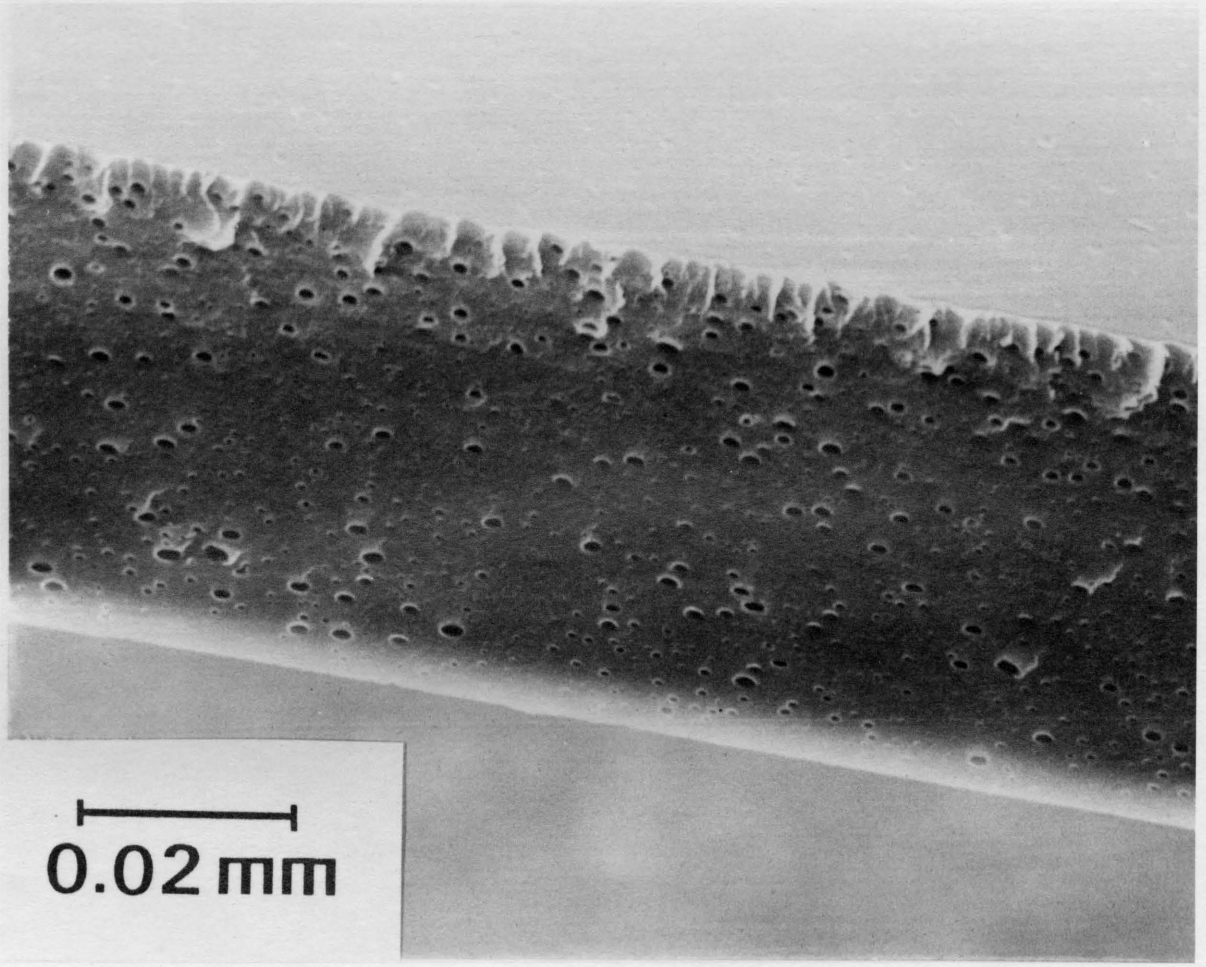

Figure 38. SEM photomicrograph of SPSF-Na (0.5) membrane prepared from maleic acid/DMF solution gelled in H_2O. (X1000)

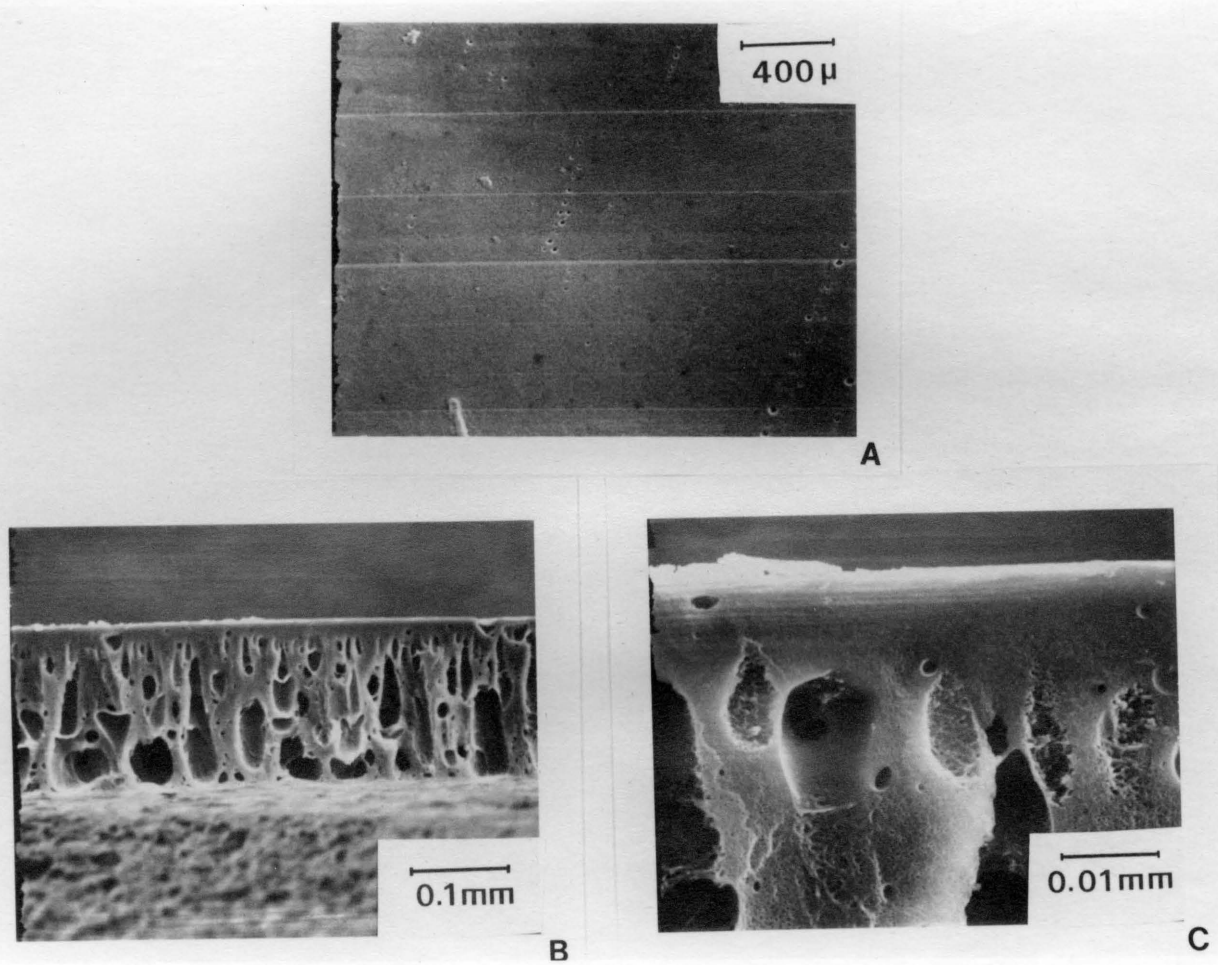

Figure 39. SEM photomicrographs of SPSF-Na (0.5) membrane prepared from a mixture of acetone, H_2O, dioxane, and maleic acid. A - Top (X5000) B - Cross-section (X200) C - Magnified cross-section (X2000)

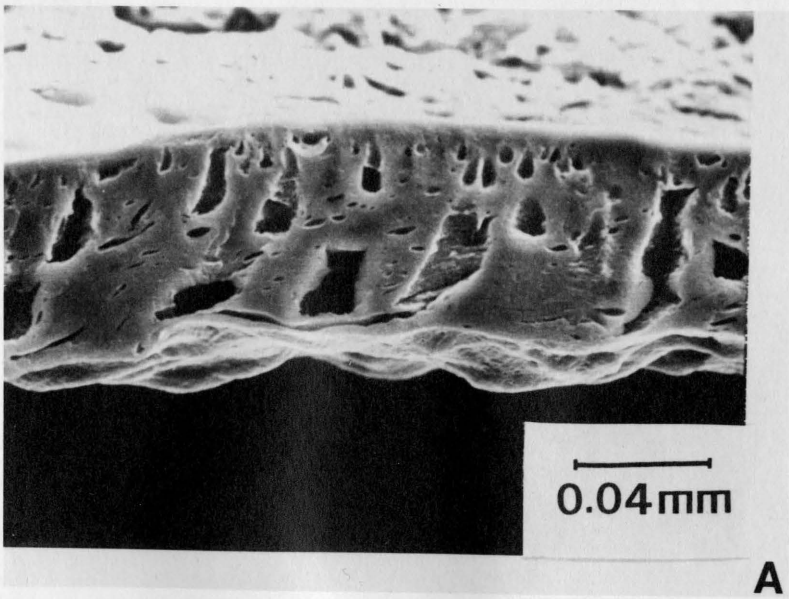

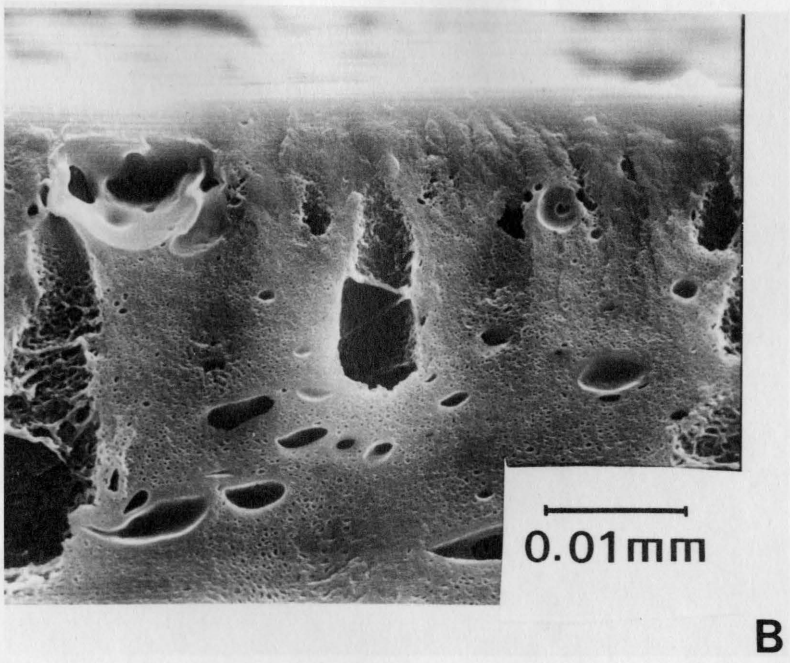

Figure 40. SEM photomicrographs of cross-section of SPSF-Na (0.5) membrane shown in Figure 39 after the reverse osmosis desalination test. A - X500
B - X2000

be due to the lower density of the pin holes. The cross-sectional views, B and C in Fig. 39, clearly indicate a dense layer on the top side of the membrane and raindrop-like macropores.

Figure 40 shows the cross-section of the same membrane after the reverse osmosis desalination test. The membrane thickness was reduced about 2.5-fold, and the voids were apparently compressed. In other words, the membrane was more compact and dense after the reverse osmosis test.

In conclusion, the membrane morphology was extensively investigated by means of SEM. SEM clearly indicated the effect of solution composition on the membrane morphology. In addition, in some cases examination of SEM photomicrographs led to prediction of the membrane's performance as a reverse osmosis membrane.

V. SUMMARY

The variety of characterization processes carried out in this study provided a better understanding of SPSF membrane properties in addition to demonstrating the feasibility of using sulfonated polysulfone as a material for reverse osmosis membranes. While some of the techniques, such as water uptake, contact angle measurement, and ion exchange studies, have been used previously by other workers in a variety of systems, the present study was directed specifically to sulfonated polysulfone characterization. In addition, a novel study of the electrical properties and analysis of SPSF membranes with ESCA and SEM were performed for the first time. The major conclusions of this study are summarized below.

Sulfonation introduced hydrophilicity into an essentially hydrophobic polysulfone. Thus, the water uptake was consistently greater for the membranes with higher degrees of sulfonation. The degree of sulfonation was preserved during the membrane fabrication process. The extent of water sorption was dependent on the nature of the counter ion in that SPSF-Na membranes showed greater hydrophilicity than SPSF-K membranes for a given degree of sulfonation. Water is less hydrogen-bonded in a SPSF membrane as compared to bulk water, as evidenced by shifts in the near IR absorption.

The hydrophilicity of the dense SPSF membranes, as determined by contact angles, mimics the bulk membrane characteristics. The contact angle of water decreased for higher degrees of sulfonation. Further, the contact angle of water on the SPSF-Na membrane was less than on the SPSF-K membrane for a given degree of sulfonation.

Only Si was found to be a surface contaminant on the membrane surface by ESCA. Neither the membrane surface not the polymer powder surface had the same stoichiometry as the bulk. There was no trend in the surface chemical composition for varying degrees of sulfonation. The counter ion concentration on the membrane surface was greater for SPSF-Na compared to SPSF-K, as determined by the angle-resolved ESCA analysis. It was not possible to predict the membrane performance in the reverse osmosis desalination process based on ESCA analysis. Ion exchange occurred not only on the SPSF membrane surface but also throughout the bulk.

The electrolyte/membrane/electrolyte system exhibited ohmic behaviour. The membrane potential difference under transient current was greatly dependent on the nature of the cation whereas the nature of the anion had no effect. The activation energy was minimally dependent on the membrane thickness. The rate-limiting step in the ion transport process is likely to be the disruption

of bound water. The membrane resistance was significantly dependent on the degree of sulfonation. The greater degree of sulfonation resulted in lower membrane resistance. The membrane performance could be predicted from the electrical property measurements. The membrane conductivity had to be > 1 $\mu mho.cm^{-2}$, but less than the solution conductivity for the membrane to be suitable as a reverse osmosis membrane.

SEM photomicrographs provided valuable information on the membrane morphology and, in some cases, the performance as a reverse osmosis membrane could be predicted apriori from the SEM photomicrographs of the cast films.

REFERENCES

1. State and National Water Use Trends to the Year 2000. A report prepared by the Congressional Research Service of the Library of Congress. May, 1980. Serial 96-12.

2. U.S. Geological Survey; Skinner, B.J. "Earth's Resources;" Prentice-Hall: Englewood Cliffs, N.J., 1969.

3. Ross, W. D., ed. "The Works of Aristotle Translated into English," Problemata, Vol. VII, Book XXIII. Clarendon Press: Oxford, 1963, p. 18.

4. Loeb, S.; Sourirajan, S. UCLA Department of Engineering 1961 Report No. 60-60.

5. Chemical and Engineering News, 1980, February 4, p. 26.

6. Noshay, A.; Robeson, L.M. J. Appl. Polym. Sci. 1976, 20, 1885.

7. Graefe, A.F.; Schell, W.J.; Saltonstall, C.W., Jr.; Stannett, V.T.; Hopfenberg, H.B. "Research on Advanced Membranes for Reverse Osmosis." 1974, NTIS, PB-230-690.

8. Brousse, C.L.; Chapurlat, R.; Quentin, J.P. Desalination, 1976, 18, 137.

9. Erschler, B. Kolloid Z, 1934, 68, 289.

10. McBain, J.W.; Stuewer, R.F. J. Phys. Chem., 1936, 40 1157.

11. Trautman, S.; Ambard, L. J. Chim. Phys., 1952, 49, 220.

12. Hacker, W. Kolloid Z., 1941, 95, 194.

13. Wintgren, R. Kolloid Z., 1940, 93, 257.

14. Yuster, S.T.; Sourirajan, S.; Bernstein, K. "Sea Water Demineralization by the Surface Skimming Process." 1958, Department of Engineering UCLA Report No. 58-26.

15. Breton, E.J., Jr. "Water and Ion Flow Through Imperfect Osmotic Membranes." 1957, Office of Saline Water

Research and Development Progress Report No. 16.

16. Reid, C.E.; Breton, E.J. J. Appl. Polym. Sci., 1959, 1, 133.

17. Reid, C.E.; Spencer, J.G. J. Phys. Chem., 1960, 64, 1587.

18. Loeb, S.; Sourirajan, S. UCLA Department of Engineering 1960 Report No. 60-5.

19. Dobry, A. Bull. Soc. Chim., 1936, (5) 3, 312.

20. Biget, A.M. Ann. Chim., 1950, (12) 5, 66.

21. Sourirajan, S. "Reverse Osmosis." Academic Press: New York, 1970.

22. Lonsdale, H.K. in "Desalination by Reverse Osmosis." Merte, U., ed. MIT Press: Cambridge, Mass., 1966.

23. Vos, K.D.; Barris, F.O.; Riley, R.L. J. Appl. Polym. Sci., 1966, 10, 825.

24. Reese, E.T.; Mandels, M. in "Cellulose and Cellulose Derivatives." Bikales, N.M.; Segal, L. ed. Wiley Interscience: New York, 1971, Part V, p. 1079.

25. Hassid, W.Z.; Ballou, C.E. in "The Carbohydrates: Chemistry, Biochemistry, Physiology." Pigman, W., ed. Academic Press: New York, 1957, p. 489.

26. Kesting, R.E. "Synthetic Polymeric Membranes." McGraw-Hill: New York, 1971.

27. Lonsdale, H.K.; Podall, H.E., ed. "Reverse Osmosis Membrane Research." Plenum Press: New York, 1972.

28. Sourirajan, S., ed. "Reverse Osmosis and Synthetic Membranes." National Research Council of Canada Publications: Ottawa, Canada, 1977.

29. Turbak, A.F.; Noshay, A. U.S. Patent 3, 206, 492, 1965.

30. Johnson, R.N.; Farnham, A.G.; Clendinning, R.A.; Hale, W.F.; Merriam, C.N. J. Polym. Sci. A-1, 1967, 5, 2399.

31. Yasuda, H. in Reference 28, Chapter 13.

32. Rozelle, L.T.; Cadotte, J.E.; Senechal, A.J.; King, W.L.; Nelson, B.R. in Reference 27, p. 419.

33. Turbak, A.F.; Noshay, A.; Karoly, G. U.S. Patent 3, 205, 285, 1965.

34. O'Farrell, C.P.; Surniuk, G.E. U.S. Patent 3, 836, 511, 1974.

35. Goethals, E.J. in "Encyclopedia of Polymer Science and Technology." Wiley: New York, 1970, Vol. 13, p. 465.

36. LaConti, A.B.; Chludzinski, P.J.; Fickett, A.P. in Reference 27, p.263.

37. Quentin, J.P. U.S. Patent 3, 709, 841, 1973.

38. Bourganel, J. U.S. Patent 3, 855, 122, 1974.

39. Bourganel, J. U.S. Patent, 4, 026, 977, 1977.

40. Quentin, J.P.; Milas, M.; Rinaudo, M. 5th Int. Symp. on Fresh Water from the Sea. 1976, 4, 157.

41. Graefe, A.F.; Wong, D. "Development of a Chlorine-Resistant Composite Membrane for Reverse Osmosis." Office of Water Research and Technology, Department of the Interior, Report No. 2001-20, August, 1980.

42. Riley, R.L.; Gardner, J.O.; Merten, U. Science, 1964, 143, 801.

43. Riley, R.L.; Merten, U.; Gardner, J.O. Desalination, 1966, 1, 3.

44. Kimoto, S. On Scanning Electron Microscopy, JEOLCO Publication, SM-67013.

45. Kesting, R.E.; Menefee, A. Kolloid Z.Z. Polymere, 1969, 230, 2, 341.

46. Kesting, R.E.; Engdahl, M.; Stone, W. J. Macromol. Sci. Chem., 1969, A3, 157.

47. Kesting, R.E. in Reference 28, Chapter 5.

48. Fox, H.W.; Zisman, W.A. J. Colloid Sci., 1950, 5, 514.

49. Shafrin, E.G.; Zisman, W.A. J. Phys. Chem., 1960, 64, 519.

50. Fowkes, F.M. "Contact Angle, Wettability, and Adhesion." Advances in Chemistry Series, No. 43. Gould, R.F., ed. ACS Press: Washington, D.C., 1964.

51. Johnson, R.E., Jr.; Dettre, R.H. in "Surface and Colloid Science." Vol. 2. Matijevic, E., ed. Wiley: New York, 1969, p. 85.

52. Good, R.J. in "Colloid and Surface Science." Vol. 11. Good, R.J.; Stromberg, R., ed.; Plenum: New York, 1979, Chapter 1.

53. Dwight, D.W.; McGrath, J.E.; Wightman, J.P. J. Appl. Polym. Sci. Appl. Polym. Symp., 1978, 34, 35.

54. Clark, D.T. in "Progress in Theoretical Organic Chemistry." Vol. 2. Crizmadia, I.G., ed. Elsevier: Amsterdam, 1976.

55. Ratner, B.O.; Weathersby, P.K.; Hoffman, A.S.; Kelley, M.A.; Sharpen, L.H. J. Appl. Polym. Sci., 1978, 22, 643.

56. Thomas, H.R.; O'Malley, J.J. Macromolecule, 1979, 12 (2), 323.

57. Fadley, C.S.; Baird, R.J.; Siekhaus, W.; Navakov, T.; Biegstrom, S.A. J. Electron Spectros Related Phenom., 1974, 4, 93.

58. Clark, D.T. Advances in Polym. Sci., 1977, 24, 126.

59. Clark, D.T.; Adams, D.B.; Dilks, A.; Peeling, J.; Thomas, H.R. J. Electron Spectros Related Phenom., 1976, 8, 51.

60. Everhart, D.S.; Reilley, C.N. Anal. Chem., 1981, 53, 665.

61. Merten, U.; Lonsdale, H.K.; Riley, R.L.; Vos, K.D.; U.S. Department of Interior, OSW, Research and Development Progress Report, No. 265. Washington, D.C., 1967.

62. Speigler, K.S. Desalination, 1971, 9, 367.

63. Ramp, F.L. Desalination, 1975, 16, 321.

64. Kumins, C.A.; Condon, A. J. Polym. Sci., 1960, 46, 395.

65. Horigome, S.; Taniguchi, Y. J. Appl. Polym. Sci., 1977, 21, 343.

66. Wong, S. G.; Kwak, J.C.T. Desalination, 1974, 15, 213.

67. Choi, K.W.; Bennon, D.N. UCLA Engineering Report 7370, 1973.

68. Demisch, H.U.; Pusch, W. J. Colloid Interface Sci., 1980, 76 (2), 445.

69. Kimjo, N.; Sato, M. Desalination, 1978, 27, 71.

70. Kimjo, N. J. Colloid Int. Sci., 1980, 73 (2), 438.

71. Myers, A.W.; Meyer, J.A.; Rogers, C.E.; Stannett, U.; Szware, M. Tappi, 1961, 44, 58.

72. Flory, P.J. "Principles of Polymer Chemistry." Cornell University Press: Ithaca, 1953, p. 495.

73. Huggins, M.L. Ann NY Acad. Sci., 1942, 43, 1.

74. Brunauer, S.; Emmett, P.H.; Teller, E. J. Am. Chem. Soc., 1938, 60, 309.

75. Bull, H.B., ibid., 1944, 66, 1499.

76. Pauling, L., ibid., 1945, 67, 555.

77. White, H.J., Jr.; Eyring, H. Textile Res. J., 1947, 17, 523.

78. Zimm, B.H.; Landberg, J.L. J. Phys. Chem., 1956, 60, 425.

79. Zimm, B.H. Rev. Mod. Phys., 1959, 31, 123.

80. Reid, C.E.; Kuppers, J.R. J. Appl. Polym. Sci., 1959, 2, 264.

81. Reid, C.E.; Spencer, H.G. ibid., 1960, 4, 384.

82. Rowland, S.P., ed. "Water in Polymer." ACS Sym. Series, 127, American Chemical Society Press: Washington, D.C., 1980.

83. Luck, W.A.; Schioberg, D.; Siemann, U. JCS Faraday II, 1980, 76, 136.

84. Frommer, M.A.; Shporer, M.; Messalem, R.M. J. Appl. Polym. Sci., 1973, 17, 2263.

85. Almagor, E.; Belfort, G. J. Colloid Interface Sci., 1978, 66 (1), 146.

86. Burghoff, H.G.; Pusch, W. J. Appl. Polym. Sci., 1979, 23, 473.

87. Chang, Y.T.; Chen C.T.; Tobolsky, A.V. J. of Polym. Sci., Polym.-Physics Ed., 1974, 12, 1.

88. Belfort, G.; Sinai, N. in Reference 73, Chapter 19.

89. Scott, J. "Membrane and Ultrafiltration Technology, Recent Advances." Noyes Data Corporation: Park Ridge, N.J., 1980.

90. Havens Industries, Sea Water Conversion by Reverse Osmosis. Technical Broch., San Diego, California, 1964.

91. Loeb, S. Desalination, 1966, 1, 35.

92. Merten, U., ed. "Desalination by Reverse Osmosis." MIT Press: Cambridge, Mass., 1966.

93. Lonsdale, H.K.; Merten, U.; Riley, R.L. J. Appl. Polym. Sci., 1965, 9, 1341.

94. Lloyd, D.R.; McGrath, J.E.; Wightman, J.P.; Iqbal, M.; Kang, Y.; Tran, C.; Gerlowski, L.E.; Sunderland, C. OWRT Annual Report, Washington, D.C., April 15, 1980.

95. Kopf, P.W. Private Communication. Union Carbide Corporation Chemicals and Plastics. River Road, Bound Brook, N.J. 08805.

96. Neumann, A.W.; Good, R.J. in "Colloid and Surface Science," Vol. 11. Good, R.J.; Stromberg, R., ed. Wiley: New York, 1980, Chapter 2.

97. Scofield, J.H. J. Electron Spectros. Relatd. Phenom., 1976, 8, 129.

98. Dulany, G.W. MADCAP IV, A Multiplex ADC and Analog Plotting Program. DECUS No. 8-237, Digital Equipment Corporation: Maynard, Mass., 1969.

99. Tran, C. MS Thesis, Virginia Polytechnic Institute and State University, Blacksburg, Virginia, 1980.

100. Skoog, D.A.; West, D.M. "Principles of Instrumental Analysis." Holt, Rinehart, and Winston, Inc.: New York, 1971.

101. MacKnight, W.J.; Taggart, W.P.; Stein, R.S. J. Polym. Sci., 1974, Sym. No. 45, 113-128.

102. Alfrey, T., Jr.; Gurnee, E.F.; Lloyd, W. J. Polym. Sci., 1966, C12, 249.

103. Jacques, C.H.M.; Hopfenberg, H.B.; Stannett, U. Polym. Sci. and Tech., 1974, 6, 73.

104. Good, R.J.; Koo, M.N. J. Colloid Interface Sci., 1979, 71 (2), 283.

105. Luck, W.A.P. in Reference 82, Chapter 3.

106. Muilenberg, G.E. "Handbook of X-ray Photoelectron Spectroscopy.: Perkin Elmer Corporation: Eden Prarie, MN., 1978.

107. Fisher, S.; Kunin, R. Anal. Chem., 1955, 27, 1191.

108. Singh, A. Ph.D. Dissertation. Virginia Polytechnic Institute and State University, Blacksburg, Virginia, 1980.

109. Eyring, H.; Eyring, E.M. "Modern Chemical Kinetics," Reinhold Publishing Corp.: New York, 1963, p. 51.

110. Eyring, H.; Lumry, R.; Woodbury, J.W. Rec. of Chem. Prog., 1949, 10, 100.

111. Drost-Hansen, W. Ind. and Eng. Chem., 1965, 57, 18-37.

112. Etzler, F.M.; Drost-Hansen, W. in "Cell-Associated Water.: Drost-Hansen, W.; Clegg, J., ed. Adademic Press: New York, 1979, p. 125.

113. Vinnikova, N.; Tanny, G.B. in "Synthetic Membranes," Vol. 1. Turbak, A.F., ed. ACS Sym. Ser. 153. ACS Press: Washington, D.C., 1981.

114. Dinno, M.A. Virginia Polytechnic Institute and State University, Blacksburg, Virginia. Private Communication.

115. Kesting, R.; Barsch, M.; Vincent, A. J. Appl. Polym. Sci., 1965, 9, 1873.

116. Lloyd, D.G.; Gerlowski, L.E.; Sunderland, C.D.; Wightman, J.P.; McGrath, J.E.; Iqbal, M.; Kang, Y. in Turbak, A.F., ed. "Synthetic Membranes," Vol. I; ACS Sym. Ser. 153. ACS Press: Washington, D.C., 1981, Chapter 22.

APPENDIX 1

SYNTHESIS OF SULFONATED POLYSULFONE

Sulfonation of polysulfone was performed by the procedure described by Noshay and Robeson[6] where polysulfone was dissolved in 1,2-dichloroethane and reacted with a complex of SO_3-triethyl phosphate (2:1 ratio) followed by neutralization with a base. A brief summary of a typical synthetic scheme is given below:

Preparation of SO_3/Triethylphosphate Complex: The SO_3/TEP complex was freshly prepared for each sulfonation reaction. 8.2251 g of distilled triethylphosphate in 40 ml of dry dichloroethane was placed in a 250 ml, three-necked, round-bottom flask. The flask was kept under N_2 gas and cooled with an ice water mixture. 7.232 g of sulfur trioxide was added drop-by-drop during 25-30 minutes with stirring, and the solution was kept stirred for another 30 minutes. The reaction flask was then allowed to warm up to room temperature.

Sulfonation of Polysulfone: 100 ml of dry 1,2-dichloroethane was placed in a 1 liter, four-necked, round-bottom flask attached to a mechanical stirrer, a condenser, and two dropping funnels, and the flask was kept under N_2 gas. 20 g of 5% solution of polysulfone (Union Carbide P-1700) in 1,2-dichloroethane and the SO_3/TEP complex was placed in each funnel. The two reagents were introduced

simultaneously during 10 minutes with vigorous stirring. The reaction was completed in 30 minutes forming a tan-colored precipitate. The precipitate was then dissolved by the addition of 100-125 ml of isopropanol. To clear the solution, sodium methylate in methanol or potassium hydroxide was added to neutralize the acid to prepare SPSF-Na or SPSF-K. The precipitate was filtered through a fritted funnel and washed with distilled water. The polymer was dried at 100°C for 24 hours under vacuum.

Compositional Analysis: The degree of sulfonation of the prepared polymer was determined by elemental sulfur analysis and NMR analysis and the results are tabulated in Table A-I. The elemental analysis was performed at Galbraith Laboratories in Knoxville, Tennessee. The degree of sulfonation (from the NMR analysis) was calculated following the method developed by Kopf.[95] The integration of the ring protons defined in Figure A-1 was utilized in the equation where the degree of sulfonation is defined as:

$$D = \frac{12 - 4R}{2 + R}$$

where D = degree of sulfonation and R = ratio of peak intensities, $\frac{a + b + c}{d + c}$.

Table A-I.

Degree of Sulfonation Determined by Sulfur Analysis and NMR

Sample No.	Target Degree of Sulfonation	Sulfur Analysis	NMR Analysis
SPSF-Na(0.2)	0.2	0.12	0.16
SPSF-Na(0.4)	0.4	ND*	0.34
SPSF-Na(0.5)	0.5	0.40	0.38
SPSF-Na(0.6)	0.6	0.39	0.53
SPSF-Na(0.8)	0.8	0.61	0.68
SPSF-Na(1.0)	1.0	0.80	1.00
SPSF-K(0.2)	0.2	ND	0.12
SPSF-K(0.4)	0.4	0.30	0.32
SPSF-K(0.6)	0.6	0.38	0.48
SPSF-K(0.8)	0.8	0.57	0.72
SPSF-K(1.0)	1.0	0.65	0.87

*ND = Not Determined

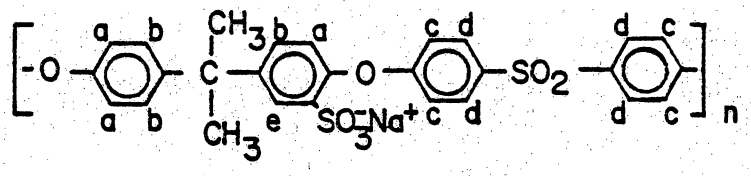

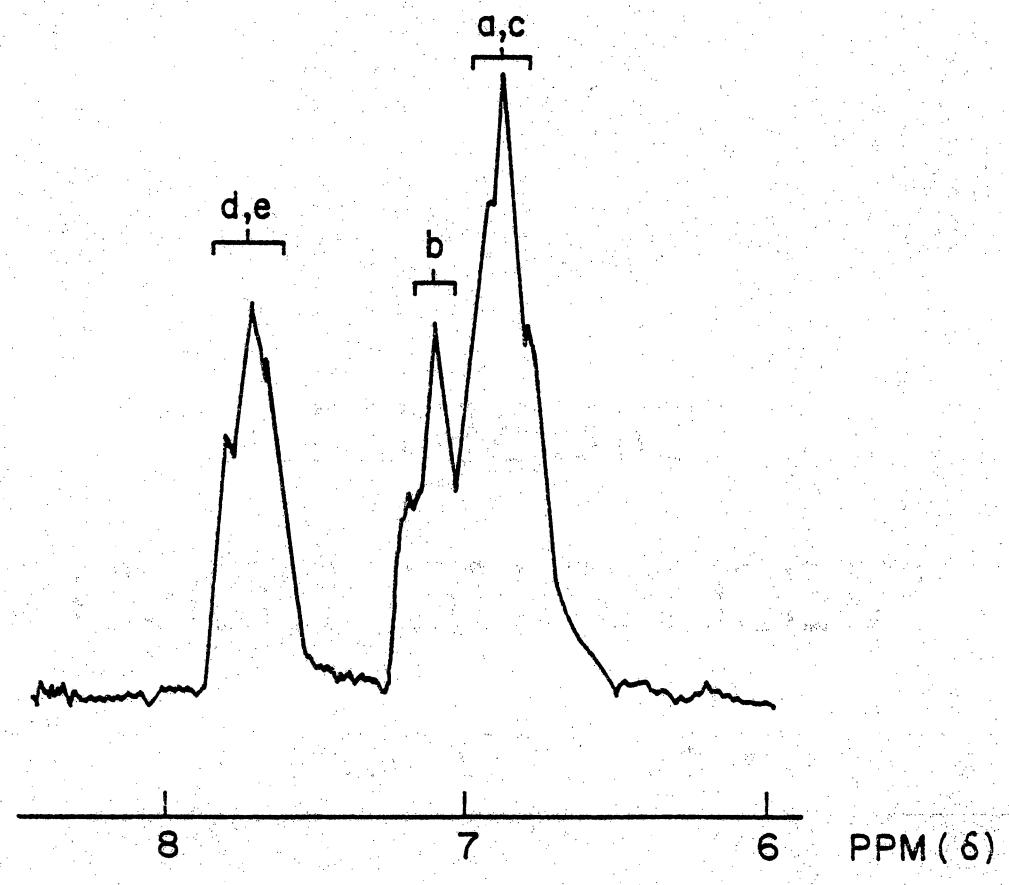

Figure A-1. Proton NMR spectrum of Sulfonated Polysulfone : SPSF-Na (1.0).

APPENDIX II

PREPARATION OF ASYMMETRIC MEMBRANES

The preparation of the asymmetric membranes was done by a method similar to the one described by Loeb and Sourirajan.[4] In all cases, a casting solution was placed on the top of a glass plate and cast into a sheet with a doctor's knife set at a predetermined thickness, typically 8 to 16 mil. After a brief evaporation period, the glass plate was immersed in a gelation bath. Finally, the membrane was thoroughly washed in distilled water.

Numerous compositions of casting solution were prepared using the classical approach, i.e., dissolving the polymer in a solvent and adding a less-volatile non-solvent or swelling agent. The initial solution, depending on the solubility parameter and the boiling point, contained dimethyl formamide (DMF), and diethyl glycol monoethyl ether (DEGME) as a solvent and swelling agent. The performance of such membranes were not acceptable, however, as shown by the low flux in Table A-II. Other combinations, such as using $CaCl_2$ and maleic acid as swelling agents, also failed to show any improvement.

Attention was then given to a non-classical casting solution formulation. The investigation of the solubility diagram for SPSF-Na(0.5) indicated that while two liquids may be non-solvents by themselves, the right combination of two liquids may form a solution which falls within the solubility envelope[116] and becomes a co-solvent,

Table A-II.

Performance of Membranes Prepared from Classical Casting Solutions[116]

SPSF-Na(0.42) (wt-%)	DMF (wt-%)	DEGME (wt-%)	Oven Temp (°C)	Oven Time (min)	Flux ($kg/m^2.s$) x10^2	Salt Rejection (percent)
16.4	80.5	3.1	65	45	0.0037	85
17.5	79.5	3.0	70	45	0.0014	<2
17.5	79.5	3.0	70	30	0.0021	50
17.5	79.5	3.0	70	45	0.0014	<2
17.5	80.9	1.6	70	30	0.0014	<2
17.5	80.9	1.6	70	45	0.0014	<2
17.5	81.0	1.5	72	20	31.22	2
17.5	81.0	1.5	72	20	22.02	2
17.5	79.5	3.0	72	20	0.0083	<2
17.5	79.5	3.0	72	20	3.39	2

as shown in Figure A-2. Various combinations of the THF-Formamide system were investigated based on the high volatility and, thus, the quick drying time of the THF. The performance of such membranes is listed in Table A-III, and although none looked too promising, some were better than others as judged by the wide variations in flux and salt rejection.

The best asymmetric membrane produced in this study with a reasonable performance was prepared from the casting solution composition given in Table A-IV. The composition is a modified version of the solution used by Graefe et al.[7] The solution was chilled in a refrigerator. The membrane was cast as an 8 mil film on a glass plate at room temperature in a box under an acetone vapor environment. The drying time was minimal in that the glass plate was immersed in water upon completion of casting. Prior to the performance test in a reverse osmosis cell, the membrane was heat-treated in 50% $NaNO_3$ at 60°C for 5 minutes. Typical membrane performance was about 25% separation at a flux of 0.035 $kg/m^2.S$.

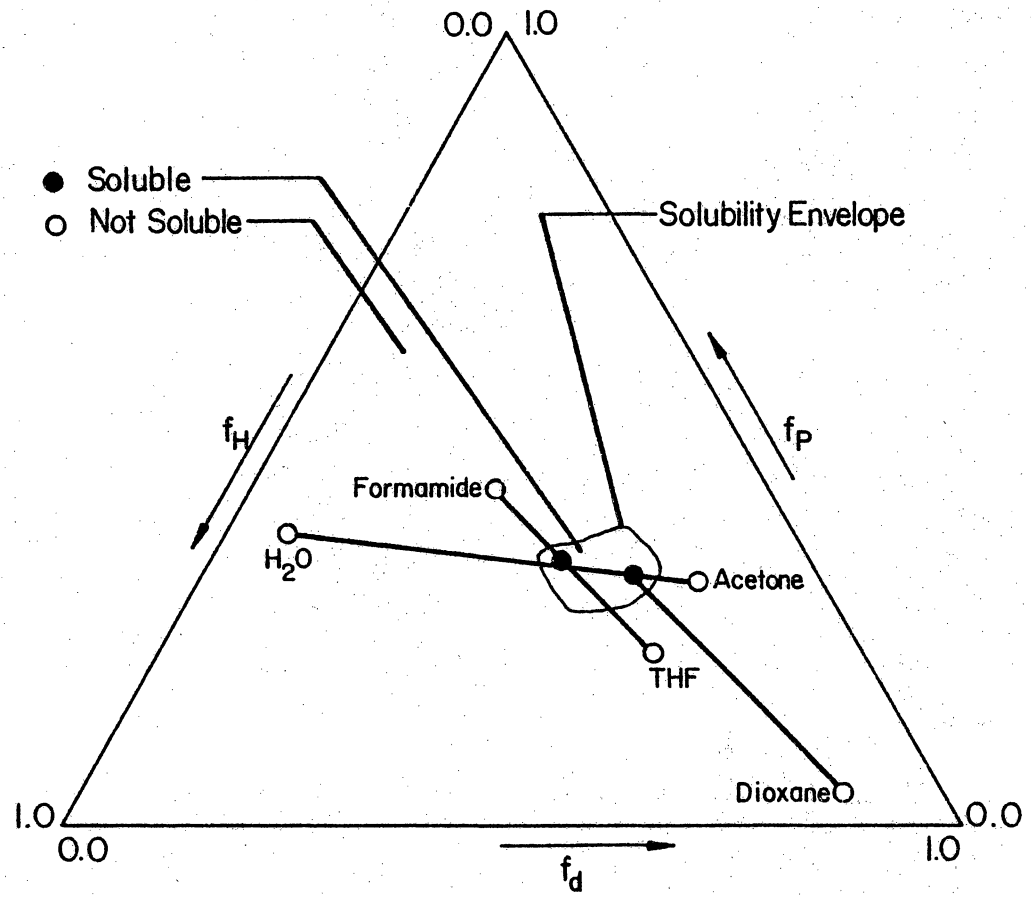

Figure A-2. Solubility diagram for SPSF-Na (0.5):

f_H - Hydrogen bonding factor

f_d - Dispersion factor

f_p - Polar factor

Table A-III.

Effect of Co-Solvent Composition and Gelation Medium on Reverse Osmosis Performance[114]

THF (Vol-%)	Formamide (Vol-%)	Gelation Medium	Flux ($kg/m^2.s$) x10^2	Salt Rejection (%)
70	30	H_2O	1.34	<2
70	30	.75H_2O-.25IPA	1.43	3
70	30	.50H_2O-50IPA	1.48	7
70	30	.25H_2O-.75IPA	1.72	11
70	30	IPA	0.25	50
70	30	methyl alcohol	----	<2
60	40	n butyl alcohol	9.26	1
60	40	t butyl alcohol	2.31	7
60	40	H_2O	----	<2
40	60	n butyl alcohol	8.16	0
40	60	IPA	0.61	45
40	60	IPA	0.63	44
40	60	H_2O	**	**

**membrane swelled in gelation bath

Table A-IV.

Composition of Cast Solution of SPSF-Na(0.5) for an Asymmetric Membrane

Component	Weight (g)
Maleic Acid	0.11
H_2O	0.29
Dioxane	4.0
Acetone	0.57
Polymer	1.75
Polymer %	26%

APPENDIX III

REVERSE OSMOSIS TEST PROCEDURES

A conventional reverse osmosis stainless steel cell, as described by Loeb and Sourirajan[4], was used. Circular sections were cut from the film and placed in the reverse osmosis cells with the membrane top side facing down. The test area was 1.443×10^{-3} m^2 for each membrane. Six cells were placed in parallel to allow 6 simultaneous rejection studies. The membranes were pre-pressurized at 1200 psi until the pure water flux varied less than 3% per hour. The membranes were then allowed to relax for at least 6 hours.

Desalination studies were conducted with a 3.5 wt% NaCl (aq) solution. The feed rate was 400 ml/min at 1000 psi at 25°C. The pure water flux was taken before and after each separation study. Feed, permeate, and retardate samples were analyzed by conductivity (YSI 31 conductivity meter) to determine the salt concentration.

Photographs of the test set-up are shown in Figures A-3 through A-6. Figure A-3 is a close-up of the interior of the cell; Figures A-4 and A-5 show the assembled cell; Figure A-6 shows the 6 connected cells.

The membrane is placed top-side down on the O-ring. The saline solution is fed in from the lower left-hand tubing and comes out from the upper right-hand tubing attached on the lower section of the cell. The desalted permeate comes out through the tubing on the top section

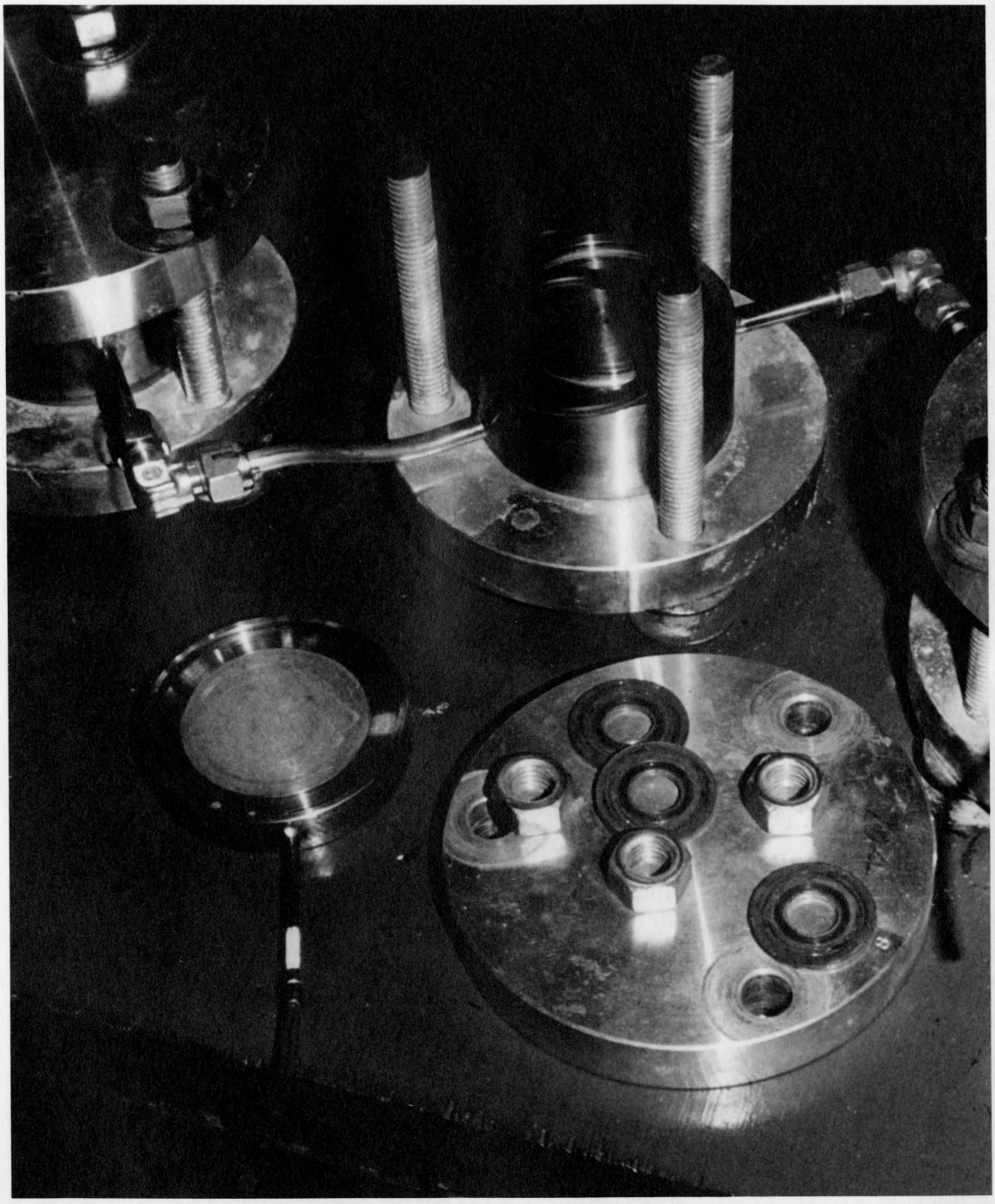

Figure A-3. Disassembled reverse osmosis unit cell showing the interior.

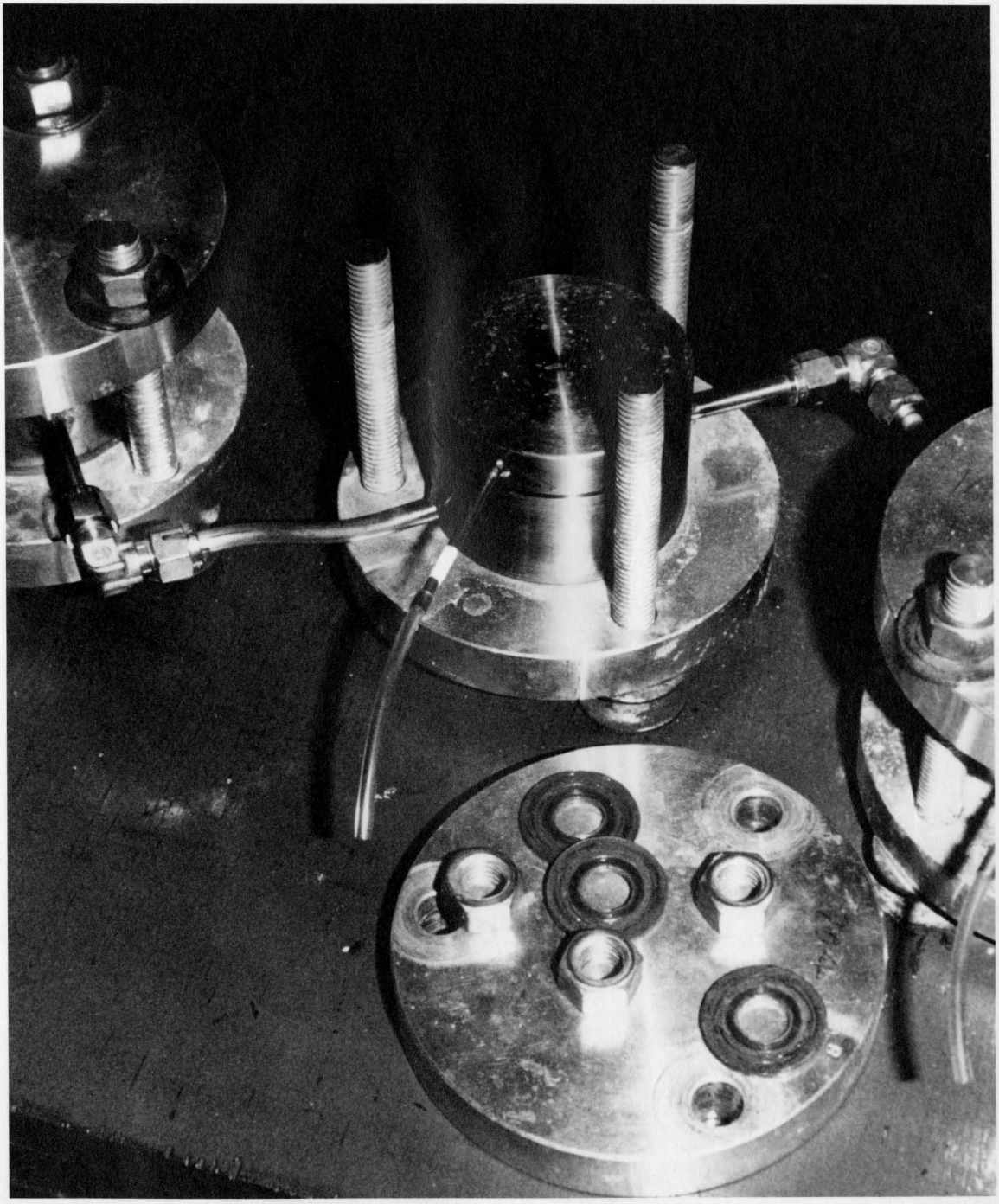

Figure A-4. Half-assembled reverse osmosis unit cell.

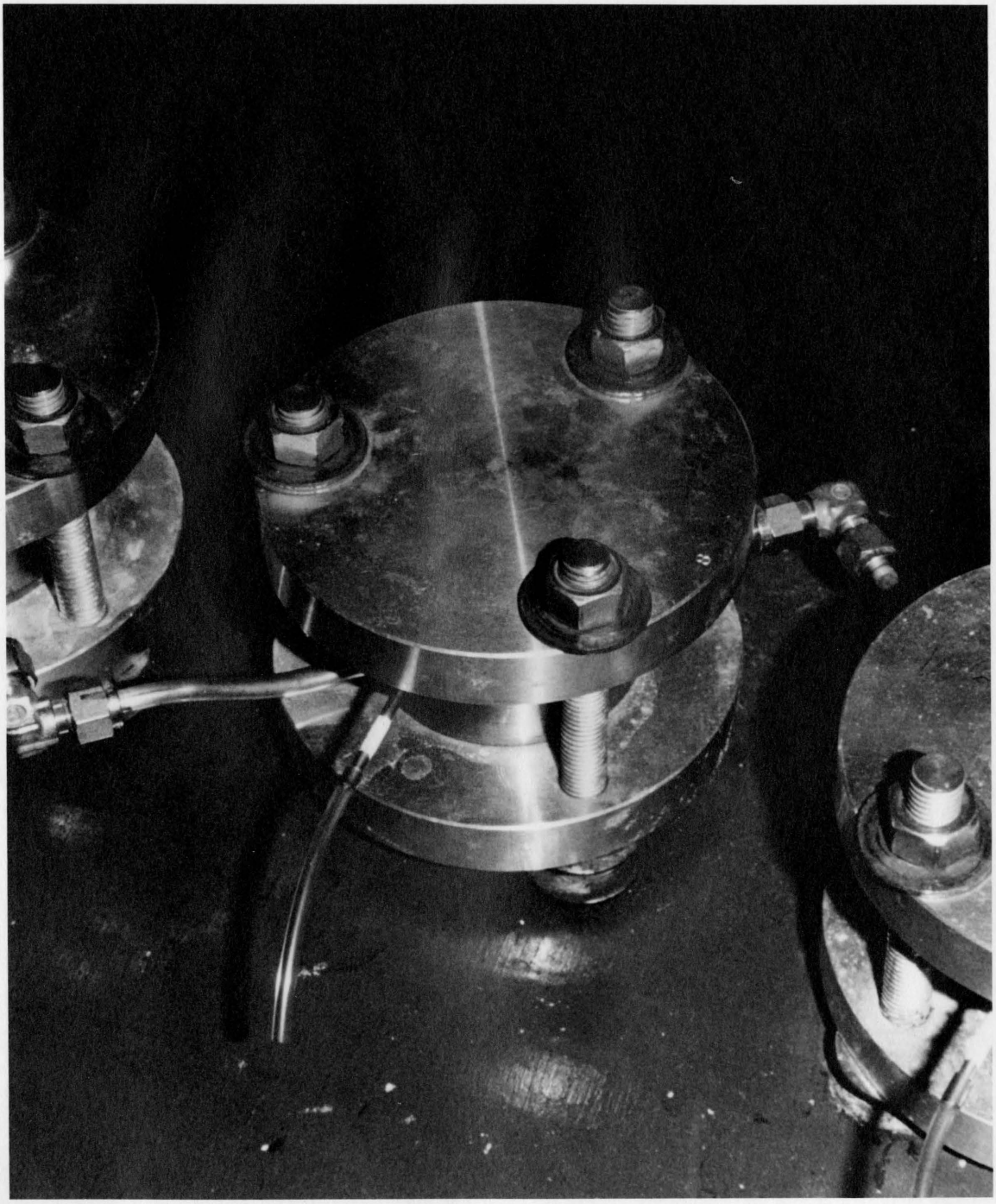

Figure A-5. Fully assembled reverse osmosis unit cell.

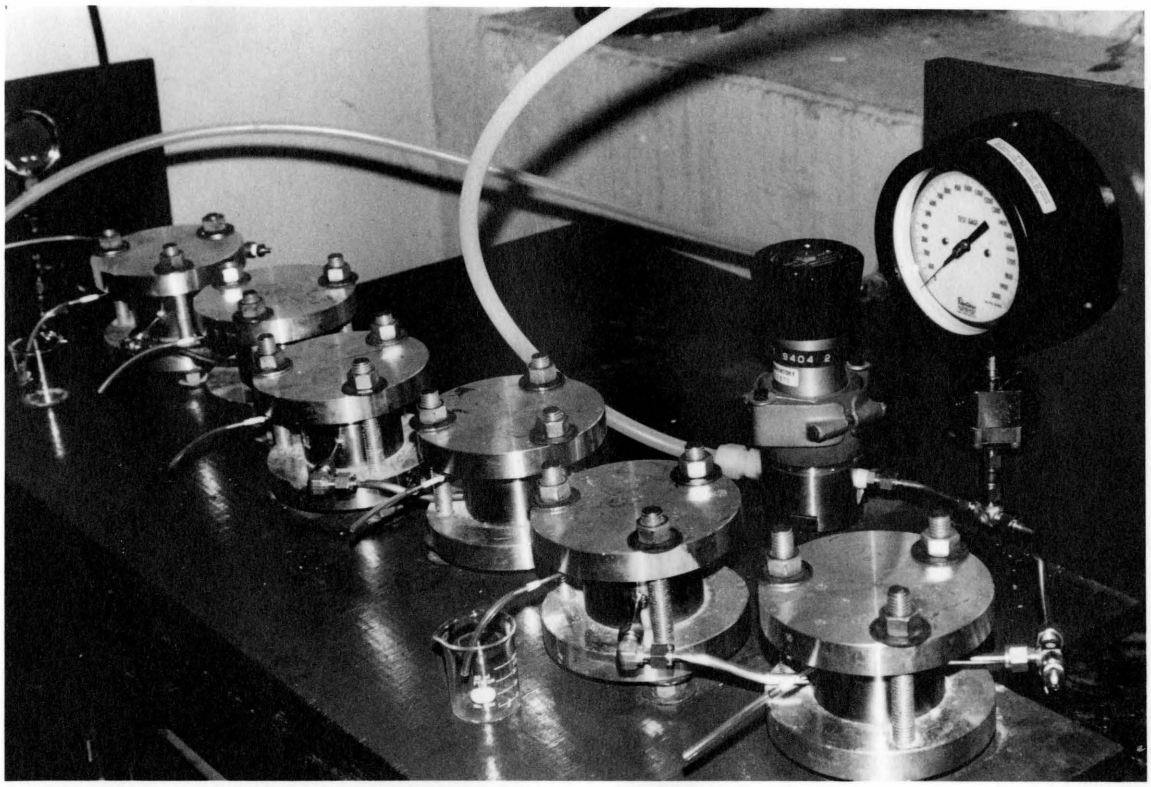

Figure A-6. Six reverse osmosis unit cells connected in series.

of the cell.

The two page vita has been removed from the scanned document. Page 1 of 2

The two page vita has been removed from the scanned document. Page 2 of 2

CHARACTERIZATION OF POLYMERIC MEMBRANES: SULFONATED POLYSULFONES

by

Yoonok Kang

(ABSTRACT)

Sulfonated polysulfone has been shown to possess desirable physical properties for use as a reverse osmosis desalination membrane. In this work, an extensive of dense membranes made from sulfonated polysulfone having 0.2, 0.4, 0.5, 0.6, 0.8, and 1.0 degree of sulfonation is described. The degree of sulfonation (D.S.) was maintained during the membrane fabrication process as evidenced by IR analysis.

The effect of the degree of sulfonation and the counter ion, namely Na and K, on the properties of the membrane were examined. The hydrophilic nature of the material increased with increasing degrees of sulfonation, as evidenced by water uptake and the contact angle of water on the membrane surface. The amount of water increased from 0.6% for polysulfone to 19.2% for sodium salt of sulfonated polysulfone with D.S. of 1.0, and 12.2% for potassium salt of sulfonated polysulfone with D.S. of

1.0. The contact angle of water on polysulfone membranes was 75.1°. The contact angle of water decreased to 25.5° and 60.3° for sodium and potassium salt of sulfonated D.S. = 1.0) polysulfone, respectively. The decrease in the contact angle of water indicated an increase in the hydrophilicity of the membrane surface. Both the water uptake study and the contact angle measurement indicated greater hydrophilicity for the sodium salts of sulfonated polysulfone when compared to the potassium salts of sulfonated polysulfone for a given degree of sulfonation. The nature of the water within the membrane was found to be less hydrogen-bonded when compared to the bulk water.

The surface of the membrane and the polymer powder was found to be different by ESCA analysis, and were also different from the bulk of the material. Neither the membrane surface nor the polymer powder surface had the same stoichiometry as the bulk. Ion exchange occurred not only on the membrane surface, but extended into the bulk with an overall ion exchange of about 80%.

Electrical properties of the membranes were investigated by measuring the partial ionic conductivity and the selectivity of the membrane. The electrolyte/membrane/electrolyte system showed ohmic behaviour. The membrane potential difference under applied transient current

was greatly dependent on the nature of the cation, whereas the nature of the anion had no effect. The activation energy had minimal dependence on the membrane thickness, but depended on the nature of the electrolyte system. The effective size of the ion-conducting channels seemed to increase with higher degrees of sulfonation, probably due to a swelling process.

SEM photomicrographs were taken to study membrane morphology and, in some cases, performance as a reverse osmosis membrane could be predicted from the SEM photomicrographs.